Assessment of whole-head magnetoencephalography during transcranial electric entrainment of brain oscillations

Thesis submitted as requirement to fulfill the degree „Doctor of Philosophy“ (Ph.D.)

at the
Faculty of Medicine
Eberhard Karls University
Tübingen

by

Bankim, Subhash Chander

from

New Delhi, India

2018

Dean:	Professor Dr. I. B. Autenrieth
1. Reviewer:	Privatdozent Dr. S. R. Soekadar
2. Reviewer:	Professor Dr. G. Eschweiler

Dedicated to my parents

Contents

1. Chapter 1 – Introduction 1
   1.1 Magnetoencephalography (MEG) 1
   1.2 Brain Oscillations: A feature representing brain states 2
   1.3 Transcranial Electric Stimulation 6
   1.4 Publication 1: Mapping entrained brain oscillations during transcranial alternating current stimulation (tACS) 8
   1.5 Working Memory 9
   1.6 Publication 2: tACS phase locking of frontal midline theta oscillations disrupts working memory performance 11
   1.7 Limitations of simultaneous assessment of MEG recordings during tACS 13
   1.8 Publication 3: Amplitude-modulated transcranial alternating current stimulation (tACS) during magnetoencephalography (MEG): An update 13
   1.9 Summary 14
2. Chapter 2 – Publications 16
   2.1. Mapping entrained brain oscillations during transcranial alternating current stimulation (tACS) 17
   2.2. TACS phase locking of frontal midline theta oscillations disrupts working memory performance 28
   2.3. Amplitude-modulated transcranial alternating current stimulation (tACS) in magnetoencephalography (MEG): An update 42
   2.4. Unpublished work 59
3. Chapter 3 – Discussion 63
4. Chapter 4 – Summary 69
5. German Summary 71
6. Bibliography 74
7. Declaration of Author Contributions 81

Acknowledgements 84

1. Chapter 1 – Introduction

Diverse cognitive functions have been associated with dynamic brain states that emerge due to simultaneous activity of neural ensembles. Disentangling activity of these neural ensembles as representative features of brain states and forming an association with the emergent cognitive function remains a challenge. However, it has been possible to record brain states using advanced neuroimaging techniques while executing different cognitive tasks. Furthermore, by assessing the recorded brain states while performing various cognitive tasks could hint towards the associations between brain states and cognitive functions. Such associations are further strengthened by correlating the alterations in brain states induced by an external intervention with alterations in cognitive functions.

Using a novel strategy allowing for assessment of brain states recorded by magnetoencephalography (MEG) during transcranial electric stimulation (TES) (*Soekadar et al. 2013, Witkowski et al. 2015, Garcia Cossio et al. 2015*), effects of TES on cognitive brain functions are investigates.

After Soekadar et al. (*2013*) showed that assessment of MEG recordings performed during TES is possible, it has recently been shown that currently available stimulation artifact rejection methods cannot completely remove all stimulation artifacts (*Noury et al. 2016*). Thus, in addition to demonstrations of successful applications of TES to influence cognitive function, this dissertation also highlights possible strategies to infer TES effects on neural activity despite these artifacts. Due to their non-linearity, however, interpretation of neuroimaging data recorded during TES must be interpreted with great care.

1.1 Magnetoencephalography (MEG)

Magnetoencephalography (MEG) is a brain imaging technique that can record ongoing fluctuations in magnetic fields originating from the brain on a millisecond-by-millisecond time scale. Such fluctuations in magnetic fields occur in the brain due to dynamic neuronal transmembrane electro-chemical currents.

These dynamic magnetic field fluctuations generated within the human head are a billion times smaller than the earth's magnetic field. Therefore, MEG captures magnetic field fluctuation from the brain through highly sensitive magnetic field sensors using superconducting quantum interference devices (SQUID). Due to high sensitivity of SQUID, MEG recordings are performed in a shielded room to prevent interference from fluctuating environmental magnetic fields.

The small size of the SQUID sensors allows high spatial resolution of MEG with simultaneous recordings from 275 sensors. Due to high the spatial resolution, mathematical models allow localizing the sources of magnetic activity in the brain with millimeter precision. While mathematical models can determine the magnetic field strength as projected on the MEG sensors by a dipole source of known strength, location and orientation, inverse methods based on these models allow determining the location, orientation and strength of a dipole source from the magnetic activity recorded by MEG sensors. However, due to multiple dipole sources such inverse methods do not uniquely determined a solution and require additional mathematical constraints based on prior knowledge in order to obtain a unique solution. Furthermore, the accuracy of determining the location, orientation and strength of a dipole source depends on these additional mathematical constraints.

After recording MEG, to determine the anatomical location of the brain activity as determined using the inverse solution requires co-registration with individual's brain anatomy. Thus, during MEG recordings, head location is digitized and monitored using head coils attached to nasion and pre-auricle fiducial points.

1.2 Brain Oscillations: A feature representing brain states

Brain oscillations reflect fluctuations in the activity of neuronal ensembles. Hans Berger made the first report of brain oscillations in 1929 by recording electrical activity from the scalp (*Berger, 1929*). Since then technological advances have not only improved recording of brain oscillations but also introduced novel techniques like magnetoencephalography (MEG) that can

measure fluctuations in magnetic activity originating from the brain. Such a brain imaging technique allows associating ongoing brain oscillations with various cognitive functions. Furthermore, clinical observations could associate brain oscillations in various frequency bands to diverse brain functions (*Tatum, 2014*).

- **Delta oscillations: 0 – 4 Hz**

  Delta oscillations are large amplitude oscillations that are predominant during sleep in humans. Delta oscillations predominantly originate from thalamus and cortex (*Neske, 2016*). Brain functions like regulation of hormone release such as growth hormone, prolactin and thyroid stimulation hormone are associated with delta oscillations (*Brandenberger, 2003*).

  Various neurological disorders have also been associated with aberrant alterations in delta oscillations. For example, disruption of delta oscillations during sleep is observed in people suffering from dementia, schizophrenia and Parkinson's disease (*Kryzhanovskiĭ et al. 1990*).

- **Theta oscillations: 4 – 8 Hz**

  Jung & Kornmüller (*1938*) first observed theta oscillations in rabbits. As the function role of theta oscillations remained unclear, the interest of the scientific community in theta band oscillations continued to grow. It was only in 1972 when Landfield et al. correlated observation of theta oscillations with memory of foot shocks in rats. Since then, numerous studies suggested the relevance of theta oscillations for different kinds of learning and memory processes.

  Existence of theta oscillations in humans was a matter of debate until recently (*Klimesch et al. 1994, Tesche et al. 2000).* Since then, numerous studies have linked theta oscillations to various brain functions in humans. Many studies have reported an increase in power of theta oscillation while engaging in cognitive tasks (*Burgess et al. 2000, Gevins et al. 1997, Krause et al. 2000*). Also, theta oscillations have been

observed during rapid eye movement sleep stage in humans and are linked to consolidation of memory (*Diekelmann et al. 2010*).

Various neurological disorders have been associated with aberrant alterations in theta oscillations. For example, people suffering from disorders like major depressive disorders, schizophrenia and Alzheimer's disease that reveal deficits in memory related brain functions show reduction in amplitude of theta oscillation (*Basar et al. 2008*).

- **Alpha oscillations: 8 – 14 Hz**

  Hans Berger first reported alpha oscillations in 1931. Berger observed increase in amplitude of alpha oscillations over the occipital brain areas while human participants closed their eyes. In addition, alpha oscillations originating from sensory or motor cortex are associated with voluntary control of movement (*Arroyo et al. 1993*). Apart from wakeful state, alpha oscillations occur during sleep (*Cantero et al. 2002*). While sleeping, alpha oscillations occur during rapid eye movement (REM) stage mainly due to combination of eye movement related motor component and dreaming related occipital component.

  Various neurological disorders have been associated with aberrant alterations in alpha oscillations. For example, patients suffering from bipolar disorders, schizophrenia and Alzheimer's disease show reduction in amplitude of alpha oscillation (*Basar et al. 2012*).

- **Beta oscillations: 15 – 30 Hz**

  Hans Berger first reported beta oscillations along with alpha oscillations in 1931. Berger observed an increase in amplitude of beta oscillations during eyes open compared to eyes closed in humans. However, currently beta oscillations are more commonly associated with muscle contractions and originate from sensory-motor cortex (*Baker, 2007, Lalo et al. 2007*). Apart from contraction of muscles, increase in amplitude of beta oscillations is also associated with suppression of movement (*Pfurtscheller, 1981*). However, the most pronounced

increase in power of beta oscillations occurs shortly after termination of voluntary movement (*Pfurtscheller, 1981*). More recently, Hanslmayr (*2014*) showed that interrupting desynchronization of beta oscillations originating from prefrontal cortex impairs memory formation.

Various neurological disorders have been associated with aberrant alterations in beta oscillations. For example, patients having bipolar disorders, Alzheimer's disease show reduction in power of beta oscillation (*Basar et al. 2012*). Patients suffering from Parkinson's disease show pronounced increase in power of beta oscillations (*Brown et al. 2001*).

- **Gamma oscillations: 30 – 90 Hz**

  Jasper & Andrews (*1938*) first used the term gamma waves to designate low-amplitude beta-like waves at 35 – 45 Hz. They recorded gamma oscillations from the cortex of epileptic patients. Since then several studies have linked gamma oscillations to various cognitive processes such as attention, arousal, language perception and object recognition (*Herrmann et al. 2004*). However, gamma oscillations are not uniquely associated only with above mentioned brain functions. Gamma oscillations are occurring across the whole brain. The widely accepted function of gamma oscillations is binding of different neuronal populations to form a network for performing cognitive or motor functions (*Niedermeyer et al. 2004*).

  Various neurological disorders have been associated with aberrant alterations in gamma oscillations. In disorders like attention deficit hyperactivity disorder (ADHD) and epilepsy, an increase in amplitude of gamma oscillations occurs. Whereas in case of Alzheimer's disease, autism, migraine, stroke and brain injury, a decrease in power of gamma oscillations occurs (*Arroyo et al. 1992, Yordanova et al. 2001, Ribary et al. 1991, Grice et al. 2001, Hall et al. 2004, Molnár et al. 1997, Thornton, 1999*).

Even though, there are abundant studies investigating fluctuations in brain oscillations, the role of brain oscillations in performing cognitive tasks remains still obscure. Thus, perturbing ongoing brain oscillations in a specific frequency band while performing cognitive tasks and subsequently correlating the perturbations with task performance can reveal certain roles of brain oscillations. One of the most promising methods for perturbing brain oscillations is by applying transcranial electric stimulation as described below.

1.3 Transcranial Electric Stimulation

During transcranial electric stimulation (tES), weak electrical currents are applied across the brain to stimulate neurons and modulate various brain functions. Neurons maintain electrochemical gradients across the neuronal membrane, which are essential for transmission of information across neurons. Neurons are susceptible to various forms of external stimulations that can alter the electrochemical gradients maintaining the membrane potential across neurons. In-vitro experiments demonstrate neuronal membrane potential can be dynamically altered by externally applying electric currents (*Hodgkin et al. 1952*). Application of weak electric currents induces sub-threshold alterations of neuronal resting membrane potential that can modulate functional response of neurons to external stimuli (*Kuo et al. 2015*).

Usually tES is applied for few minutes by passing electric currents in order of milliamperes through the stimulation electrodes attached to the scalp. Unlike classical electro convulsive therapy that applies electrical currents in order of one ampere magnitude and cause extreme discomfort, tES applied in milliampere range might cause only mild headache, itching and tingling sensations felt under the stimulation electrodes by the receiver (*Been et al. 2007*). The only disadvantage of such sensations in research is that the receiver is aware of tES, which might trigger a placebo effect. Nevertheless, a rhythmic variant of tES, the transcranial alternating current stimulation (tACS) can perturb brain oscillations at frequency of the applied rhythmic stimulation as described below.

Transcranial Alternating Current Stimulation (tACS) – tACS is usually applied as oscillatory current with alternating polarity, resembling a sinusoidal wave. It is possible to alter excitability of motor cortex by applying tACS within beta band at 20 Hz (*Feurra et al. 2011*). tACS when applied within theta band at 5 Hz, alpha band at 10 Hz and gamma band at 40 Hz over the motor cortex did not change cortical excitability (*Feurra et al. 2011*), thus demonstrating that tACS can induce frequency specific modulation in cortical excitability. Computational modeling and human experiments have shown that tACS can increase power of brain oscillations at the frequency of applied stimulation (*Ali et al. 2013*, *Helfrich et al. 2014*).

Application of tACS can also alter receiver's performance in cognitive tasks. tACS when applied over motor cortex at a frequency within beta band slows voluntary movement (*Pogosyan et al. 2009, Joundi et al. 2012*). Whereas, tACS when applied over motor cortex within gamma band at 70 Hz accelerates voluntary movements (*Joundi et al. 2012*). Apart from execution of motor functions, tACS can also modulate performance in memory tasks. After receiving tACS in theta band, receivers could remember more items in a recall by memory task (*Jausovec et al. 2014*).

Studying the mechanisms of tACS induced cognitive enhancements remained challenging as artifacts from tACS impedes investigating the recordings of brain activity acquired during tACS. However, the recording of brain signals is essential for revealing the mechanisms of tACS mediated cognitive enhancements. A solution to this problem at least to a certain extent is a novel tACS paradigm, the amplitude modulated tACS ($tACS_{AM}$) as described below.

1.4 Publication 1: Mapping entrained brain oscillations during transcranial alternating current stimulation (tACS)

This publication describes $tACS_{AM}$ as a novel method for interacting with brain oscillations and simultaneous assessment of brain activity during tACS by applying the strategy proposed by *Soekadar et al. 2013*. $tACS_{AM}$ is applied as tACS at a carrier frequency beyond the physiological frequencies of interest and the amplitude of the applied tACS signal is modulated at the physiological frequency of interest (*Witkowski et al. 2016*). The rationale of testing $tACS_{AM}$ for perturbing brain oscillations originates from amplitude modulated peripheral nerve stimulation for evoking somatosensory potentials (*Noss et al. 1996*). When amplitude modulated electric currents were applied to median nerve, the stimulation noise was observed at high carrier frequency while allowing recovery of somatosensory evoked potentials. Furthermore, the frequency spectrum showed increase in power at the modulation frequency only from the electroencephalography (EEG) recorded over the somatosensory cortex contralateral to the stimulated peripheral nerve (*Noss et al. 1996*). This observation confirms that neurons are responsive to the modulation signal of the applied amplitude modulated stimulation. Based on this report, we suspected that neurons might be responsive to the modulation signal of the applied $tACS_{AM}$ signal. Thus, the main advantage of $tACS_{AM}$ over classical tACS is that the stimulation noise is concentrated around the carrier frequency. This allows assessment of brain activity during $tACS_{AM}$ with low stimulation noise in the physiological frequencies of interest compared to tACS while neurons respond to modulation frequency.

To extract and localize brain activity with millimeter precision from MEG recordings acquired $tACS_{AM}$, adaptive spatial filtering technique, the synthetic aperture magnetometry (SAM) is applied (*Robinson, 1999, Soekadar et al. 2013*). While it was possible to extract self-paced finger movement related brain activity with high fidelity, the quantification of the $tACS_{AM}$-induced perturbations of brain oscillations required another metric. As power changes due to $tACS_{AM}$ were concentrated at the carrier frequency and were not statistically detectable

in the physiological frequencies, there was a need to test other metrics independent of power to quantify the physiological effects of $tACS_{AM}$.

As $tASC_{AM}$ induced power changes are not detectable in the physiological frequencies, we assessed phase changes induced by $tACS_{AM}$ to quantify synchronization of ongoing brain oscillation to the applied stimulation in the physiological frequencies of interest. The process of synchronizing brain oscillations to the applied rhythmic stimulation such as $tACS_{AM}$ is *entrainment* (*Thut et al. 2011*). While entrainment might be one of the mechanisms of interacting with ongoing brain oscillations, the feature of brain oscillations, such as amplitude or phase, showing tACS-induced modulation was unknown. Helfrich et al. (*2014*) showed phase entrainment of brain oscillations using the EEG recordings acquired from close proximity to the applied tACS at 10 Hz over occipital cortex.

Even though effects of tACS-entrainment on brain activity has been shown using EEG, it was not possible to record brain activity at the site of tACS over the scalp. Therefore, it remains a challenge to estimate brain oscillations from the brain region targeted for stimulation with EEG recordings. Simultaneous MEG recordings during $tACS_{AM}$ not only made it possible to record brain physiological activity below the stimulation electrode but also to estimate stimulation-related PLV increase (*Lachaux et al. 1999*) with millimeter precision. It remained open, however, to what degree this PLV increase relates to neural entrainment. Also, it remained unclear whether purposeful entrainment of brain oscillations can manipulate performance in a cognitive task. To establish entrainment dependent manipulation of performance in a cognitive task, we applied $tACS_{AM}$ while the receivers were engaging in a working memory task.

1.5 Working Memory

Working memory (WM) is associated with temporary storage and processing of information, which is essential for performing complex cognitive tasks such as mental calculations, language comprehension, learning and reasoning.

According to the model of WM proposed by Baddeley (*2000*), WM is categorized into the following three subcomponents.

- **Central executive** – This subcomponent of WM is responsible for controlling attention. Additionally, this subcomponent suppresses irrelevant information and coordinating between multiple cognitive tasks when performed at the same time.
- **Visuospatial sketchpad** – This WM subcomponent is usually associated with processing of visual images. Visual sketchpad is further classified into visual and spatial components. The visual component processes shape, color and texture related information, whereas the spatial component processes information related to the location, orientation and movement in space.
- **Phonological loop** – This WM subcomponent associated with processing of speech and language. All forms of auditory and verbal information are processed through the phonological loop. Even language information in form of images is also transferred into the phonological loop through silent articulation.

One of the cognitive tasks to assess WM performance is an n-back task. Wayne Kirchner first introduced N-back task in 1958. During an n-back task, a continuous sequence of sensory stimuli is presented to a participant and the participant has to indicate when the currently perceived stimulus matches with the n^{th} previous stimulus. Here 'n' refers to the number of stimulus to remember during the n-back task and the difficulty level of n-back task increases by increasing the 'n'. In an n-back task all the above mentioned component of WM are active at the same time. Central executive function keeps a record of the sensory stimuli while the participant relies on the visuospatial sketchpad and the phonological loop to recall and update the sensory stimuli.

While performing an n-back task, an increase in power of frontal midline theta (FMT) oscillations (4 – 8 Hz) originating from medial prefrontal cortex (mPFC) was reported (*Brookes et al. 2011*). The power increase of theta

oscillations is also related with the increase in n-back task difficulty (*Brookes et al. 2011*). In addition, 6 Hz tACS of healthy volunteers could influence reaction times in WM task but did not alter the WM task accuracy (*Polanía et al. 2012*).

Atypical alterations of theta oscillations have been linked to WM deficits in various psychiatric disorders such as bipolar disorder, schizophrenia, attention deficit hyperactivity disorder (ADHD) and dementia associated with Alzheimer disease (*Ozerdema et al. 2012, Doege et al. 2010, Lenartowicz et al. 2014, Yener et al. 2007*). Such WM deficits that are associated with theta oscillations can be compensated by externally applying various forms of brain stimulations. For example, WM task performance of depressed patients improved after receiving tACS at a frequency within theta band (*Jaušovec et al. 2014, Jaušovec et al. 2014*). Hence, WM served as the most appropriate cognitive function to study purposeful manipulation by $tACS_{AM}$ mediated entrainment of FMT oscillations.

1.6 Publication 2: tACS phase locking of frontal midline theta oscillations disrupts working memory performance

This publication focuses on purposefully entraining FMT oscillations to study whether $tACS_{AM}$ mediated entrainment can modulate a cognitive function associated with FMT oscillations such as working memory. We applied $tACS_{AM}$ modulated at individual's theta peak frequency while engaging them in an n-back task. Engaging in an n-back task increases the power of FMT oscillations and the phase of the FMT oscillations encodes the temporal order of stimulus presented (*Brookes et al. 2011, Axmacher et al. 2010*). Furthermore, to perform the n-back task hippocampus regulates the phase of FMT oscillations in order to suppress competing cortical representations of the sensory stimuli presented in n-back task (*Gordon, 2011, Norman et al. 2007*). Thus, manipulating phase of the ongoing FMT oscillations through $tACS_{AM}$-mediated entrainment would interfere with maintenance of temporal order information necessary for performing n-back task.

To test this hypothesis, 20 volunteers were invited to receive $tACS_{AM}$ modulated at each individual's theta peak frequency while performing a 2-back task. The theta peak frequency was determined by analyzing MEG recordings acquired while familiarizing the volunteers to the 2-back task. Usually the performance on n-back tasks improves with practice. To control for any confound by learning, volunteers were randomly selected to receive either $tACS_{AM}$ or no stimulation while performing the 2-back task. Another confounding factor could be the sensations associated with the application of stimulation. However, participants were not able to identify whether they received $tACS_{AM}$ or not. Thus, placebo effects associated with $tACS_{AM}$, could be ruled out and $tACS_{AM}$ can be regarded as a powerful tool to establish a link between performance on a cognitive task and the perturbed brain oscillation.

Interestingly, apart from entrainment of FMT oscillations to the modulation frequency of the applied $tACS_{AM}$, an inhibition of 2-back task related increase of FMT power occurred. Contrary to the expected increase in power of ongoing brain oscillations as observed while applying tACS, application of $tACS_{AM}$ resulted in inhibition of n-back task related power of FMT oscillations. Furthermore, as hypothesized, there was a decrease in the accuracy on the 2-back task as the $tACS_{AM}$ inhibited the power increase of FMT oscillations.

Summarizing, $tACS_{AM}$ was not only associated with increased PLV under the frontal stimulation electrode in close proximity, but also modulated performance in an n-back task. However, identification of the exact mechanism causing inhibition of n-back task related increase in power of FMT oscillations would require further investigation. We speculate as hippocampus drives the phase of the FMT oscillations, entrainment of FMT oscillations to phase of the applied $tACS_{AM}$ signal envelope would interfere with hippocampus-driven endogenous phase regulation of FMT oscillations and prevent FMT power increase related to suppression of competing cortical representations.

1.7 Limitations of simultaneous assessment of MEG recordings during tACS

Even though it was possible to modulate performance in a cognitive task and observe simultaneous entrainment of FMT oscillations, it is not possible to conclude full suppression of $tACS_{AM}$ artifacts with complete certainty. Neuling et al. (*2015*) suggested the recovery of brain activity from MEG recordings acquired during tACS and complete suppression of tACS noise by applying spatial filters based on beamforming algorithms. However, Karsten et al. (2018) showed non-linearities in the stimulation setup induce artifacts associated with demodulation of $tACS_{AM}$ signal. In addition, Noury et al. (*2017*) reported steady phase shifts in the MEG recordings due to such modulations of the tACS signal. Thus, it might seem possible to attenuate $tACS_{AM}$ artifact at the modulation frequency while recording MEG by implementing advanced spatial filtering algorithms based on beamforming techniques, but certainly distinguishing brain activity from $tACS_{AM}$ artifact at the modulation frequency is not possible. The presence of undetectable residual artifact from $tACS_{AM}$ in MEG recordings cannot be eliminated. Therefore, the following publication shows functional interaction of $tACS_{AM}$ signal with neurons in the brain apart from only demodulation due interaction with biological membranes.

1.8 Publication 3: Amplitude-modulated transcranial alternating current stimulation (tACS) during magnetoencephalography (MEG): An update

In this publication, sources of linear and non-linear stimulation artifacts are described (*Karsten et al. 2018, Noury et al. 2016*) and validity of phase-locking value (PLV), a well-established measure to estimate neural entrainment, further tested. For this purpose, comparison between human brains and a melon phantom was performed while tACS or $tACS_{AM}$ was applied. It was suggested that a melon can be considered an appropriate model for human head without neurons (*Neuling et al. 2017*). The concentric tissue layers with different electrical properties resemble different tissue layers of the human head.

Following the assumption that melon phantom has only passive electrical properties, the power at the $tACS_{AM}$ modulation frequency is due to the demodulation by non-linear interaction with biological tissue and is referred to as power leakage. In case of human brains, in addition to power leakage, neural entrainment contributes to power increase at the modulation frequency. Therefore, the ratio of power at the modulation frequency and the carrier frequency of $tACS_{AM}$ signal was compared between human brains and melon phantom. A higher ratio for human brain compared to melon phantom would indicate an additional contribution of neural entrainment to the power leakage.

Apart from the power spectral analysis, a PLV analysis revealed larger increase in PLV for $tACS_{AM}$ compared to tACS for human brain. In comparison, the PLV for melon phantom during $tACS_{AM}$ and tACS are approximately the same. Even though the power of $tACS_{AM}$ at the modulation frequency is lower in comparison to tACS, a larger PLV at modulation frequency underlines the independence of power and phase. It remains unclear whether the observed increase in power and PLV at the modulation frequency is possibly a combination of demodulations induced by non-linearities in the stimulation circuit and neural entrainment. Further investigations are essential to disentangle the contributions of demodulation due to nonlinearities of the stimulation setup and functional interactions of stimulation current with neurons.

1.9 Summary

Even though it is possible to perturb ongoing brain oscillations through various brain stimulation methods, the assessment of brain oscillations during brain stimulation remains a challenge due to stimulation-induced artifacts. As the artifacts associated with brain stimulation methods are concentrated in the frequency range of the brain oscillations to be perturbed, the recovery of brain activity and the quantification of the induced perturbations remain difficult.

Application of $tACS_{AM}$ allows concentrating the stimulation artifact in the frequency range beyond the physiological frequencies of brain oscillations intended for perturbations. Therefore, assessment of brain activity acquired

during $tACS_{AM}$ while perturbing ongoing brain oscillations is possible. Furthermore, advanced spatial filtering algorithms allow estimation of induced perturbation with millimeter precision from MEG recordings acquired during $tACS_{AM}$. In addition, applying $tACS_{AM}$ can purposefully perturb brain oscillations through entrainment and modulate performance of the cognitive function associated with the entrained frequency. For example, applying $tACS_{AM}$ modulated at each individual's theta peak frequency entrains FMT oscillations and interferes with maintenance of temporal order information in a working memory task. Thus, $tACS_{AM}$ has the potential to serve as a novel tool for perturbing ongoing brain oscillations through entrainment and modulating the performance of cognitive functions associated with entrained brain oscillations, while allowing assessment of entrained brain oscillations.

While the presented data suggest $tACS_{AM}$-mediated entrainment of brain oscillations, established measures to quantify such entrainment, e.g. PLV, must be interpreted with caution. The combination of non-linearities in the stimulation circuit and possible functional interactions with neurons demodulate the $tACS_{AM}$ signal and contribute both towards an increase in power and neural entrainment. The characterization of demodulation induced by each component would possibly allow for reliable quantification of neural entrainment in the future.

2. Chapter 2 – Publications

2.1. Mapping entrained brain oscillations during transcranial alternating current stimulation (tACS)

NeuroImage 140 (2016) 89–98

Contents lists available at ScienceDirect

NeuroImage

journal homepage: www.elsevier.com/locate/ynimg

Mapping entrained brain oscillations during transcranial alternating current stimulation (tACS)

Matthias Witkowski [a,1], Eliana Garcia-Cossio [a,b,c,1], Bankim S. Chander [a], Christoph Braun [d,e], Niels Birbaumer [b], Stephen E. Robinson [f], Surjo R. Soekadar [a,b,*]

[a] Applied Neurotechnology Lab, Department of Psychiatry and Psychotherapy, University Hospital of Tübingen, Germany
[b] Institute of Medical Psychology and Behavioral Neurobiology, University of Tübingen, Tübingen, Germany
[c] Donders Centre for Brain, Cognition and Behavior, Department of Artificial Intelligence, Radboud University Nijmegen, Nijmegen, The Netherlands
[d] MEG Center, University of Tübingen, Tübingen, Germany
[e] CIMeC, Center for Mind/Brain Sciences, University of Trento, Trento, Italy
[f] National Institute of Mental Health (NIMH), MEG Core Facility, Bethesda, USA

ARTICLE INFO

Available online 17 October 2015

Keywords:
Neuromagnetic brain oscillations
Entrainment
Transcranial alternating current stimulation
Whole-head magnetoencephalography

ABSTRACT

Transcranial alternating current stimulation (tACS), a non-invasive and well-tolerated form of electric brain stimulation, can influence perception, memory, as well as motor and cognitive function. While the exact underlying neurophysiological mechanisms are unknown, the effects of tACS are mainly attributed to frequency-specific entrainment of endogenous brain oscillations in brain areas close to the stimulation electrodes, and modulation of spike timing dependent plasticity reflected in gamma band oscillatory responses. tACS-related electromagnetic stimulator artifacts, however, impede investigation of these neurophysiological mechanisms. Here we introduce a novel approach combining amplitude-modulated tACS during whole-head magnetoencephalography (MEG) allowing for artifact-free source reconstruction and precise mapping of entrained brain oscillations underneath the stimulator electrodes. Using this approach, we show that reliable reconstruction of neuromagnetic low- and high-frequency oscillations including high gamma band activity in stimulated cortical areas is feasible opening a new window to unveil the mechanisms underlying the effects of stimulation protocols that entrain brain oscillatory activity.

Introduction

Transcranial application of weak alternating electric currents via two or more scalp electrodes can affect perception (Kanai et al., 2008), memory (Marshall et al., 2006), motor function (Brignani et al., 2013; Joundi et al., 2012) and higher-order cognition (Santarnecchi et al., 2013). While the exact neurophysiological mechanisms underlying these effects are widely unknown, the main mechanisms by which tACS influences brain physiology were attributed to frequency specific entrainment, i.e. phase alignment of endogenous brain oscillations to externally applied oscillating electric currents (Thut et al., 2011; Zaehle et al., 2010), and modulation of spike-timing dependent plasticity (Polanía et al., 2012; Vossen et al., 2015). There is, however, no established method for precise source localization and artifact-free source reconstruction of tACS-entrained brain oscillations near and underneath the stimulator electrodes. Nonlinear stimulation artifacts reflected by broadband noise and a signal peak at the stimulation frequency impedes investigation of local and distant mechanisms underlying tACS effects on low- and high-frequency brain oscillatory activity. Besides providing the possibility to further elucidate the causal link between brain oscillations and behavior, the ability to precisely map entrained brain oscillations could further improve stimulation effectiveness by refining the positions of tACS electrodes according to the individual brain anatomy.

Recently, simultaneous recording of electroencephalography (EEG) during tACS was demonstrated using signal subtraction and filtering (Voss et al., 2014) or by estimating a template of the tACS artifact from an adjacent ~3-second EEG-recording window and subsequent application of an independent component analysis (ICA) to remove residual stimulation artifacts (Helfrich et al., 2014). However, spatial resolution of EEG is limited and recording of brain oscillations in close proximity or underneath the stimulation electrodes is not possible due to saturation of the EEG signal amplifier in case of direct contact with the stimulation electrode (Soekadar et al., 2014a). Also, the EEG is increasingly insensitive towards higher frequencies due to the low-pass filtering properties of the skin and skull (Nunez, 1981) limiting its capacity to assess high frequency oscillations, e.g. gamma band responses related to spike timing dependent plasticity (Fründ et al., 2009).

* Corresponding author at: Applied Neurotechnology Lab, Department of Psychiatry and Psychotherapy, University Hospital of Tübingen, Calwerstr. 14, 72076 Tübingen, Germany.
E-mail address: surjo.soekadar@uni-tuebingen.de (S.R. Soekadar).
[1] Both authors contributed equally.

http://dx.doi.org/10.1016/j.neuroimage.2015.10.024
1053-8119/

In contrast to EEG, the spatial resolution of MEG is not influenced by the conduction properties of the skull, and allows localization of cortical signal sources at precision of a few millimeters (Poghosyan and Ioannides, 2007; Papadelis et al., 2009; Suk et al., 1991). Also, the MEG allows for assessing brain oscillatory activity directly underneath the stimulation electrodes as neuromagnetic fields pass the stimulation electrodes undistorted. Being independent of the conducting boundaries of the skull, MEG allows recordings of neuromagnetic brain activity beyond 600 Hz (Curio et al., 1997; Kotecha et al., 2009). MEG would, thus, be an ideal candidate to map entrained brain oscillations and to investigate local and distant effects of tACS.

Recently, we have introduced a novel strategy to record whole-head magnetoencephalography (MEG), the assessment of the brain's neuromagnetic fields, during transcranial direct current stimulation (tDCS) (Soekadar et al., 2013a; Garcia-Cossio et al., 2016). It remains unclear, however, to what extent the MEG system's hardware would tolerate the application of high-frequency tACS (mainly limited by the maximum slew rate and occurrence of flux locks), and whether reliable removal of tACS-dependent artifacts in source-reconstructed signals is feasible.

An extensive series of experiments (unpublished data, available upon request) showed that application of alternating currents at 2 mA (currently the accepted maximum intensity for tACS in humans) and 600 Hz stimulation frequency in the MEG is possible without harming the hardware as tested in a 275 whole-head MEG by CTF Systems (Port Coquitlam, Canada) (Fig. 1A). Feasibility of tACS during MEG recordings was recently likewise shown for the Elekta Neuromag Vectorview device (Electa, Oy, Finland) (Neuling et al., 2015).

A crucial challenge in the assessment of brain oscillations during tACS is, however, the distinction between physiological brain activity and the stimulator-dependent non-linear artifacts, as the frequency of interest (FOI) is usually equal to the stimulation frequency (FOS). Thus, cancellation of stimulator-dependent artifacts during tACS, particularly at the FOI, is desirable. While localization of neuromagnetic source activity, e.g. source localization of motor task related synchronized beta activity ('beta-rebound') (Jurkiewicz et al., 2006), during tACS was possible using the previously described strategy (Soekadar et al., 2013a), a fast Fourier transform (FFT) of reconstructed source activity showed a large spectral power peak at the stimulation frequency, however, as well as broadband noise distorting the physiological signal (Fig. 2A). This suggested that noise cancelling features of Synthetic Aperture Magnetometry (SAM) beamforming and possibly all linearly constrained minimum variance (LCMV) beamformers fail to reliably distinguish between physiological brain activity and tACS-dependent artifacts, particularly at the FOI. Besides that tACS artifacts are not reliably removed from LCMV beamformer reconstructed source activity (Figs. 2A,B,C), linear transformation of that signal with the aim to remove the stimulation artifact, e.g. baseline normalization or template subtraction, does not take any non-linear components of the tACS artifact into account and may thus lead to misinterpretation of data processed in such way.

Here we introduce and evaluate a new experimental protocol that solves this problem and allows for mapping of entrained brain oscillations at millimeter precision. To avoid contamination of the FOI by FOS (Fig. 2A), the amplitude of a high frequency carrier signal far beyond FOI (e.g. >150 Hz) was purposefully modulated at FOI (e.g. 1 Hz, 11 Hz or 23 Hz) (Fig. 1B), so that the carrier signal's frequency components and its sideband do not contaminate the frequency bands of physiological oscillations (i.e. 0–150 Hz). The frequency of the AC component in such stimulation protocol is, in contrast to the classical tACS protocol, not identical with the FOI, but oscillates at a considerably higher frequency beyond the physiological bands of interest. In both stimulation protocols, DC-offset over time remains zero.

Based on previous animal studies showing FOI-specific neuronal responses to the amplitude-modulated stimulation (Beason and Semm, 2002) up to the cortical levels of both auditory and visual systems (Middleton et al., 2006) and rectification of signal envelopes that was attributed to non-linear properties of neural cell membranes (Goldman, 1943; Bawin et al., 1975), we reasoned that amplitude-modulated tACS might be a viable strategy to modulate and entrain

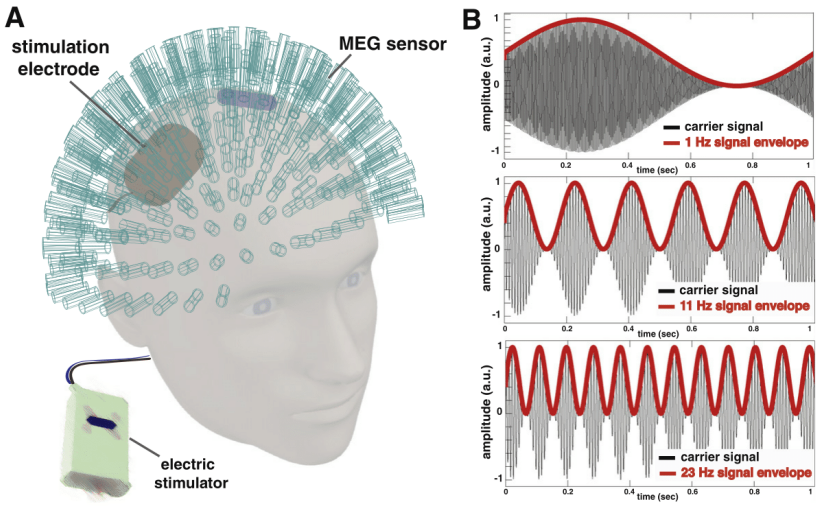

Fig. 1. A: Experimental setup. A 275-sensor whole-head magnetoencephalography (MEG) was used to record neuromagnetic activity while alternating current (AC) was delivered via two radiotranslucent electrodes. B: Illustration of the stimulator output signal during amplitude modulated transcranial alternating current stimulation (tACS). Amplitude of a carrier signal (here a 220 Hz signal) was modulated at 1 Hz, 11 Hz and 23 Hz generating a signal envelope at the frequency of interest (FOI).

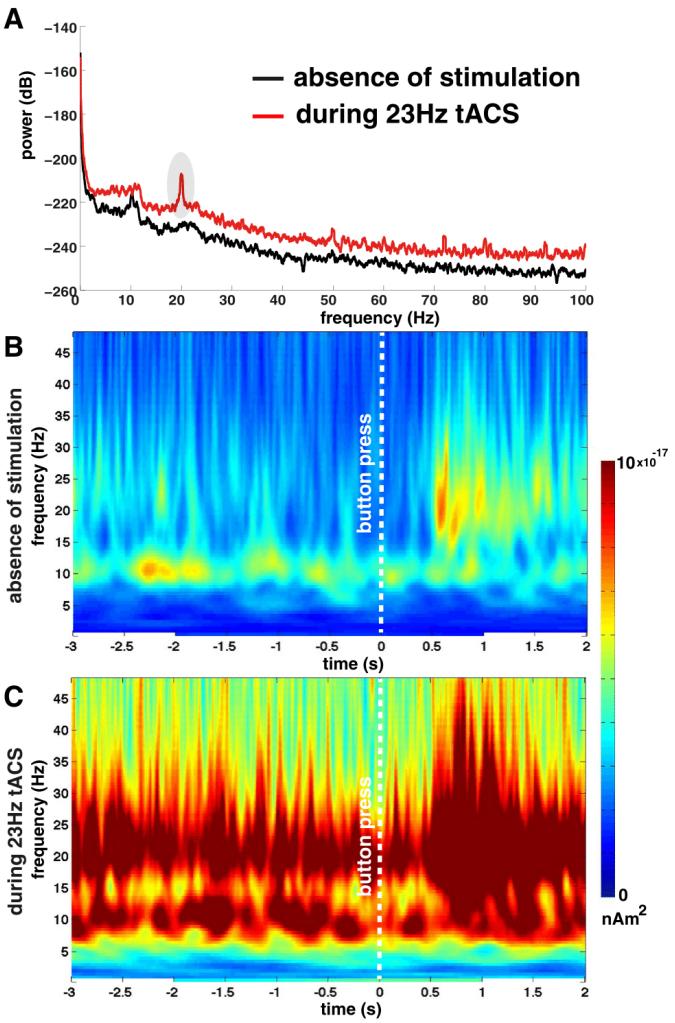

Fig. 2. A: Frequency spectrum of source reconstructed brain oscillatory activity of the primary motor cortex (M1) in absence and during 23 Hz tACS while a healthy volunteer engaged in a self-paced button press task. Stimulation is associated with increase in broadband noise and results in a stimulation artifact at frequency of interest (FOI). B: Time frequency representation (TFR) of the reconstructed source in absence of stimulation. Note the alpha synchronization before and the beta rebound activity after button press. C: During 23 Hz tACS, reconstructed signals are substantially distorted, particularly at FOI. As linear transformations of the signal e.g. baseline normalization does not eliminate any non-linear components of the tACS, data processed in such way may lead to misinterpretations as stimulation artifacts and brain oscillatory activity cannot be discriminated correctly.

neural activity at FOI while avoiding artifact contamination of the FOI and physiological frequency bands <150 Hz.

It was unclear, though, whether beamformer-based spatial filtering could be used to achieve artifact-free source reconstruction of brain oscillations during tACS documenting reliable distinction between a given signal source and stimulator-dependent artifacts, and importantly, whether amplitude-modulated tACS would indeed result in entrainment of brain oscillations that could be mapped at millimeter precision.

To test whether such stimulation protocol allows for artifact-free source reconstruction, a phantom head model was used across three MEG sessions in which a dipole signal source oscillating at different FOIs (session 1 = 1 Hz, session 2 = 11 Hz, session 3 = 23 Hz) was active at a fixed position while different forms of tACS were applied. Source space analysis was performed on data recorded in absence (condition 1) and during amplitude-modulated tACS delivered at 1 Hz (condition 2A), 11 Hz (condition 2B) and 23 Hz (condition 2C) for each session.

Deviation in localization of artificial source activity from the known position of the dipole signal source were computed and compared between sessions and conditions. To test for reliability of source reconstruction across sessions and conditions, coherence values between the reconstructed source activity and known dipole activity in absence and during tACS were compared.

To evaluate precision of localizing phase-locked activity during tACS, phases of the oscillating dipole and tACS signal were synchronized and drop in phase-lock value (PLV) (Eugenio et al., 1999) as function of distance from the known fixed dipole position (at 0 mm, 5 mm, 10 mm, 15 mm, 20 mm, 25 mm, 75 mm) assessed.

Finally, four healthy human volunteers were invited to two sessions in which MEG was recorded in absence (condition 1) and during tACS applied to their primary motor cortex (M1) while they engaged in a self-paced button press task. Depending on the session, tACS was applied at alpha frequency (condition 2A = 11 Hz) or beta frequency (condition 2B = 23 Hz). M1 time-frequency representations (TFR) of physiological frequency bands (δ, θ, α, β, γ_1, γ_2) were computed (Fig. 4) and compared between conditions to evaluate feasibility of artifact-free reconstruction of physiological frequency bands. To rule out that the 220 Hz carrier signal would influence oscillatory brain activity, a control experiment was conducted in which 220 Hz tACS was applied without amplitude modulation. As a last step, whole-head mapping of tACS entrained brain oscillations was performed to evidence capability of this new approach to identify brain regions in which endogenous brain oscillations follow the tACS signal's phase (Fig. 5).

Materials and procedures

Localization and reconstruction of source activity in absence and during tACS using a phantom ('study 1')

Magnetoencephalography (MEG)

All studies were performed using a 275-channel whole head MEG system (CTF Systems Inc., Port Coquitlam, Canada) situated in a magnetically shielded room (Vakuumschmelze GmbH, Hanau, Germany). Magnetic signals were recorded at 584 Hz with a bandwidth of 0–150 Hz. Synthetic 3rd gradient balancing was used to remove online background noise.

Phantom dipole model

A spherical phantom head (CTF/MISL phantom, CTF Systems Inc., Port Coquitlam, Canada) with a diameter of 13 cm containing two electrodes and filled with a saline electrolyte solution was used to generate an electric dipole oscillating at a fixed location relative to the center of the sphere (coordinates [−40 mm, 0 mm, 25 mm] according to the right/anterior/inferior, RAI, reference system). The dipole-generating electrodes had an inter-electrode distance of 4 mm. The dipole signal was set to oscillate at different frequencies (1 Hz, 11 Hz and 23 Hz) and changed its amplitude from 3 to 10 nAm^2 source strength to resemble physiological task-related changes of human brain oscillatory activity.

Transcranial alternating current stimulation (tACS)

Alternating current (AC) was applied to the phantom head using a commercial stimulator (NeuroConn GmbH, Ilmenau, Germany). A conductive paste (Ten20®, D.O. Weaver, Aurora, CO, USA) was applied to the surface of the phantom maintaining impedance between the stimulating electrodes within a range of 10–12 kΩ. Radiotranslucent stimulator electrodes were placed in a bipolar montage over C4 and P3 according to the International 10–20 system, and had a size of 4 × 7 cm. The battery-driven stimulator device was located outside the magnetically shielded room and delivered electric currents via a twisted pair of wires with an intensity of 1 mA. For stimulation, AC was applied at 220 Hz and modulated in amplitude by 1 mA at 1 Hz (condition 2A), 11 Hz (condition 2B) and 23 Hz (condition 2C) (Fig. 1B). Accordingly, the resulting stimulator output had signal envelopes at 1 Hz, 11 Hz and 23 Hz that were co-registered and saved by the MEG acquisition system.

Localization and reconstruction of dipole activity

MEG source analysis was performed for data recorded in absence (condition 1) and during tACS (condition 2) using Synthetic Aperture Magnetometry (SAM) beamforming (Robinson and Vrba, 1999).

Assessment of precision in localizing the phantom's dipole oscillating at 1 Hz (session 1), 11 Hz (session 2) or 23 Hz (session 3) during tACS modulated at 1 Hz (condition 2A), 11 Hz (condition 2B) and 23 Hz (condition 2C) involved three different processing steps. First, a dual-state (contrast) SAM analysis was applied by calculating signal source power of two different time windows: of a 'baseline window' ranging from 1 s and 2 s relative to a trigger signal and of an 'active window' ranging from −1 s to 0 s relative to the trigger signal. Signal source power was estimated at 5 mm resolution on a regular three-dimensional grid throughout the phantom head modeled as single sphere. To identify the location of the voxel with the most significant amplitude change, a non-parametric U-test between both time windows was performed.

To reconstruct source activity, SAM was applied at the estimated source location using the whole time series for estimating global signal source power. Before applying SAM beamformer signals were filtered from 0 to 30 Hz using Butterworth bandpass filter. To investigate whether tACS-related artifacts, particularly at the FOI, distort the reconstructed source signal, a time-frequency analysis of the reconstructed signals was performed for each session and condition using a multitaper spectral method (Mitra and Pesaran, 1999) implemented in Fieldtrip (Oostenveld et al., 2011) that included frequencies between 0.5 to 150 Hz.

Assessing precision of localization and reliability of source reconstruction

Precision of source localization was measured as the deviation in millimeters (mm) of the estimated source location from the fixed known position of the simulated dipole. To test whether localizations differed between sessions and conditions, a two-way repeated measures ANOVA with 'session' as between-subject factor and 'condition' as within-subject factor was applied. To compare reliability of source reconstruction in absence (condition 1) and during tACS delivered at different frequencies (conditions 2A, 2B and 2C), coherence values between the reconstructed source activity and the actual simulated dipole activity (Soekadar et al., 2013a) were computed for each session and condition using the following equation:

$$C_{xy}(f) = \frac{|P_{xy}(f)|^2}{P_{xx}(f)P_{yy}(f)}$$

where P_{xy} is the cross power spectral density, and P_{xx} and P_{yy} the power spectral density of each signal, x and y, respectively.

To test whether tACS had an impact on coherence values, a two-way repeated measures ANOVA with 'session' as between-subject factor and 'condition' as within-subject factor was performed. Post-hoc t-tests were used when applicable. P-values were corrected for multiple comparisons using FDR. For all statistical tests, the significance level was set to $p < 0.05$.

Localization of tACS phase-locked activity

To assess the accuracy of localizing an oscillating signal that is phase-locked to tACS when using SAM beamforming, phase locking value (PLV) (Eugenio et al., 1999) was used to estimate the temporal variability of phase differences between the reconstructed dipole signal's time series at each voxel and the synchronized stimulator output signal envelope's time series.

The phase information of these signals was obtained by spectrally decomposing the signal at the frequency of interest (FOI) to estimate the instantaneous phase for each time point. A Hilbert transform was

used to estimate the instantaneous phase. Given that the electric dipole and tACS envelope signals were synchronized, decrease of PLV at the coordinates of the known dipole signal would document the impact of the signal processing strategy and other systematic factors like sensor noise on the validity of phase reconstruction using SAM beamforming. Furthermore, drop in PLV as function of distance reflects the spatial resolution of the applied strategy to identify phase-locked signal sources.

The time averaged PLV was computed using the following equation:

$$PLV = \frac{1}{N}\left|\sum_{n=1}^{N} e^{i(\Phi_{sa}(n) - \Phi_{stim}(n))}\right|$$

where N is the number of sampled time points, Φ_{stim} and Φ_{sa} are the instantaneous phase values at the time points *n* of the stimulator's output signal envelope (*stim*) and the reconstructed source activity (*sa*), respectively. The PLV can reach values between 0 and 1. Values close to 0 indicate a random signal phase relationship, while values close to 1 indicate a fixed signal phase relationship.

To assess precision of PLV-based mapping, tACS phase-locked activity was localized under different stimulation conditions (1 Hz, 11 Hz, 23 Hz) and activity evaluated as function of distance from the artificial dipole's known source location at 5 mm, 10 mm, 15 mm and 20 mm distance. For comparison of localization of tACS phase-locked activity between stimulation conditions, a one-way ANOVA was applied. To evaluate the effect of distance on PLV values, a one-way within subjects repeated-measures ANOVA was applied with 'distance' (0 mm, 5 mm, 10 mm, 15 mm, 20 mm, 25 mm, 75 mm) as within-subject factor and 'condition' (1 Hz, 11 Hz, 23 Hz) as between-subject variable.

Localization and reconstruction of physiological source activity during tACS ('study 2')

Study participants

Four healthy human volunteers (3 male, 1 female, age 30 ± 3.6 years, all right-handed) without a history of neurological or psychiatric disorders were invited to two MEG sessions on two consecutive days. The study was approved by the ethics committee of the Medical Faculty at the University of Tübingen. Before entering the study, written informed consent was obtained by all participants. Before the first MEG measurement, location of the abductor pollicis brevis (APB) muscle's motor cortical representation in the primary motor cortex (M1) was assessed by single pulse transcranial magnetic stimulation (TMS) according to Rossini et al. (1994). The APB's motor 'hot spot' was identified by detecting the most excitable stimulation site eliciting maximum APB motor evoked potentials (MEPs) at rest. For TMS, a single-pulse TMS system (Magstim 200®, Withland, UK) with a figure-of-eight coil was used. The APB 'hot spot' was marked with a water-resistant skin marker allowing precise placement of the tACS electrode centered above the M1 hand-knob area. Three fiducial localization coils were placed at the nasion and pre-auricular points (right and left) to determine the head position in real time during MEG recordings. Before each measurement, coil positions were photographed for offline co-registration of the recorded MEG data with structural T1 magnetic resonance (MR) images assessed in a separate MR session.

Anatomical magnetic resonance imaging (MRI)

A cranial MRI exam in a 3-Tesla whole body scanner with a 12-channel head coil (Magnetom Trio®, Siemens, Erlangen, Germany) was acquired while the participants were placed supine in the scanner. Vitamin E capsules served as radiological markers for the nasion and pre-auricular points corresponding to locations used for MEG head localization. To minimize movement, the subject's head was secured on either side within the MRI head coil by means of two pieces of foam rubber. T1-weighted structural MRI scans of the whole brain were obtained using an MPRAGE sequence (matrix size = 256 × 256, 160 partitions, 1 mm^3 isotropic voxels, TA = 5:17 m, TR = 2300 ms, TE = 3.93 ms, flip angle = 8°, FOVRO = 256, FOVPE = 224, PAT = 2, PAT mode = GRAPPA) and were used as anatomical reference for corregistration with functional data.

Transcranial alternating current stimulation (tACS)

The same AC stimulator device was used as in study 1. Before the MEG sessions, stimulation electrodes were placed in a bi-cephalic montage (in which one electrode was placed over the right M1 and the other electrode over the left parietal cortex) with an inter-electrode distance of 8–10 cm depending on the head size (Fig. 1). For stimulation, amplitude-modulated tACS at 11 Hz (condition 2A) and 23 Hz (condition 2B) was applied in analogy to study 1. To avoid possible discomfort during the onset of tACS, stimulation current was gradually ramped up from 0 to 1 mA over 10 s and kept constant during the stimulation.

Recording of neuromagnetic activity during a motor task using magnetoencephalography (MEG)

Participants were seated comfortably inside the shielded MEG room and were asked to perform a self-paced button press task, in which they had to press a button with the left index finger every 8 to 12 s at their own volition. Participants were asked to keep their eyes open throughout the sessions and to minimize head and body movements. After a screening run lasting 4 min that included approximately 20 button presses, data were recorded either in absence of stimulation (condition 1) or during tACS (condition 2A and 2B) for approximately 20 min in each session (including approximately 120 button presses). Each condition consisted of two blocks with durations of approximately 8 min that were terminated once 60 button presses were reached.

Localization and reconstruction of physiological source activity

For localization of motor task-related synchronized beta activity ('beta-rebound'), a dual-state SAM analysis was applied in analogy to study 1 using a 'baseline window' ranging from −1 s and 0 s relative to voluntary button presses and an 'active window' ranging from 1 s to 2 s relative to the button presses. Mean power activity was estimated at 5 mm resolution per voxel on a regular three-dimensional grid using a single shell head model (Nolte, 2003). The covariance matrix was estimated based on the entire time-series. Before application of SAM beamforming, data was filtered from 15–30 Hz using a Butterworth bandpass filter. Motor task related source activity was averaged across all trials, co-registered with the anatomical MR images and voxels showing significant increase of beta-synchronization were then displayed using AFNI (Cox, 1996).

After localization, source reconstruction was performed in analogy to study 1 using the SAM beamforming approach. Finally, a time-frequency analysis of the reconstructed signal from the estimated voxel with highest task-related beta synchronization was performed for data recorded in absence (condition 1) and during tACS (condition 2A and 2B) using Fieldtrip (Oostenveld et al., 2011).

To test for reliability of source localization across different conditions, a one-way repeated measures ANOVA with 'condition' as within-subject factor was applied to the identified coordinates of task-related synchronized beta activity. To compare reliability of reconstructing source activity in absence (condition 1) and during tACS (condition 2A and 2B), mean power across different frequency bands (δ = 0–4 Hz, θ = 4–8 Hz, α =

Table 1
Deviation (in mm) of localized signal source from fixed know dipole location (study 1).

Session	Condition 1 tACS off	Condition 2A tACS on (1 Hz)	Condition 2B tACS on (11 Hz)	Condition 2C tACS on (23 Hz)
1 (1 Hz)	1.667 ± 2.887	1.667 ± 2.887	5.000 ± 5.000	3.333 ± 5.773
2 (11 Hz)	3.333 ± 2.887	9.024 ± 1.691	5.000 ± 0.000	3.333 ± 2.886
3 (23 Hz)	3.333 ± 2.887	1.667 ± 2.887	3.333 ± 2.886	8.333 ± 2.888
mean	2.778	4.119	4.444	5.000
std	2.887	2.488	2.629	3.849

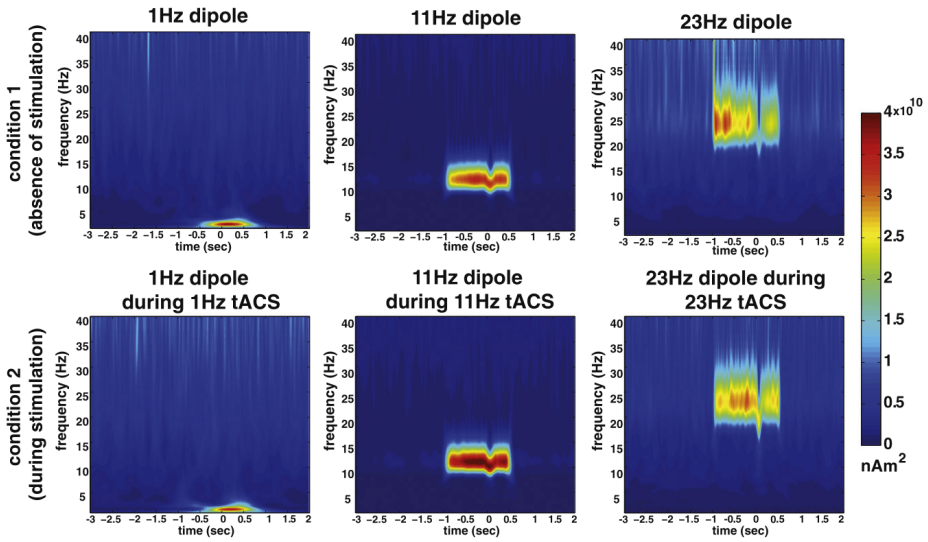

Fig. 3. Time frequency representation (TFR) of source-reconstructed activity using a phantom model with an artificial dipole oscillating at 1 Hz, 11 Hz and 23 Hz in absence of stimulation (condition 1, upper panels) and while transcranial alternating current was applied at 1 Hz, 11 Hz and 23 Hz (lower panels). TFRs evidenced artifact-free reconstruction of signal sources during stimulation.

8–15 Hz, $\beta = 15–30$ Hz, $\gamma_1 = 30–60$ Hz, $\gamma_2 = 60–150$; averaged window: −4 to 2 s. relative to button press) were computed and compared between conditions using a one-way ANOVA. Post-hoc t-tests were used when applicable. To rule out that the 220 Hz carrier-signal would influence brain oscillatory activity across physiological frequency bands, mean power of MEG data recorded in absence (condition 1) and during application of 220 Hz tACS without amplitude modulation (condition 2) while participants performed the same task as in 'study 2' was computed for each frequency band(δ–γ_2) and compared using Student's t-tests for paired samples ('control experiment'). Across all statistical tests, p-values were FDR corrected and significance level set to $p < 0.05$.

Mapping of entrained brain oscillations

To map entrained oscillating signal sources during 23 Hz tACS delivered over M1, PLV was computed in analogy to study 1 for the whole brain. To identify tACS-specific increase in PLV, a simulated 23 Hz sine wave was used as a reference signal in absence of stimulation. Entrained oscillating signal sources were identified by applying a paired-samples t-test on each voxel's PLV calculated for condition 1 (absence of stimulation) and condition 2B (23 Hz tACS). The statistical maps were computed for each participant separately. The recorded data was segmented into epochs overlapping by 20 s. Statistical comparison between PLV values reached during condition 1 and condition 2 was performed using AFNI (Cox, 1996). Results were corrected for multiple comparisons using a family-wise error (FEW) threshold set to $p < 0.05$. As a last step, topographic images from superior and lateral viewpoints were generated highlighting voxels with significant PLV increase under 23 Hz tACS. PLV values for these voxels were color-coded using SUMA (Saad and Reynolds, 2012) (Fig. 6).

Results

Localization and reconstruction of source activity in absence and during tACS using a phantom ('study 1')

Localization and reconstruction of dipole activity during tACS

Mean average deviation in localization of source activity (oscillating at 1 Hz, 11 Hz and 23 Hz) from the known fixed location of the artificial dipole signal was 2.78 ± 2.89 mm in absence of stimulation (condition 1), and 4.12 ± 2.48 mm (condition 2A), 4.44 ± 2.63 mm (condition 2B) and 5.00 ± 3.85 mm (condition 2C) (Table 1).

A two-way repeated-measures ANOVA showed no significant main effect for 'session' ($F(2, 4) = 0.966$, $p = 0.454$) and 'condition' ($F(3, 6) = 2.156$, $p = 0.194$), and no interaction ($F(6, 12) = 1.68$, $p = 0.201$) indicating that neither frequency of source activity nor stimulation condition influenced source localization.

Time-frequency representations of reconstructed source activity showed the expected activity of the artificial dipole source oscillating

Table 2
Coherence value between reconstructed signal in absence of stimulation and during modulated tACS.

Session	Condition 1 tACS off	Condition 2A tACS on (1 Hz)	Condition 2B tACS on (11 Hz)	Condition 2C tACS on (23 Hz)
1 (1 Hz)	0.9883 ± 0.0033	0.9861 ± 0.0035	0.9881 ± 0.0029	0.9882 ± 0.0029
2 (11 Hz)	0.9890 ± 0.0010	0.9878 ± 0.0038	0.9899 ± 0.0029	0.9867 ± 0.0029
3 (23 Hz)	0.9870 ± 0.0035	0.9896 ± 0.0029	0.9869 ± 0.0029	0.9884 ± 0.0029
mean	0.9881	0.9878	0.9883	0.9878
std	0.0026	0.0034	0.0029	0.0029

at 1 Hz, 11 Hz and 23 Hz under all stimulation conditions (Fig. 3), and did not evidence any stimulation-dependent distortions, particularly at the FOI.

Averaged coherence values between reconstructed time-series and actual dipole activity across sessions were 0.9881 ± 0.0026 under condition 1 (absence of stimulation) and 0.9878 ± 0.0034 under condition 2A (1 Hz tACS), 0.9883 ± 0.0029 under condition 2B (11 Hz tACS) and 0.9878 ± 0.0029 mm under condition 2C (23 Hz tACS) (Table 2). A two-way repeated-measures ANOVA showed no main effect for 'session' ($F(2, 4) = 0.145$, $p = 0.866$) and 'condition' ($F(3, 6) = 0.059$, $p = 0.981$) and no interaction ($F(6, 12) = 0.712$, $p = 0.643$) indicating that coherence of source reconstruction was not influenced by the frequency of source activity or stimulation.

Accuracy of localizing tACS phase-locked activity

Mean deviation in localizing tACS phase-locked source activity was 5.69 ± 5.14 mm under condition 2A (1 Hz), 5.00 ± 0.00 mm under condition 2B (11 Hz) and 7.35 ± 2.51 mm under condition 2C (23 Hz). A one-way ANOVA indicated that 'condition' had no significant effect on the localization of tACS phase-locked activity ($F(2, 4) = 0.311$, $p = 0.749$).

Evaluation of drop in tACS phase-locked activity as function of distance from the artificial dipole's known source location using a one-way within subjects repeated-measures ANOVA showed a main effect for 'distance' ($F(5, 10) = 42{,}87$, $p < 0.001$). Post-hoc t-tests indicated a significant drop of PLV at 5 mm ($p < 0.001$) and further distances across all sessions (Fig. 4). Drop of PLV followed an exponential function with a maximum decrease between 0 and 5 mm underlining that localization of tACS phase-locked activity is precise (Table 3).

75 0.0856 ± 0.0016 0.0658 ± 0.0286 0.0207 ± 0.0066

Localization and reconstruction of physiological source activity during tACS ('study 2')

Motor-task related beta-synchronization ('beta rebound') under condition 1 and condition 2 was reliably localized in right M1 (Fig. 4), and showed minimal variation across conditions (condition 1 vs. condition 2A: 0.90 ± 0.47 mm, condition 1 vs. condition 2B: 1.51 ± 0.81 mm) (Table 4).

A one-way repeated measures ANOVA showed that coordinates of physiological beta-source activity across stimulation conditions were not different across conditions (x-coordinate: $F(2, 11) = 0.34$, $p = 0.72$; y-coordinate: $F(2, 11) = 0.05$, $p = 0.95$; and z-coordinate: $F(2, 11) = 1.97$, $p = 0.22$).

Time-frequency representations in absence (condition 1) and during tACS (conditions 2A and 2B) showed typical alpha desynchronization preceding button presses and beta synchronization after button presses (Fig. 5).

A one-way repeated measures ANOVA showed no significant effect in any of the frequency bands (δ: $F(2, 11) = 0.61$, $p = 0.56$; θ: $F(2, 11) = 0.16$, $p = 0.85$; α: $F(2, 11) = 0.11$, $p = 0.90$; β: $F(2, 11) = 0.22$, $p = 0.81$; γ_1: $F(2, 11) = 0.3$, $p = 0.75$; γ_2: $F(2, 11) = 0.21$, $p = 0.81$).

Evaluation of the control experiment in which 220 Hz tACS was applied in analogy to study 2, but without amplitude modulation, did not indicate any significant effect of such stimulation in any of the physiological frequency bands (δ: $p = 0.23$; θ: $p = 0.26$; α: $p = 0.31$; β: $p = 0.32$; γ_1: $p = 0.45$; γ_2: $p = 0.37$). Time-frequency representations in absence (condition 1) and during 220 Hz tACS (condition 2) did not show any stimulation artifacts and were comparable to TFRs recorded in study 2 (Supplementary data, Fig. S1).

Mapping of entrained brain oscillations in healthy human volunteers

Mapping of entrained brain oscillations using PLV showed alignment of the neuromagnetic source activity's and the tACS signal's phase in brain areas immediately underneath and in proximity to the stimulation electrodes. These included the right pre- and post-central gyri as well as the right inferior parietal gyrus neighboring the stimulation electrode placed over the right M1, and left precuneus and superior parietal lobule close to the left parietal stimulation electrode (Fig. 6).

Table 3
PLV values of source activity at different distances from the reconstructed source of the artificial dipole signal.

Distance relative to known dipole source (in mm)	Dipole oscillating at 1 Hz	Dipole oscillating at 11 Hz	Dipole oscillating at 23 Hz
0	0.9914 ± 0.0084	0.9320 ± 0.0875	0.9984 ± 0.0013
5	0.5596 ± 0.0081	0.5248 ± 0.0544	0.6571 ± 0.0009
10	0.3872 ± 0.0057	0.4463 ± 0.0404	0.4533 ± 0.0028
15	0.2660 ± 0.0045	0.4443 ± 0.0265	0.3513 ± 0.0052
20	0.2224 ± 0.0037	0.4230 ± 0.0180	0.2948 ± 0.0072
25	0.1964 ± 0.0031	0.4036 ± 0.0084	0.2566 ± 0.0085
75	0.0856 ± 0.0016	0.0658 ± 0.0286	0.0207 ± 0.0066

Discussion

Besides evidencing that amplitude-modulated tACS has electrode site-specific effects and can be used for frequency-specific entrainment of brain oscillations, this study showed successful cortical mapping of entrained brain oscillations during tACS. After validation of reliable localization as well as stimulator artifact-free reconstruction of source

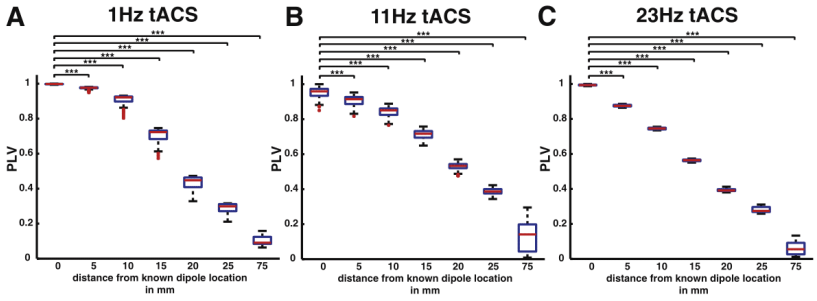

Fig. 4. Spatial resolution of localizing tACS phase-locked activity across different stimulation frequencies. Decrease of phase lock values (PLV) between the synchronized tACS signal and artificial electric dipole signal is shown as a function of distance at 0, 5, 10, 15, 20, 25 and 75 mm from the known dipole location. Drop in PLV at 5 mm distance from the known dipole location was highly significant following an exponential function for further distances. Drop in PLV is shown for 1 Hz (A), 11 Hz (B) and 23 Hz (C).

Table 4
Coordinates of motor-task related beta-synchronization across conditions and participants, and deviations (*d*) in mm from coordinates localized in absence of stimulation. Condition 1 = absence of stimulation; condition 2A = 11 Hz tACS; condition 2B = 23 Hz tACS.

Condition	Participant	x	y	z	*d*
1	1	0	−3.75	9.25	–
1	2	1.25	−5.25	7.25	–
1	3	0.25	−2.75	11.5	–
1	4	0	−4.25	9.75	–
2A	1	0.25	−3.75	8.75	0.559
2A	2	0.75	−4.25	8	1.346
2A	3	0.25	−3.5	10.5	1.250
2A	4	0.25	−4	9.5	0.433
2B	1	−0.25	−3.5	8.25	1.061
2B	2	−0.5	−4.25	7.5	2.031
2B	3	1.25	−4.25	10	2.345
2B	4	−0.25	−3.75	9.5	0.612

activity during amplitude-modulated tACS in a phantom model, we showed millimeter-precise localization of phase-locked activity dropping exponentially as a function of distance from a known signal source. In a second study, whole-head MEG was recorded during application of 23 Hz tACS delivered over the motor cortex of four healthy human volunteers engaging in a voluntary finger-tapping task. Time-frequency analysis of brain oscillations evidenced complete cancellation of tACS-related artifacts at FOI up to high-gamma band oscillations (0–150 Hz). Amplitude-modulated tACS entrained brain oscillations underneath and in proximity of the stimulation electrodes as measured by PLV that could be precisely mapped.

While amplitude modulation at FOI (1 Hz, 11 Hz, 23 Hz) was performed in this specific setup using a carrier frequency of 220 Hz, any other carrier frequency could be also chosen. It is unknown, though, whether the carrier signal itself exerts an effect on brain physiology and whether such effect would depend on the carrier signal's frequency, an issue to be investigated in future studies. It was shown, for example, that transcranial high frequency stimulation in the ripple range (140 Hz) applied over M1 can influence the amplitude of motor evoked potential (MEP) (Moliadze et al., 2010), which was similarly shown for stimulation at 250 Hz, but with a less pronounced and persistent effect. While we could not find any influence of the 220 Hz carrier signal on brain oscillatory activity ranging from 0–150 Hz, possible physiological effects of such high-frequency stimulation cannot be entirely ruled out. Given the maximum slew rate of the MEG system used in this investigation (CTF MEG® by MISL, Coquitlam, Canada) that translates into a theoretical boundary of 6.13×10^3 nT/s for the application of an oscillating magnetic field (Soekadar et al., 2013a, Supplementary Material), use of carrier signals above 220 Hz seem theoretically possible and their applicability should be investigated in subsequent studies.

While our study showed frequency-specific entrainment of brain oscillations at FOI in cortical areas close to the stimulation electrodes, it is possible that mechanisms underlying effects of classical tACS are different from those underlying amplitude-modulated tACS. Amplitude modulation is very common in biological systems shown to be important e.g. in neural transmission and processing in the somatosensory (Lundstrom et al., 2010), visual (Grosof et al., 1993; Mareschal and Baker, 1998) or auditory domain (Giraud and Poeppel, 2012). While the mechanisms underlying the effects elicited by classical tACS are still not well understood, they were mostly attributed to modifications of synaptic activity related to accumulation of calcium ions in the presynaptic nerve terminals leading to short-term synaptic plasticity effects (Citri and Malenka, 2008; Antal and Paulus, 2013). In contrast, entrainment of brain oscillatory activity by a signal envelope, which contains no power at the FOI, requires non-linear operations such as rectification (Rice, 1954). It was shown that neural cell membranes exhibit properties of non-linear asymmetrical systems and can thus perform such operations (Goldman, 1943). While the biological substrate is not entirely clear, this property may be mediated by configurational changes of membrane proteins resulting in modifications of ionic binding sites and membrane permeability as shown for high-frequency electromagnetic fields modulated in amplitude at brain wave frequencies, e.g. 16 Hz (Bawin et al., 1975). Besides resulting in calcium efflux, such protocol also influenced receptor binding of neurotransmitters, such as GABA, acetylcholine and glutamate (Kolomytkin et al., 1994).

The cellular basis for further processing of the rectified envelope signal could attribute to two-cell networks consisting of an interneuron connected to a pyramidal cell by means of a slow synapse (Middleton et al., 2006) tuned to a specific envelope frequency. This frequency tuning might explain why tACS-based entrainment is specific for a particular brain area and depends on the similarity in temporal structure of the stimulation signal and endogenous network activity (Ali et al., 2013). Further studies are, however, needed that investigate possible differences in mechanisms underlying the effects of amplitude-modulated tACS and classical tACS on brain oscillations, neuroplasticity and behavior.

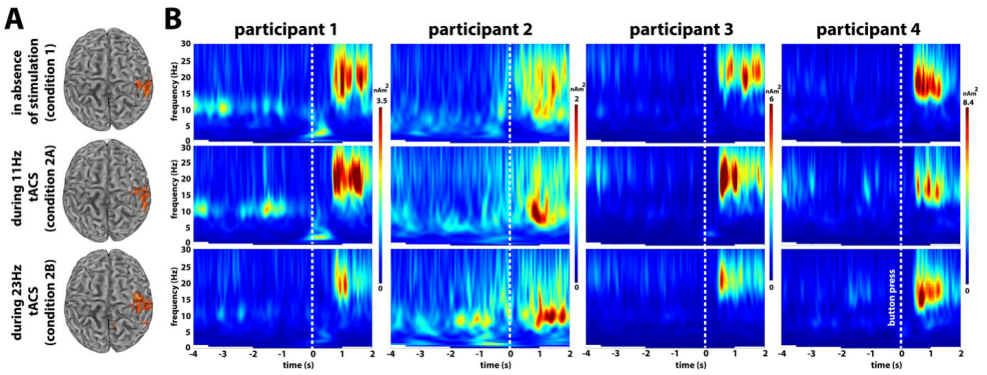

Fig. 5. A) Localization of motor task-related beta rebound in absence (condition 1) and across different transcranial alternating current stimulation (tACS) frequencies (11 Hz, 23 Hz). B) Time-frequency representation of brain oscillatory activity of the right primary motor cortex across participants in absence (upper row, condition 1) and during 11 Hz (middle row, condition 2A) and 23 Hz (lower row, condition 2B) tACS.

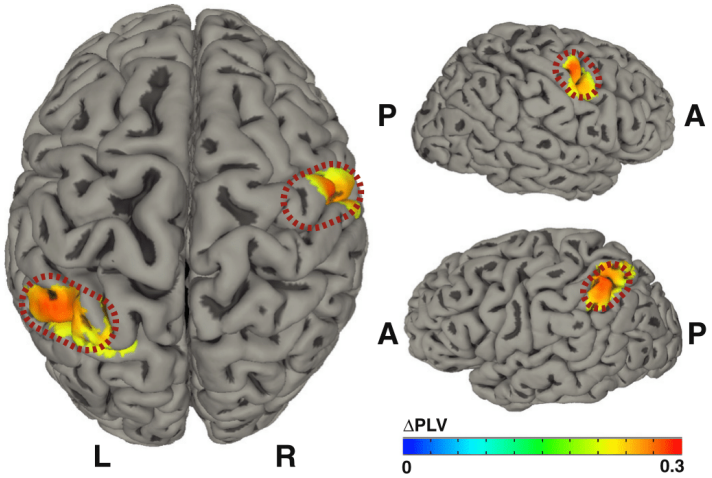

Fig. 6. Topographic map of voxels showing significant increase of phase-lock value (PLV) during amplitude modulated 23 Hz transcranial alternating current stimulation (tACS) delivered over the right primary motor cortex (M1) and contralateral left parietal cortex in contrast to simulated PLV in absence of stimulation. Significant voxels are color-coded indicating the difference in PLV values between the 23 Hz tACS and sham condition (ΔPLV). L = left, R = right, A = anterior, P = posterior.

As pointed out in the introduction, SAM beamforming was insufficient to cancel stimulation artifacts at FOI when tACS was applied as mono-sinusoidal signal. Subsequent linear transformations with the purpose to separate simulator artifacts from the physiological signal may not be sufficient to eliminate non-linear components of the stimulator artifact and lead to misinterpretations. More studies are needed that address this difficulty in depth and compare different solution strategies to identify the optimal approach depending on the exact research question and study hypothesis. Clearly, an approach for frequency-specific entrainment allowing for artifact-free source reconstruction as demonstrated here provides the broadest range of applications as no further processing steps, such as linear transformations or template subtractions, are necessary in pursuing a separation of physiological brain activity and stimulator-dependent non-linear artifacts. Such additional processing steps also limit implementation in real-time applications, e.g. in closed-loop brain stimulation (Liew et al., 2014) or brain-machine interfaces (Soekadar et al., 2013b). Importantly, our results further corroborate previous findings from animal studies (Beason and Semm, 2002) that modulation of brain activity, e.g. entrainment of endogenous brain oscillations, using amplitude-modulated stimulation is possible. While evidencing that the brain tissue underneath and in proximity of the stimulation electrodes exhibited demodulation characteristics (i.e. responsiveness to the envelope signal), a clear physiological effect of 11 Hz and 23 Hz amplitude-modulated tACS on motor-related brain oscillations was not detected in our study. As this may account to the small sample size, sufficiently powered studies addressing such possibility are needed.

Mapping of brain areas showing entrained activity as described here could be used to trace the path of electric currents applied in other NIBS protocols, e.g. direct current (DC) or random noise (RN) stimulation (Paulus, 2011) to complement and corroborate computational models of transcranial current flow. Furthermore, the described protocol allows for identifying factors that influence tACS-related entrainment of brain oscillations, e.g. neuroanatomical, metabolic or functional factors. Having identified such factors, improved computational models predicting stimulation effects or more effective tACS protocols may evolve. In this context, systematic mapping of entrained brain oscillations under varying stimulation parameters, e.g. using electrodes of various sizes or using multiple stimulation electrodes that are distributed over the skull may be useful.

The here introduced and evaluated approach will allow further investigating mechanisms underlying tACS-related effects that cannot be assessed by other non-invasive techniques such as EEG or metabolic neuroimaging, e.g. spike timing dependent plasticity reflected in gamma band responses (Fründ et al., 2009).

Having shown that real-time reconstruction of brain oscillatory activity is possible during tDCS (Soekadar et al., 2013b; Garcia-Cossio et al., 2016), implementation of the described experimental protocol in such real-time paradigm would allow for brain-state dependent (closed-loop) stimulation. Once available, such paradigm could help to further elucidate the causal link between brain oscillatory activity, e.g. slow cortical potentials, sensorimotor rhythms (SMR) or sleep spindles, and brain functions, such as memory (Klimesch et al., 1996), motor (Pfurtscheller et al., 1997; Soekadar et al., 2015) or cognitive functions (Kolev et al., 2001). Beyond this, it is conceivable that implementation of closed-loop tACS during neurofeeback paradigms, e.g. in stroke (Soekadar et al., 2014b) or depression, will lead to novel and more personalized treatment options for neurological and psychiatric disorders and pave the way for the development of non-invasive bidirectional brain-machine (-brain) interfaces (Fetz, 2015).

Supplementary data to this article can be found online at http://dx.doi.org/10.1016/j.neuroimage.2015.10.024.

References

Ali, M.M., Sellers, K.K., Fröhlich, F., 2013. Transcranial alternating current stimulation modulates large-scale cortical network activity by network resonance. J. Neurosci. 33, 11262–11275.

Antal, A., Paulus, W., 2013. Transcranial alternating current stimulation (tACS). Front. Hum. Neurosci. 7, 317.

Bawin, S.M., Kaczmarek, L.K., Adey, W.R., 1975. Effects of modulated VHF fields on the central nervous system. Ann. N. Y. Acad. Sci. 247, 74–81 (No abstract available).

Beason, R.C., Semm, P., 2002. Responses of neurons to an amplitude modulated microwave stimulus. Neurosci. Lett. 333, 175–178.

Brignani, D., Ruzzoli, M., Mauri, P., Miniussi, C., 2013. Is transcranial alternating current stimulation effective in modulating brain oscillations? PLoS One 8, e56589.

Citri, A., Malenka, R.C., 2008. Synaptic plasticity: multiple forms, functions, and mechanisms. Neuropsychopharmacology 33, 18–41 (Review).

Cox, R.W., 1996. AFNI: software for analysis and visualization of functional magnetic resonance neuroimages. Comput. Biomed. Res. 29, 162–173.

Curio, G., Mackert, B.M., Burghoff, M., Neumann, J., Nolte, G., Scherg, M., Marx, P., 1997. Somatotopic source arrangement of 600 Hz oscillatory magnetic fields at the human primary somatosensory hand cortex. Neurosci. Lett. 234, 131–134.

Eugenio, J.P.L., Rodriguez, E., Martinerie, J., Varela, F.J., 1999. Measuring phase synchrony in brain signals. Hum. Brain Mapp. 8, 194–208.

Fetz, E.E., 2015. Restoring motor function with bidirectional neural interfaces. Prog. Brain Res. 218, 241–252.

Fründ, I., Ohl, F.W., Herrmann, C.S., 2009. Spike-timing-dependent plasticity leads to gamma band responses in a neural network. Biol. Cybern. 101, 227–240.

Garcia-Cossio, E., Witkowski, M., Robinson, S.E., Cohen, L.G., Birbaumer, N., Soekadar, S.R., 2016. Simultaneous transcranial direct current stimulation (tDCS) and whole-head magnetoencephalography (MEG): assessing the impact of tDCS on slowcortical magnetic fields. Neuroimage 140, 33–40.

Giraud, A.L., Poeppel, D., 2012. Cortical oscillations and speech processing: emerging computational principles and operations. Nat. Neurosci. 15, 511–517.

Goldman, D.E., 1943. Potential impedance, and rectification in membranes. J. Gen. Physiol. 27, 37–60.

Grosof, D.H., Shapley, R.M., Hawken, M.J., 1993. Macaque V1 neurons can signal 'illusory' contours. Nature 365, 550–552.

Helfrich, R.F., Knepper, H., Nolte, G., Strüber, D., Rach, S., Herrmann, C.S., Schneider, T.R., Engel, A.K., 2014. Selective modulation of interhemispheric functional connectivity by HD-tACS shapes perception. PLoS Biol. 12, e1002031.

Joundi, R.A., Jenkinson, N., Brittain, J.S., Aziz, T.Z., Brown, P., 2012. Driving oscillatory activity in the human cortex enhances motor performance. Curr. Biol. 22, 403–407.

Jurkiewicz, M.T., Gaetz, W.C., Bostan, A.C., Cheyne, D., 2006. Post-movement beta rebound is generated in motor cortex: evidence from neuromagnetic recordings. NeuroImage 32, 1281–1289.

Kanai, R., Chaieb, L., Antal, A., Walsh, V., Paulus, W., 2008. Frequency-dependent electrical stimulation of the visual cortex. Curr. Biol. 18, 1839–1843.

Klimesch, W., Schimke, H., Doppelmayr, M., Ripper, B., Schwaiger, J., Pfurtscheller, G., 1996. Event-related desynchronization (ERD) and the Dm effect: does alpha desynchronization during encoding predict later recall performance? Int. J. Psychophysiol. 24, 47–60.

Kolev, V., Yordanova, J., Schürmann, M., Başar, E., 2001. Increased frontal phase-locking of event-related alpha oscillations during task processing. Int. J. Psychophysiol. 39, 159–165.

Kolomytkin, O., Kuznetsov, V., Yurinska, M., Zharikov, S., Zharikova, A., 1994. Response of brain receptor systems to microwave energy exposure. In: Frey, A.H. (Ed.), On the Nature of Electromagnetic Field Interactions with Biological Systems. R.G. Landes Co, Austin, TX, pp. 194–206.

Kotecha, R., Xiang, J., Wang, Y., Huo, X., Hemasilpin, N., Fujiwara, H., Rose, D., deGrauw, T., 2009. Time, frequency and volumetric differences of high-frequency neuromagnetic oscillation between left and right somatosensory cortices. Int. J. Psychophysiol. 72, 102–110.

Liew, S.L., Santarnecchi, E., Buch, E.R., Cohen, L.G., 2014. Non-invasive brain stimulation in neurorehabilitation: local and distant effects for motor recovery. Front Hum Neurosci. 8, 378.

Lundstrom, B.N., Fairhall, A.L., Maravall, M., 2010. Multiple timescale encoding of slowly varying whisker stimulus envelope in cortical and thalamic neurons in vivo. J. Neurosci. 30, 5071–5077.

Mareschal, I., Baker Jr., C.L., 1998. A cortical locus for the processing of contrast-defined contours. Nat. Neurosci. 1, 150–154.

Marshall, L., Helgadóttir, H., Mölle, M., Born, J., 2006. Boosting slow oscillations during sleep potentiates memory. Nature 444, 610–613.

Middleton, J.W., Longtin, A., Benda, J., Maler, L., 2006. The cellular basis for parallel neural transmission of a high-frequency stimulus and its low-frequency envelope. Proc. Natl. Acad. Sci. U. S. A. 103, 14596–14601.

Mitra, P.P., Pesaran, B., 1999. Analysis of dynamic brain imaging data. Biophys. J. 76, 691–708.

Moliadze, V., Antal, A., Paulus, W., 2010. Boosting brain excitability by transcranial high frequency stimulation in the ripple range. J. Physiol. 588, 4891–4904.

Neuling, T., Ruhnau, P., Fuscà, M., Demarchi, G., Herrmann, C.S., Weisz, N., 2015. Friends, not foes: magnetoencephalography as a tool to uncover brain dynamics during transcranial alternating current stimulation. NeuroImage 118, 406–413.

Nolte, G., 2003. 3D imaging, planning, navigation. Minim. Invasive Ther. Allied Technol. 12, 3–4.

Nunez, P.L., 1981. A study of origins of the time dependencies of scalp EEG: ii—experimental support of theory. IEEE Trans. Biomed. Eng. 28, 281–288.

Oostenveld, R., Fries, P., Maris, E., Schoffelen, J.M., 2011. FieldTrip: open source software for advanced analysis of MEG, EEG, and invasive electrophysiological data. Comput. Intell. Neurosci. 2011, 156869.

Papadelis, C., Poghosyan, V., Fenwick, P.B., Ioannides, A.A., 2009. MEG's ability to localise accurately weak transient neural sources. Clin. Neurophysiol. 120, 1958–1970.

Paulus, W., 2011. Transcranial electrical stimulation (tES – tDCS; tRNS, tACS) methods. Neuropsychol. Rehabil. 21, 602–617.

Pfurtscheller, G., Neuper, C., Andrew, C., Edlinger, G., 1997. Foot and hand area mu rhythms. Int. J. Psychophysiol. 26, 121–135.

Poghosyan, V., Ioannides, A.A., 2007. Precise mapping of early visual responses in space and time. NeuroImage 35, 759–770.

Polanía, R., Nitsche, M.A., Korman, C., Batsikadze, G., Paulus, W., 2012. The importance of timing in segregated theta phase-coupling for cognitive performance. Curr. Biol. 22, 1314–1318.

Rice, S.O., 1954. Mathematical analysis of random noise. In: Wax, N. (Ed.), Selected papers on noise and stochastic processes. Dover, New York, pp. 133–294.

Robinson, S., Vrba, J., 1999. Functional neuroimaging by synthetic aperature magnetometry (SAM). In: Yoshimoto, T., Kotani, M., Kuriki, S., Karibe, H., Nakasato, N. (Eds.), Recent advances in biomagnetism. Tohoku University Press, Tohoku, Japan, pp. 302–305.

Rossini, P.M., Barker, A.T., Berardelli, A., Caramia, M.D., Caruso, G., Cracco, R.Q., Dimitrijević, M.R., Hallett, M., Katayama, Y., Lücking, C.H., et al., 1994. Non-invasive electrical and magnetic stimulation of the brain, spinal cord and roots: basic principles and procedures for routine clinical application. Report of an IFCN committee. Electroencephalogr. Clin. Neurophysiol. 91, 79–92.

Saad, Z.S., Reynolds, R.C., 2012. SUMA. NeuroImage 62, 768–773.

Santarnecchi, E., Polizzotto, N.R., Godone, M., Giovannelli, F., Feurra, M., Matzen, L., Rossi, A., Rossi, S., 2013. Frequency-dependent enhancement of fluid intelligence induced by transcranial oscillatory potentials. Curr. Biol. 23, 1449–1453.

Soekadar, S.R., Witkowski, M., Cossio, E.G., Birbaumer, N., Robinson, S.E., Cohen, L.G., 2013a. In vivo assessment of human brain oscillations during application of transcranial electric currents. Nat. Commun. 4, 2032.

Soekadar, S.R., Witkowski, M., Robinson, S.E., Birbaumer, N., 2013b. Combining electric brain stimulation and source-based brain-machine interface (BMI) training in neurorehabilitation of chronic stroke. J. Neurol. Sci. 333-e542.

Soekadar, S.R., Witkowski, M., García Cossio, E., Birbaumer, N., Cohen, L.G., 2014a. Learned EEG-based brain self-regulation of motor-related oscillations during application of transcranial electric brain stimulation: feasibility and limitations. Front. Behav. Neurosci. 8, 93.

Soekadar, S.R., Birbaumer, N., Slutzky, M.W., Cohen, L.G., 2014b. Brain-machine interfaces in neurorehabilitation of stroke. Neurobiol Dis. (in press), pii: S0969-9961(14)00371-4. http://dx.doi.org/10.1016/j.nbd.2014.11.025.

Soekadar, S.R., Witkowski, M., Birbaumer, N., Cohen, L.G., 2015. Enhancing Hebbian Learning to Control Brain Oscillatory Activity. Cereb Cortex 25, 2409–2415.

Suk, J., Ribary, U., Cappell, J., Yamamoto, T., Llinás, R., 1991. Anatomical localization revealed by MEG recordings of the human somatosensory system. Electroencephalogr. Clin. Neurophysiol. 78, 185–196.

Thut, G., Schyns, P.G., Gross, J., 2011. Entrainment of perceptually relevant brain oscillations by non-invasive rhythmic stimulation of the human brain. Front. Psychol. 2, 170.

Voss, U., Holzmann, R., Hobson, A., Paulus, W., Koppehele-Gossel, J., Klimke, A., Nitsche, M.A., 2014. Induction of self awareness in dreams through frontal low current stimulation of gamma activity. Nat. Neurosci. 17, 810–812.

Vossen, A., Gross, J., Thut, G., 2015. Alpha power increase after transcranial alternating current stimulation at alpha frequency (α-tACS) reflects plastic changes rather than entrainment. Brain Stimul. 8, 499–508 (pii: S1935-861X(14)00436-7).

Zaehle, T., Rach, S., Herrmann, C.S., 2010. Transcranial alternating current stimulation enhances individual alpha activity in human EEG. PLoS One 5, e13766.

2.2. TACS phase locking of frontal midline theta oscillations disrupts working memory performance

frontiers in Cellular Neuroscience

ORIGINAL RESEARCH
published: 06 May 2016
doi: 10.3389/fncel.2016.00120

tACS Phase Locking of Frontal Midline Theta Oscillations Disrupts Working Memory Performance

*Bankim S. Chander[1], Matthias Witkowski[1], Christoph Braun[2,3], Stephen E. Robinson[4], Jan Born[5], Leonardo G. Cohen[6], Niels Birbaumer[5] and Surjo R. Soekadar[1,2]**

[1] Applied Neurotechnology Lab, Department of Psychiatry and Psychotherapy, University Hospital of Tübingen, Tübingen, Germany, [2] MEG Center, University Hospital of Tübingen, Tübingen, Germany, [3] CIMeC, Center for Mind/Brain Sciences, University of Trento, Trento, Italy, [4] National Institute of Mental Health (NIMH), MEG Core Facility, Bethesda, MD, USA, [5] Institute of Medical Psychology and Behavioral Neurobiology, University of Tübingen, Tübingen, Germany, [6] National Institute of Neurological Disorders and Stroke (NINDS), Bethesda, MD, USA

Background: Frontal midline theta (FMT) oscillations (4–8 Hz) are strongly related to cognitive and executive control during mental tasks such as memory processing, arithmetic problem solving or sustained attention. While maintenance of temporal order information during a working memory (WM) task was recently linked to FMT phase, a positive correlation between FMT power, WM demand and WM performance was shown. However, the relationship between these measures is not well understood, and it is unknown whether purposeful FMT phase manipulation during a WM task impacts FMT power and WM performance. Here we present evidence that FMT phase manipulation mediated by transcranial alternating current stimulation (tACS) can block WM demand-related FMT power increase (FMTΔpower) and disrupt normal WM performance.

Methods: Twenty healthy volunteers were assigned to one of two groups (group A, group B) and performed a 2-back task across a baseline block (block 1) and an intervention block (block 2) while 275-sensor magnetoencephalography (MEG) was recorded. After no stimulation was applied during block 1, participants in group A received tACS oscillating at their individual FMT frequency over the prefrontal cortex (PFC) while group B received sham stimulation during block 2. After assessing and mapping phase locking values (PLV) between the tACS signal and brain oscillatory activity across the whole brain, FMT power and WM performance were assessed and compared between blocks and groups.

Results: During block 2 of group A but not B, FMT oscillations showed increased PLV across task-related cortical areas underneath the frontal tACS electrode. While WM task-related FMTΔpower and WM performance were comparable across groups in block 1, tACS resulted in lower FMTΔpower and WM performance compared to sham stimulation in block 2.

Conclusion: tACS-related manipulation of FMT phase can disrupt WM performance and influence WM task-related FMTΔpower. This finding may have important implications for the treatment of brain disorders such as depression and attention deficit disorder associated with abnormal regulation of FMT activity or disorders characterized by dysfunctional coupling of brain activity, e.g., epilepsy, Alzheimer's or Parkinson's disease (AD/PD).

Keywords: frontal midline theta (FMT), entrainment, transcranial alternating current stimulation (tACS), magnetoencephalography (MEG), working memory performance

OPEN ACCESS

Edited by:
Hansen Wang,
University of Toronto, Canada

Reviewed by:
Minah Suh,
Sungkyunkwan University, South Korea
Domenica Veniero,
University of Glasgow, UK

****Correspondence:***
Surjo R. Soekadar
surjo.soekadar@uni-tuebingen.de

Received: *07 February 2016*
Accepted: *25 April 2016*
Published: *06 May 2016*

Citation:
Chander BS, Witkowski M, Braun C, Robinson SE, Born J, Cohen LG, Birbaumer N and Soekadar SR (2016) tACS Phase Locking of Frontal Midline Theta Oscillations Disrupts Working Memory Performance. Front. Cell. Neurosci. 10:120. doi: 10.3389/fncel.2016.00120

INTRODUCTION

Brain oscillations reflect rhythmic fluctuations in neuronal excitability modulating long-range communication between cortical and subcortical areas important for cognition and adaptive behavior in humans (Buzsáki and Draguhn, 2004). Cognitive functions such as memory processing (Düzel et al., 2010; Hanslmayr and Staudigl, 2014), arithmetic problem solving (De Smedt et al., 2009) and sustained attention (for review, see Clayton et al., 2015) required for many working memory (WM) tasks were linked to theta (4–8 Hz) and gamma (>30 Hz) frequency oscillations (Buzsáki, 2006) in a subcortical-cortical network that includes the hippocampus and fronto-medial brain regions. Fronto-medial theta (FMT) oscillations (Ishihara and Yoshi, 1972) were particularly attributed to the prefrontal and anterior cingulate cortex (PFC, ACC), the latter being a highly interconnected brain area shown to be involved in various cognitive and executive functions (Beckmann et al., 2009; Vogt, 2009; Cavanagh et al., 2012). Recently, a positive correlation between FMT power and WM demand was shown (Gevins et al., 1997; Jensen and Tesche, 2002; Mitchell and Cusack, 2008; Brookes et al., 2011), but the underlying mechanisms and functional significance of such FMT power increase (FMTΔpower) and its relatedness to FMT phase are still widely unknown (Hsieh and Ranganath, 2014).

While it was shown that the amplitude of brain oscillations that can be assessed as signal (SE) power at a certain frequency, e.g., in the theta band, reflects the number of simultaneously activated neurons, the phase of these brain oscillations provides information about the timing of the underlying neuronal activity (Sauseng and Klimesch, 2008). Thus, FMT power and FMT phase provide complementary information. Recently it was suggested that maintenance of temporal order information, as required e.g., in an *n*-back task, influences the length of theta cycles resulting in a shift of FMT towards lower frequencies along with increasing WM demand (Axmacher et al., 2010). Regulation of such cycles was attributed to recurrent anatomical pathways between the hippocampus and PFC (Blatow et al., 2003) with PFC activity driven by hippocampal theta phase rather than vice-versa (Anderson et al., 2010; Gordon, 2011). Based on the complementary learning systems model (Norman et al., 2005), increased FMT power during execution of an attention-demanding task with high cognitive load, e.g., during execution of an *n*-back task, on the other hand, was mainly attributed to increased inhibition of competing cortical representations related to previous WM trials (Norman et al., 2007). Correspondingly, absence of FMTΔpower during higher WM demand was reported to be associated with reduced performance (Donkers et al., 2011). However, it was unclear how FMT phase and FMT power relate to each other, and whether purposeful modulation of FMT phase can be used to target regulation of FMT power and influence cognitive control. Such knowledge would be important to gain deeper understanding of many brain disorders in which regulation of FMT oscillations is disturbed, e.g., depression (Olbrich and Arns, 2013), Alzheimers disease (AD) (Moretti et al., 2009; Laske et al., 2015) or attention deficit and hyperactivity disorder (ADHD; Missonnier et al., 2013).

Here, we investigated whether external manipulation of FMT phase during a WM task influences modulation of FMT power and WM performance. We hypothesized that manipulation of the physiological FMT phase regulation in frontal cortical regions interferes with maintenance of cortical representations related to previous WM trials and thus, results in lack of FMTΔpower associated with increase WM demand as well as disruption of normal WM performance.

To test this hypothesis, we used amplitude-modulated transcranial alternating current stimulation (tACS; Witkowski et al., 2015), a non-invasive brain stimulation (NIBS) method that can be used to modulate neural oscillations in a frequency-specific manner. In tACS, a weak (usually ≤2 mA) alternating electric current between two or more electrodes attached to the scalp is delivered. *In vitro* (Fröhlich and McCormick, 2010) and *in vivo* (Ali et al., 2013) studies have recently demonstrated that application of alternating currents can result in phase-alignment between neuronal spiking activity and the applied electrical stimulation signal (for review, see Veniero et al., 2015; Woods et al., 2016). Such tACS-based entrainment of brain oscillatory activity was shown to be accompanied by periodic fluctuations in behavioral performance providing further evidence for a causal relationship between brain oscillations and behavior (Thut et al., 2012).

Recently, we have shown that transcranial electric currents can be applied during assessment of whole-head magnetoencephalography (MEG; Soekadar et al., 2013; Garcia-Cossio et al., 2015) and that tACS-entrained cortical oscillation can be mapped at millimeter precision using amplitude-modulated stimulation signals (Witkowski et al., 2015). We reasoned that tACS oscillating at the individual FMT frequency delivered over frontal cortical regions during execution of an n-back task would lead to FMT phase-locked activity blocking hippocampus-driven phase regulation and thus, inhibition of competing cortical representations required for successful execution of a demanding WM task.

The possibility to record whole-head neuromagnetic activity during transcranial electric stimulation allowed us to verify success of the intended external manipulation of brain oscillations while, at the same time, allowing us to assess and map immediate effects of such manipulation on brain oscillatory activity throughout various brain areas and evaluate its impact on cognition and adaptive behavior.

MATERIALS AND METHODS

Study Participants

Twenty healthy volunteers (4 females, all right handed, mean Age = 27.4 ± 3.25 years) without a history of neurological or psychiatric disorders were invited to the MEG center of the University of Tübingen, Germany. The study was approved by the University's Ethics Committee (No.401/2012BO1) and written informed consent was obtained from all participants prior to their inclusion in the study.

Experimental Design

Participants were assigned to one of two groups (group A, group B) in a pseudo-randomized order following a counter balanced factorial design. Before the experimental session, all participants were invited to a familiarization session in which they were accustomed to the setup and task. FMT activity was recorded to calculate the frequency of the individual maximum theta peak in each participant. The experimental session consisted of two blocks, a baseline block (block 1) and an intervention block (block 2). Each block had a duration of approximately 4 min and consisted of 2 min of rest (task-free state) during which participants had their eyes open fixating a cross visualized on a screen in front of them, and approximately 2 min of task during which participants performed a 2-back task across two runs (**Figure 1**) separated by a short brake of 10–15 s. Each run consisted of 30 trials (2 s each) resulting in a total of 60 trials per block. During the task, letters were presented on a screen in front of the participants at an inter-stimulus interval of 2 s. For stimulus presentation, Psychotoolbox was used. The participants were instructed to indicate whether the displayed letter matched with the 2nd letter previously shown by pressing a button with their left index finger, or to indicate that the letter did not match by pressing a button with their right index finger. A total of 30 letters were shown in each of the two runs. Only 10 of these letters in each run randomly matched with the 2nd previous letter (match trials) resulting in 20 possible correct answers (match trials) per block (**Figure 1**). While group A received tACS amplitude-modulated at the individual theta peak frequency during the whole duration of block 2, sham stimulation was delivered during block 2 of group B.

Magnetic Resonance Imaging (MRI)

Before the first MEG session, participants were invited for a cranial magnetic resonance (MR) imaging exam using a 3-tesla whole body scanner with a 12-channel head coil (Magnetom Trio®, Siemens AG, Erlangen, Germany). To minimize head movements within the head coil, foam rubber was used to fixate the participant's head. A T1-weighted structural scan of the whole brain was obtained using the sequence MPRAGE (matrix size = 256 × 256, 160 partitions, 1 mm^3 isotropic voxels, TA = 5:17 m, TR = 2300 ms, TE = 3.93 ms, flip angle = 8°, FOVRO = 256, FOVPE = 224, PAT = 2, PAT mode = GRAPPA) that served as the anatomical reference for MEG source localization.

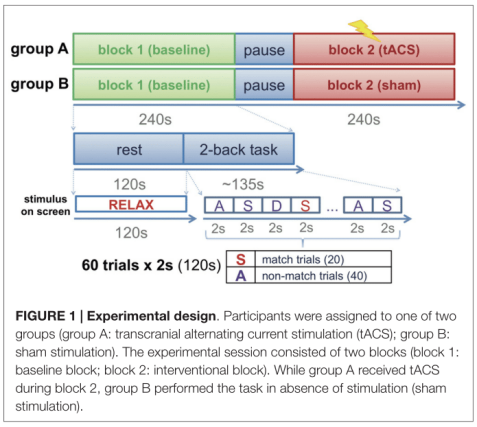

FIGURE 1 | Experimental design. Participants were assigned to one of two groups (group A: transcranial alternating current stimulation (tACS); group B: sham stimulation). The experimental session consisted of two blocks (block 1: baseline block; block 2: interventional block). While group A received tACS during block 2, group B performed the task in absence of stimulation (sham stimulation).

Whole-Head Magnetoencephalography (MEG)

Neuromagnetic activity was recorded while participants were seated in upright position using a 275-sensor whole-head MEG system (CTF MEG® by MISL, Coquitlam, BC, Canada) recording at a sampling frequency of 3906.25 Hz and bandwidth of 0–976Hz. Third order synthetic gradiometer configuration was used to attenuate environmental noise. Before MEG recordings, three fiducial localization coils were placed at the nasion, left and right pre-auricular area to determine the participant's head position during the MEG recording. Coil positions were continuously measured and locations stored to allow for offline co-registration with T1-weighted MR images. During MEG recordings, participants were asked to minimize head and body movements to avoid movement artifacts.

Transcranial Alternating Current Stimulation in the MEG Environment

tACS was delivered using a commercial transcranial brain stimulator (DC-STIMULATOR MR®, NeuroConn GmbH, Ilmenau, Germany). Two radio-translucent stimulation electrodes (5 cm × 7 cm) were placed according to the international 10–20 system over electrode positions Fpz overlying the medial frontal lope and Pz overlying the parietal cortex (Thompson and Thompson, 2003). Impedance between the stimulation electrodes was maintained below 20 kΩ using a conductive paste (Ten20®, D.O. Weaver, Aurora, CO, USA). The battery driven stimulator device was located outside the magnetically shielded room and the electric currents were delivered via a twisted pair of wires. tACS was applied at a peak-to-peak current intensity of 2 mA oscillating at 220 Hz (as in Witkowski et al., 2015), while the stimulation signal was modulated at each individual's peak theta frequency previously assessed during the familiarization session. The stimulation signal was generated using Matlab and streamed to the DC-STIMULTOR MR®'s remote input channel. The stimulator device linearly converted the input voltage into a corresponding stimulator output current (1 V = 2 mA).

To avoid possible discomfort during the onset of tACS, the stimulation current was gradually ramped up from 0 to 2.0 mA over a period of 10 s before onset of block 2, and then kept constant for the whole time of block 2. At the

end of block 2, tACS was ramped down from 2.0 to 0 mA over 10 s. For sham stimulation, no current was delivered throughout the session. The stimulator output signal was recorded along with the neuromagnetic activity using the MEG signal acquisition system so that phase-locking of reconstructed brain oscillations and the stimulator output signal could be calculated at a later stage. For sham stimulation, the stimulator output signal was recorded, but not converted into an actual output current. At the end of the session, each participant was asked to indicate whether tACS or sham stimulation was applied. To determine whether participants were able to distinguish their group assignment, a chi-square test was performed (see "Supplementary Material").

Whole-Brain Reconstruction of Source Activity

Recorded MEG data was low-pass filtered at 110 Hz using a 6th-order Butterworth filter and decimated by a factor of five. Synthetic Aperture Magnetometry (SAM) beamforming was used for reconstruction of source activity (SA) (Robinson and Vrba, 1999). The covariance matrix for all following processing steps was estimated based on the entire time-series. The weights for each voxel were estimated using the covariance matrix. Source signals were reconstructed by multiplying the estimated weights and preprocessed MEG data. SA was estimated at 5 mm resolution on a regular 3D grid using a single shell head model (Nolte, 2003).

Identification of Each Individual's Frontal Midline Theta (FMT) Peak Frequency

For identification of each individuals FMT peak frequency, MEG data recorded during the familiarization session was used to estimate each individual's theta activity by reconstructing source signals previously band-pass filtered from 4 to 8 Hz using a 3rd order Butterworth filter. The voxel with the most significant 2-back task-related theta activity increase during the familiarization session was identified and the corresponding source signal's frequency spectrum then estimated using fast Fourier transform (FFT). The frequency showing the maximum difference in signal power during the 2-back task in comparison to task-free intervals was then determined and used to set the modulation frequency of tACS in block 2.

Assessment and Mapping of tACS Phase-Locked Frontal Midline Theta Activity (FMTΔPLV)

To detect tACS phase-locked activity, phase locking value (PLV) between the theta-modulated tACS signal envelope and oscillatory SA across the whole brain was computed. In preparation for this, the instantaneous phases of the tACS signal envelope and reconstructed SA of each voxel was estimated by applying a Hilbert transformation on source signals filtered from 4 to 8 Hz (6th order Butterworth filter). PLV was then computed as a function of instantaneous phase difference between the tACS signal envelope and oscillatory SA using the following equation:

$$PLV = \frac{1}{N}\left|\sum_{n=1}^{N} e^{i(\Phi_{SA}(n)-\Phi_{SE}(n))}\right| \quad (1)$$

Where N is the number of sampled time points, Φ_{SE} and Φ_{SA} are the instantaneous phases at time point n of the stimulator's output signal *(SE)* and the reconstructed SA respectively. PLV can range between 0 and 1, where a value close to 0 indicates random phase relationship while a value close to 1 indicates a fixed signal phase relationship.

Differences in PLV were calculated between block 1 and 2 (ΔPLV). Mapping of tACS phase-locked brain activity was performed after spatial blurring using a Gaussian kernel with 5 mm full width at half maxima. Voxels were identified that exhibited increased ΔPLV between group A and B using an independent sample Wilcoxon rank sum test. Significance level was set at $p < 0.05$ and results corrected for multiple comparisons. Clusters with volumes less than 1 mL were excluded. For visualization, topographic images of frontal, sagittal and transversal view points were generated and voxels color-coded depending on ΔPLV magnitude using AFNI (Cox, 1996).

To test whether tACS was associated with an increase of theta PLV, an independent sample Wilcoxon rank sum test was performed comparing ΔPLV of the voxel with the highest ΔPLV increase in group B with ΔPLV of this voxel in group A. Additionally, ΔPLV was calculated and plotted across different frequencies to assess frequency-specificity of tACS entrainment (see "Supplementary Materials").

Assessment and Mapping of Frontal Midline Theta Power (FMTΔPower)

MEG source activity was filtered from 4 to 8 Hz (6th order Butterworth filter) and Hilbert transformed. Task-related differences in FMT power were calculated as difference in power between rest state and 2-back task and contrasted between block 1 and 2 (FMTΔpower). For visualization, topographic images of frontal, sagittal and transversal viewpoints were generated and voxels were color-coded depending on their FMTΔPower using AFNI.

To investigate whether tACS resulted in lack of FMTΔPower increase, FMTΔPower of the same voxel selected for comparison of ΔPLV between groups was calculated. Values were compared between group A and B using an independent sample Wilcoxon rank sum test. Significance level was set at $p < 0.05$ and results corrected for multiple comparisons.

Working Memory Performance

Response accuracy (nAcc) per block was calculated as percentage of correct responses normalized by the group median. To rule out difference in WM performance between groups in block 1, an independent sample Wilcoxon rank sum test with "response accuracy" was performed. As a second step, differences in WM performance between block 1 and block 2 (ΔnAcc) were

compared between group A and B using an independent sample Wilcoxon rank sum tests. Significance level was set to $p < 0.05$.

RESULTS

Source Localization of tACS Phase-Locked Frontal Midline Theta Activity (FMTΔPLV)

Localization of tACS phase-locked FMT oscillations as measured by ΔPLV in block 2 identified the right and left medial and superior frontal gyrus and ACC as cortical areas with the greatest impact of frontal theta tACS on FMT phase. These areas matched brain regions previously found to be involved in WM task execution showing WM demand-related FMTΔpower (Brookes et al., 2011, **Figure 2**). The voxel with the highest ΔPLV was located in the left PFC (Talairach coordinate [60, −6, 12]). ΔPLV at this voxel was significantly different between groups (group A: *Mdn* = 0.039; group B: *Mdn* = −0.001) evidencing that tACS, but not sham stimulation, resulted phase locking of FMT oscillations (**Figure 3**).

Assessment and Mapping of Frontal Midline Theta Power (FMTΔPower)

Voxels showing WM task-related theta power increase were located in the left and right anterior cingulate gyrus, medial and superior frontal gyrus as well as left supplementary motor cortex (SMA; **Figure 4**). A topographic map based on the difference in FMTΔPower between group A and B showed that tACS-associated lack of power increase was widespread matching cortical areas previously identified to be active during execution of a 2-back task (**Figure 5**). An independent sample Wilcoxon rank sum test revealed a significant difference in FMTΔPower in the PFC (Talairach coordinate [60, −6, 12]) of group A (tACS; *Mdn* = −0.165) compared to group B (sham stimulation; *Mdn* = 0.014; $U_{(18)} = 2.835$, $p = 0.005$; **Figure 6**) indicating that frontal theta tACS influenced regulation of FMT power during execution of a 2-back task.

Change in Working Memory Performance (ΔnAcc)

Participants were unable to differentiate to which group (A or B) they were assigned (χ^2 (2, N = 20) = 2.300, p = 0.986). While there was no difference in WM performance in block 1 (baseline block) between group A (tACS) and group B (sham stimulation; U = 1.35 p = 0.179, group A: *Mdn* = 95%, group B: *Mdn* = 95%), comparison of WM performance in block 2 between groups showed that tACS but not sham stimulation decreased response accuracy (ΔnAcc; sham; $U_{(18)} = 2.665$, $p = 0.008$, group A: *Mdn* = 2.63%, group B: *Mdn* = −2.63%; **Figure 7**).

DISCUSSION

This is the first study that assessed WM task-related FMT oscillations using whole-head MEG during simultaneous application of frequency-tuned tACS. Besides showing that FMT phase can be purposefully manipulated using frontal lobe tACS delivered at individual theta frequency, this study provides evidence that interference with endogenous FMT phase regulation, shown to be important for maintenance of temporal order information, is associated with lack of FMTΔpower and interferes with normal WM performance in an n-back task. While there was no difference in WM task-related FMTΔpower and WM performance (ΔnAcc) between both groups in block 1 in absence of any stimulation, application of frequency-tuned tACS but not sham stimulation reduced WM task-related FMTΔpower and lowered accuracy of WM performance in block 2. This finding suggests that interference

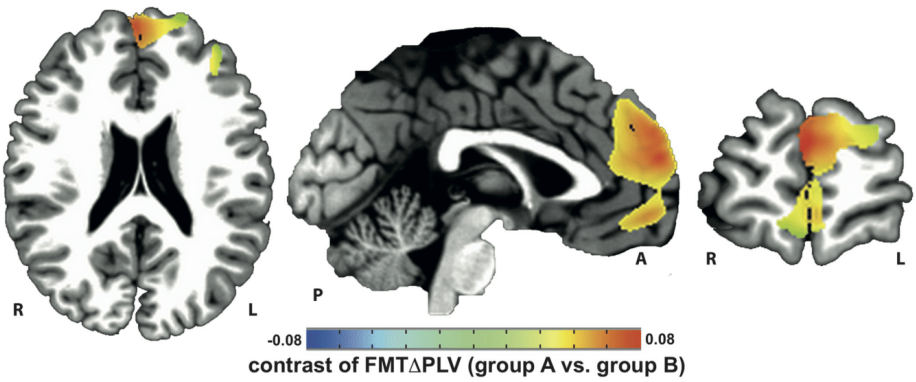

FIGURE 2 | Increase in tACS-dependent phase-locked brain activity was identified in frontal brain areas that included the prefrontal and anterior cingulate cortex (PFC/ACC) previously shown to be important for working memory (WM) task execution.

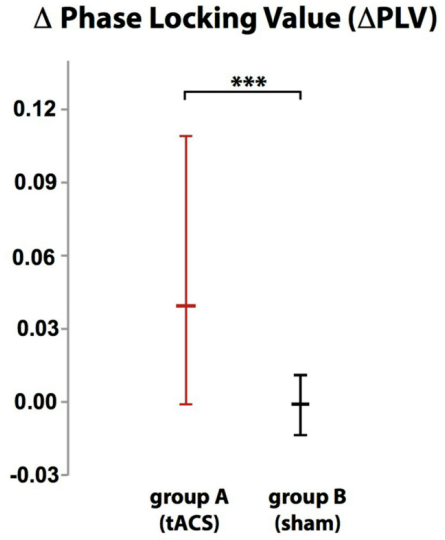

FIGURE 3 | While there was no difference in phase-locking value (ΔPLV) between blocks in group B (sham stimulation), ΔPLV increased in group A (tACS) documenting tACS-dependent manipulation of frontal midline theta (FMT) phase. Error bars indicate 95% confidence intervals. ***$p < 0.001$.

with endogenous FMT phase regulation undermines stabilization and maintenance of temporal order information required for correct responses in an n-back task. Consequently, as inhibition of competing representations is not required, task-related FMTΔpower during task execution is reduced, as shown for block 2 of group A (tACS) in our study. While our findings underline the importance of endogenous phase regulation for WM performance in an n-back task, interference with phase-regulation during other WM tasks in which maintenance of temporal order information is not required might not influence task performance or affect signal power modulation of brain oscillations, an issue that should be investigated in future studies. It is conceivable that interference with endogenous phase regulation that disrupts dysfunctionally coupled activity between relevant brain areas might, on the contrary, improve WM-related brain function, e.g., in the context of brain disorders such as depression, epilepsy, Alzheimer's or Parkinson's disease (Voytek and Knight, 2015). Better characterizations of these dysfunctional neural circuits and brain areas that can be targeted by transcranial brain stimulation to modulate these circuits are needed, however.

While in this study tACS was applied as open-loop stimulation, i.e., phase of the tACS signal was not adjusted to and independent of the phase of the endogenous brain oscillations, closed-loop stimulation in which brain stimulation is adjusted to the physiological parameters in real-time may allow for more specific and versatile modulation of brain function. Correctly adjusted, closed-loop tACS may not disrupt maintenance of temporal order information, but, on the contrary, stabilize such information, which should be reflected in an increase of task-related FMT power and improved n-back task performance. Such closed-loop paradigm allowing for precise tuning of tACS extending the currently available non-invasive tools to target brain oscillations would not only open new avenues to investigate the link between brain physiology and human behavior, but might also improve treatment options of brain disorders in which

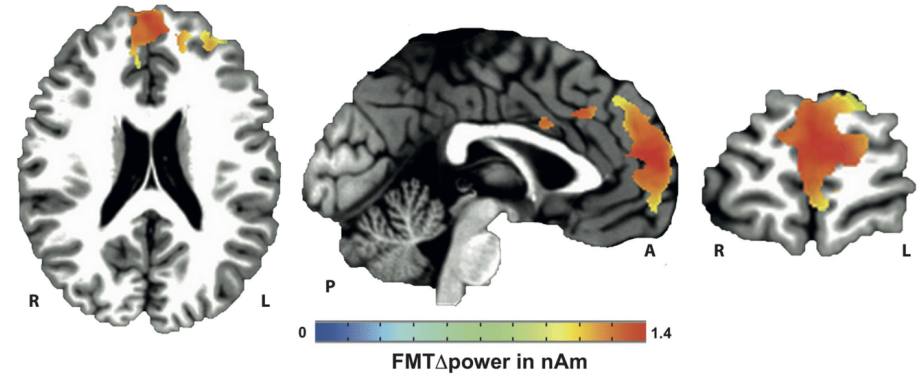

FIGURE 4 | Mapping of FMT power increase (FMTΔpower) during execution of a 2-back task.

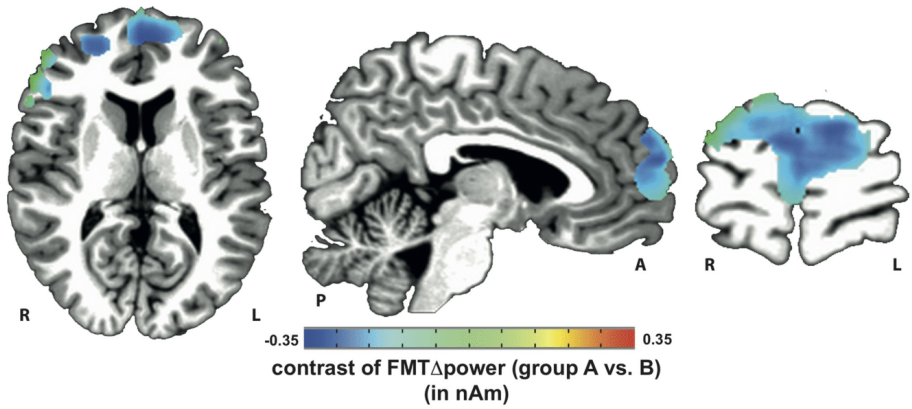

FIGURE 5 | Topographic map of voxels showing significant contrast in FMTΔpower when comparing 2-back task-related theta power increase during tACS vs. sham stimulation. Lack of theta power increase was found throughout the whole *n*-back task-related frontal cortical areas.

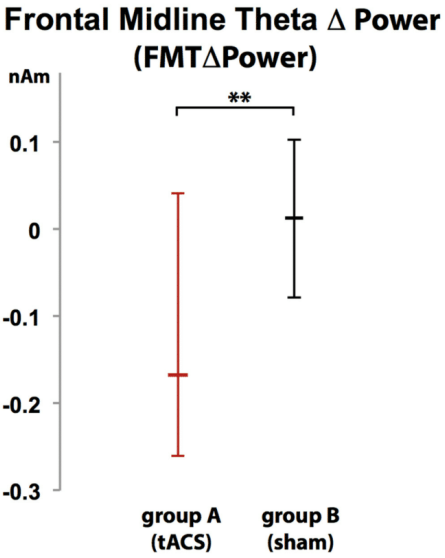

FIGURE 6 | Increase in FMT power (FMTΔpower) during execution of a 2-back task was significantly different in group A (tACS) compared to B indicating that frontal theta tACS results in lack of FMTΔpower shown to correlate with WM demand and performance. Error bars indicate 95% confidence intervals. $^{**}p < 0.01$.

coordination of activity between different brain regions is disturbed.

Mapping of tACS phase-locked (entrained) FMT oscillations showed that tACS phase locking occurred mainly in areas previously identified as generators of FMT, particularly the medial PFC and ACC. The individual role of the PFC and ACC in modulating FMT phase and power is still widely unknown. While attention coordination and error monitoring was attributed to ACC activation (Gehring and Knight, 2000), sustaining attention on task goals (MacDonald et al., 2000) and inhibiting competing cortical representations (Norman et al., 2007) was predominantly attributed to PFC activation (Munakata et al., 2011). It is not fully understood, though, how such activation (often measured as blood-oxygen-level dependent (BOLD) contrast using functional magnet resonance imaging) relates to modulations of theta activity. While our data shows that tACS-based PLV-increase affects both ACC and PFC, lack of FMT power increase during the 2-back task was only found in PFC, but not ACC. This indicates a differential role of how PFC and ACC each modulate FMT, and we'd speculate that FMT phase is influenced by both, while FMT power is predominantly modulated by PFC.

As the phase information of the tACS signal was sustained and spread across the whole task-related network independent of the tACS current flow (passing mainly through superficial cortical layers towards the parietal electrode, Laakso and Hirata, 2013), further evaluation of this phenomenon might be of great importance for the development of new transcranial stimulation strategies specifically targeting brain oscillations generated in subcortical areas. The property that tACS targeting a node of a widespread functional network can influence oscillatory activity in areas distant from the

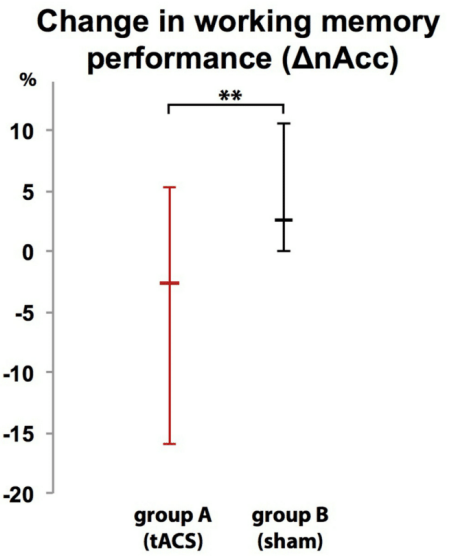

FIGURE 7 | Group-dependent difference in WM performance as measured as difference in correct responses in a 2-back task between a baseline block (block 1) and interventional block (block 2). WM performance dropped when tACS was applied (group A) but not during sham stimulation (group B). Error bars indicate 95% confidence intervals. $^{**}p < 0.01$.

stimulation electrode was recently also shown for tDCS (Garcia-Cossio et al., 2015). Interestingly, tACS phase locking was predominantly restricted to areas generating endogenous brain oscillations at frequencies similar to the tACS signal (frontal theta oscillations in our study). The fact that cortical areas underneath the parietal reference electrode did not show such differences in theta PLV or other frequencies during tACS (see "Supplementary Data Analysis") further corroborates this finding.

Whereas some previous brain stimulation studies indicated that entrainment at a specific target frequency can be associated with an increase in power at this very frequency, we did not find such entrainment-related power increase. This may relate to the different stimulation protocols that were used. Having shown that a FFT of reconstructed MEG source activity (SA) recorded during mono-sinusoidal (classical) tACS exhibits a large spectral power peak at the stimulation frequency, we concluded that noise cancelling features of SAM beamforming and possibly all linearly constrained minimum variance (LCMV) beamformers fail to reliably distinguish between physiological brain activity and stimulation-dependent artifacts of classical tACS (Witkowski et al., 2015). Additionally, Noury et al. (2016) have recently shown that heartbeat and respiration non-linearly modulate stimulation artifacts which may have resulted in misinterpretation of data acquired during classical tACS. We, thus used amplitude-modulated tACS in our study to overcome this problem. Future studies need to further elucidate the differences in the physiological effects of entrainment induced by mono-sinusoidal vs. amplitude-modulated tACS. The demonstrated tACS-dependent phase entrainment in the whole FMT network using amplitude-modulated tACS indicates, though, that increase in power related to mono-sinusoidal tACS, if not artifactual, may relate to other mechanisms than phase entrainment.

Whereas classical tACS, particularly when applied over frontal brain areas, can be associated with cutaneous retinal activation (Schutter, 2015), none of the study participants reported any photic stimulation or tACS-related discomfort leaving them unable to distinguish actual tACS from sham stimulation. Differences in specific physiological effects between classical mono-sinusoidal and amplitude-modulated tACS should be studied in future investigations. While not addressed in our study, recent studies indicate that gender can influence NIBS effects on WM performance (Meiron and Lavidor, 2013), an important issue to be considered in future studies.

After rhythmic transcranial current stimulation was already successfully used to modulate function of the motor domain, e.g., to suppress Parkinsonian resting tremor (Brittain et al., 2013), our study suggests that tACS might be a powerful tool to targeted cognitive control and adaptive behavior.

AUTHOR CONTRIBUTIONS

SRS, BSC, MW, CB designed the study. BSC, MW, SRS collected data. SRS, BSC, MW, CB analyzed data. SRS, BSC, MW, CB, SER, JB, LGC and NB interpreted data and did the literature search. SRS, BSC, MW wrote the manuscript and created the figures. SRS, BSC, MW, CB, SER, JB, LGC and NB edited the manuscript. Competing interests: All authors declare no competing financial interests. Data and materials availability: all raw data can be made available upon request.

ACKNOWLEDGMENTS

We thank Birgit Teufel for her assistance in organizing the experiments and preparing the manuscript. This study was funded by the Deutsche Forschungsgemeinschaft (DFG, SO932-2) and the University of Tübingen's *f*ortüne program, as well as the German Federal Ministry of Research and Education (BMBF, 01GQ0831 and 16SV5838K) and European Commission under the project AIDE (645322), and supported by the Open Access Publishing Fund of the University of Tübingen.

SUPPLEMENTARY MATERIAL

The Supplementary Material for this article can be found online at: http://journal.frontiersin.org/article/10.3389/fncel.2016.00120/abstract

REFERENCES

Ali, M. M., Sellers, K. K., and Fröhlich, F. (2013). Transcranial alternating current stimulation modulates large-scale cortical network activity by network resonance. *J. Neurosci.* 33, 11262–11275. doi: 10.1523/JNEUROSCI.5867-12.2013

Anderson, K. L., Rajagovindan, R., Ghacibeh, G. A., Meador, K. J., and Ding, M. (2010). Theta oscillations mediate interaction between prefrontal cortex and medial temporal lobe in human memory. *Cereb. Cortex* 20, 1604–1612. doi: 10.1093/cercor/bhp223

Axmacher, N., Henseler, M. M., Jensen, O., Weinreich, I., Elger, C. E., and Fell, J. (2010). Cross-frequency coupling supports multi-item working memory in the human hippocampus. *Proc. Natl. Acad. Sci. U S A* 107, 3228–3233. doi: 10.1073/pnas.0911531107

Beckmann, M., Johansen-Berg, H., and Rushworth, M. F. S. (2009). Connectivity-based parcellation of human cingulate cortex and its relation to functional specialization. *J. Neurosci.* 29, 1175–1190. doi: 10.1523/JNEUROSCI.3328-08.2009

Blatow, M., Rozov, A., Katona, I., Hormuzdi, S. G., Meyer, A. H., Whittington, M. A., et al. (2003). A novel network of multipolar bursting interneurons generates theta frequency oscillations in neocortex. *Neuron* 38, 805–817. doi: 10.1016/s0896-6273(03)00300-3

Brittain, J. S., Probert-Smith, P., Aziz, T. Z., and Brown, P. (2013). Tremor suppression by rhythmic transcranial current stimulation. *Curr. Biol.* 23, 436–440. doi: 10.1016/j.cub.2013.01.068

Brookes, M. J., Wood, J. R., Stevenson, C. M., Zumer, J. M., White, T. P., Liddle, P. F., et al. (2011). Changes in brain network activity during working memory tasks: a magnetoencephalography study. *Neuroimage* 55, 1804–1815. doi: 10.1016/j.neuroimage.2010.10.074

Buzsáki, G. (2006). *Rhythms of the Brain.* New York, NY: Oxford University Press.

Buzsáki, G., and Draguhn, A. (2004). Neuronal oscillations in cortical networks. *Science* 304, 1926–1929. doi: 10.1126/science.1099745

Cavanagh, J. F., Zambrano-Vazquez, L., and Allen, J. J. B. (2012). Theta lingua franca: a common mid-frontal substrate for action monitoring processes. *Psychophysiology* 49, 220–238. doi: 10.1111/j.1469-8986.2011.01293.x

Clayton, M. S., Yeung, N., and Cohen Kadosh, R. (2015). The roles of cortical oscillations in sustained attention. *Trends Cogn. Sci.* 19, 188–195. doi: 10.1016/j.tics.2015.02.004

Cox, R. W. (1996). AFNI: software for analysis and visualization of functional magnetic resonance neuroimages. *Comput. Biomed. Res.* 29, 162–173. doi: 10.1006/cbmr.1996.0014

De Smedt, B., Grabner, R. H., and Studer, B. (2009). Oscillatory EEG correlates of arithmetic strategy use in addition and subtraction. *Exp. Brain Res.* 195, 635–642. doi: 10.1007/s00221-009-1839-9

Donkers, F. C. L., Schwikert, S. R., Evans, A. M., Cleary, K. M., Perkins, D. O., and Belger, A. (2011). Impaired neural synchrony in the theta frequency range in adolescents at familial risk for schizophrenia. *Front. Psychiatry* 2:51. doi: 10.3389/fpsyt.2011.00051

Düzel, E., Penny, W. D., and Burgess, N. (2010). Brain oscillations and memory. *Curr. Opin. Neurobiol.* 20, 143–149. doi: 10.1016/j.conb.2010.01.004

Fröhlich, F., and McCormick, D. A. (2010). Endogenous electric fields may guide neocortical network activity. *Neuron* 67, 129–143. doi: 10.1016/j.neuron.2010.06.005

Garcia-Cossio, E., Witkowski, M., Robinson, S. E., Cohen, L. G., Birbaumer, N., and Soekadar, S. R. (2015). Simultaneous transcranial direct current stimulation (tDCS) and whole-head magnetoencephalography (MEG): assessing the impact of tDCS on slow cortical magnetic fields. *Neuroimage* doi: 10.1016/j.neuroimage.2015.09.068 [Epub ahead of print].

Gehring, W. J., and Knight, R. T. (2000). Prefrontal-cingulate interactions in action monitoring. *Nat. Neurosci.* 3, 516–520. doi: 10.1038/74899

Gevins, A., Smith, M. E., McEvoy, L., and Yu, D. (1997). High-resolution EEG mapping of cortical activation related to working memory: effects of task difficulty, type of processing and practice. *Cereb. Cortex* 7, 374–385. doi: 10.1093/cercor/7.4.374

Gordon, J. A. (2011). Oscillations and hippocampal-prefrontal synchrony. *Curr. Opin. Neurobiol.* 21, 486–491. doi: 10.1016/j.conb.2011.02.012

Hanslmayr, S., and Staudigl, T. (2014). How brain oscillations form memories—a processing based perspective on oscillatory subsequent memory effects. *Neuroimage* 85, 648–655. doi: 10.1016/j.neuroimage.2013.05.121

Hsieh, L. T., and Ranganath, C. (2014). Frontal midline theta oscillations during working memory maintenance and episodic encoding and retrieval. *Neuroimage* 85, 721–729. doi: 10.1016/j.neuroimage.2013.08.003

Ishihara, T., and Yoshi, N. (1972). Multivariate analytic study of EEG and mental activity in juvinile delinquents. *Electroencephalogr. Clin. Neurophysiology* 33, 71–80. doi: 10.1016/0013-4694(72)90026-0

Jensen, O., and Tesche, C. D. (2002). Frontal theta activity in humans increases with memory load in a working memory task. *Neuroscience* 15, 1395–1399. doi: 10.1046/j.1460-9568.2002.01975.x

Laakso, I., and Hirata, A. (2013). Computational analysis shows why transcranial alternating current stimulation induces retinal phosphenes. *J. Neural Eng.* 10:046009. doi: 10.1088/1741-2560/10/4/046009

Laske, C., Sohrabi, H. R., Frost, S. M., López-de-Ipiña, K., Garrard, P., Buscema, M., et al. (2015). Innovative diagnostic tools for early detection of Alzheimer's disease. *Alzheimers Dement.* 11, 561–578. doi: 10.1016/j.jalz.2014.06.004

MacDonald, A. W., III, Cohen, J. D., Stenger, V. A., and Carter, C. S. (2000). Dissociating the role of the dorsolateral prefrontal and anterior cingulate cortex in cognitive control. *Science* 288, 1835–1838. doi: 10.1126/science.288.5472.1835

Meiron, O., and Lavidor, M. (2013). Unilateral prefrontal direct current stimulation effects are modulated by working memory load and gender. *Brain Stimul.* 6, 440–447. doi: 10.1016/j.brs.2012.05.014

Missonnier, P., Hasler, R., Perroud, N., Herrmann, F. R., Millet, P., Richiardi, J., et al. (2013). EEG anomalies in adult ADHD subjects performing a working memory task. *Neuroscience* 241, 135–146. doi: 10.1016/j.neuroscience.2013.03.011

Mitchell, D. J., and Cusack, R. (2008). Flexible, capacity-limited activity of posterior parietal cortex in perceptual as well as visual short-term memory tasks. *Cereb. Cortex* 18, 1788–1798. doi: 10.1093/cercor/bhm205

Moretti, D. V., Pievani, M., Fracassi, C., Binetti, G., Rosini, S., Geroldi, C., et al. (2009). Increase of theta/gamma and alpha3/alpha2 ratio is associated with amygdalo-hippocampal complex atrophy. *J. Alzheimers Dis.* 17, 349–357. doi: 10.3233/JAD-2009-1059

Munakata, Y., Herd, S. A., Chatham, C. H., Depue, B. E., Banich, M. T., and O'Reilly, R. C. (2011). A unified framework for inhibitory control. *Trends Cogn. Sci.* 15, 453–459. doi: 10.1016/j.tics.2011.07.011

Nolte, L.-P. (2003). 3D imaging, planning, navigation. *Minim. Invasive Ther. Allied Technol.* 12, 3–4. doi: 10.1080/13645700306909

Norman, K. A., Newman, E. L., and Detre, G. (2007). A neural network model of retrieval-induced forgetting. *Psychol. Rev.* 114, 887–953. doi: 10.1037/0033-295x.114.4.887

Norman, K. A., Newman, E. L., and Perotte, A. J. (2005). Methods for reducing interference in the complementary learning systems model: oscillating inhibition and autonomous memory rehearsal. *Neural Netw.* 18, 1212–1228. doi: 10.1016/j.neunet.2005.08.010

Noury, N., Hipp, J. F., and Siegel, M. (2016). Physiological processes non-linearly affect electrophysiological recordings during transcranial electric stimulation. *Neuroimage* doi: 10.1016/j.neuroimage.2016.03.065 [Epub ahead of print].

Olbrich, S., and Arns, M. (2013). EEG biomarkers in major depressive disorder: discriminative power and prediction of treatment response. *Int. Rev. Psychiatry* 25, 604–618. doi: 10.3109/09540261.2013.816269

Robinson, S. E., and Vrba, J. (1999). "Functional neuroimaging by synthetic aperture magnetometry (SAM)," in *Recent Advances in Biomagnetism*, eds T. Yoshimoto, M. Kotani, S. Kuriki, H. Karibe, and N. Nakasato (Sendai: Tohoku University Press), 302–305.

Sauseng, P., and Klimesch, W. (2008). What does phase information of oscillatory brain activity tell us about cognitive processes? *Neurosci. Biobehav. Rev.* 32, 1001–1013. doi: 10.1016/j.neubiorev.2008.03.014

Schutter, D. J. (2015). Cutaneous retinal activation and neural entrainment in transcranial alternating current stimulation: a systematic review *Neuroimage*. doi: 10.1016/j.neuroimage.2015.09.067 [Epub ahead of print].

Soekadar, S. R., Witkowski, M., Cossio, E. G., Birbaumer, N., Robinson, S. E., and Cohen, L. G. (2013). *In vivo* assessment of human brain oscillations during application of transcranial electric currents. *Nat. Commun.* 4:2032. doi: 10.1038/ncomms3032

Thompson, M., and Thompson, L. (2003). *The Neurofeedback Book: An Introduction to Basic Concepts in Applied Psychophysiology*. Wheat Ridge, CO: Association for Applied Psychophysiology.

Thut, G., Miniussi, C., and Gross, J. (2012). The functional importance of rhythmic activity in the brain. *Curr. Biol.* 22, R658–R663. doi: 10.1016/j.cub.2012.06.061

Veniero, D., Vossen, A., Gross, J., and Thut, G. (2015). Lasting EEG/MEG aftereffects of rhythmic transcranial brain stimulation: level of control over oscillatory network activity. *Front. Cell. Neurosci.* 9:477. doi: 10.3389/fncel.2015.00477

Vogt, B. (2009). *Cingulate Neurobiology and Disease*. London: Oxford University Press.

Voytek, B., and Knight, R. T. (2015). Dynamic network communication as a unifying neural basis for cognition, development, aging and disease. *Biol. Psychiatry* 77, 1089–1097. doi: 10.1016/j.biopsych.2015.04.016

Witkowski, M., Garcia-Cossio, E., Chander, B. S., Braun, C., Birbaumer, N., Robinson, S. E., et al. (2015). Mapping entrained brain oscillations during transcranial alternating current stimulation (tACS). *Neuroimage* doi: 10.1016/j.neuroimage.2015.10.024 [Epub ahead of print].

Woods, A. J., Antal, A., Bikson, M., Boggio, P. S., Brunoni, A. R., Celnik, P., et al. (2016). A technical guide to tDCS and related non-invasive brain stimulation tools. *Clin. Neurophysiol.* 127, 1031–1048. doi: 10.1016/j.clinph.2015.11.012

Conflict of Interest Statement: The authors declare that the research was conducted in the absence of any commercial or financial relationships that could be construed as a potential conflict of interest.

Supplementary material

Supplementary data analysis

Placebo-control of stimulation

To rule out that participants could distinguish between active tACS and sham stimulation, all subjects were asked at the end of each session whether they believed to have received active brain stimulation throughout the session (*active*) or not (*inactive*) (Supplementary Table S2). A chi-square test was performed to determine whether the groups were able to distinguish active and inactive stimulation across sessions. The ability to distinguish was equally distributed in the population, $\chi^2_{(2,\ N\ =\ 20)} = 2.300$, $p = .986$ suggesting that participants were unable to reliable distinguish whether active tACS was applied or not.

Modulation of PLV underneath the parietal electrode in other frequency bands

To investigate whether theta tACS applied over the parietal lobe results in PLV increase in other frequency bands, ΔPLV was estimated at a frequency resolution of 0.5 Hz in each band (delta: 0.1-4Hz; alpha: 9-15Hz; and beta: 15-30Hz) and compared between groups using a two-sided Student′s t-test. Resulting p-values were corrected for multiple comparisons using Bonferroni correction. Theta tACS did not result in any significant PLV increase in any of the tested frequency bands (delta: $p = .4703$; alpha: $p = .4264$; beta: $p = .1866$).

Supplementary Tables

Table S1: Theta peak frequencies across participants

Participant (group A)	**Theta peak frequency**
1	6.6 Hz
2	5.9 Hz
3	6.2 Hz
4	5.8 Hz
5	6.6 Hz
6	5.4 Hz
7	5.5 Hz
8	6.5 Hz
9	5.2 Hz
10	6.5 Hz
Participant (group B)	**Theta peak frequency**
1	6.2 Hz
2	5.2 Hz
3	5.9 Hz

4	4.9 Hz
5	4.9 Hz
6	5.6 Hz
7	6.4 Hz
8	6.3 Hz
9	6.9 Hz
10	5.3 Hz

Table S2: Response of participants when asked whether they believed to have received active or inactive brain stimulation during block 2

Participant (group A)	**Response** (active / inactive)
1	Inactive
2	Active
3	Inactive
4	Inactive
5	Active
6	Inactive
7	Inactive
8	Inactive
9	Active
10	Inactive
Participant (group B)	**Response** (active / inactive)
1	Inactive
2	Inactive
3	Inactive
4	Active
5	Inactive
6	Active
7	Active
8	Active
9	Inactive
10	Inactive

Supplementary Table S1: Placebo-control of stimulation type. Participants were asked at the end of each session whether they believed to have received active stimulation during block 2 (*active*) or not (*inactive*). Responses were not different between stimulation types suggesting that participants were unable to reliable distinguish whether active stimulation was applied or not.

Supplementary Figures

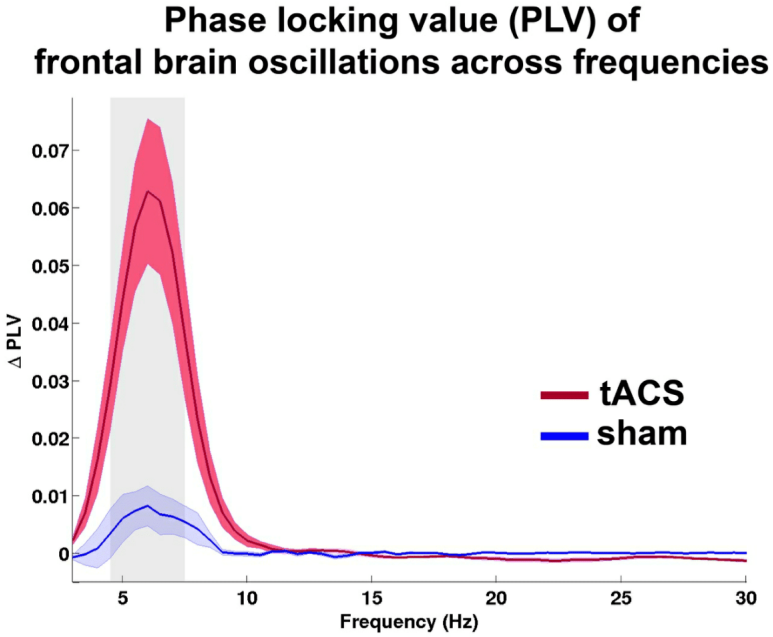

Fig. S1: Frequency specificity of transcranial alternating current stimulation (tACS)-dependent phase locking of brain oscillations. Difference in phase locking value (ΔPLV) between block 1 (baseline block) and block 2 (intervention block) in group A (tACS, red line) and group B (sham, blue line) across different frequency bands in the left prefrontal cortex (PFC) (Talairach coordinate [60 -6 12]). Shaded areas indicate standard error (SE). ΔPLV increased only in theta band and matched with the frequency of the amplitude modulated tACS signal's envelope oscillating at each individual's frontal midline theta (FMT) frequency. The grey shaded area indicates a significance level of $p < .01$.

2.3. Amplitude-modulated transcranial alternating current stimulation (tACS) in magnetoencephalography (MEG): An update

Amplitude-modulated transcranial alternating current stimulation (tACS) during magnetoencephalography (MEG): An update

Bankim S. Chander[1], Matthias Witkowski[1], David Haslacher[1], Shuka Shibusawa[2], Stephen E. Robinson[3], Christoph Braun[4,5], Surjo R. Soekadar[1]*

[1] Applied Neurotechnology Lab, Department of Psychiatry and Psychotherapy, University Hospital of Tübingen, Germany

[2] Keio University, Tokyo, Japan

[3] National Institute of Mental Health (NIMH), MEG Core Facility, Bethesda, USA

[4] MEG Center, University of Tübingen, Tübingen, Germany

[5] CIMeC, Center for Mind/Brain Sciences, University of Trento, Trento, Italy

* Correspondence to: Surjo R. Soekadar, MD, Applied Neurotechnology Lab, Department of Psychiatry and Psychotherapy, University Hospital of Tübingen, Calwerstr. 14, 72076 Tübingen, Germany. Email: surjo.soekadar@uni-tuebingen.de

Key words: neuromagnetic brain oscillations, transcranial electric stimulation, magnetoencephalography, EEG, MEG, stimulation artifacts

Abstract

Transcranial alternating current stimulation (tACS) is a non-invasive and well-tolerated technique to influence brain function. The direct effects of tACS on brain oscillations are not well understood as simultaneous recordings of neural activity, e.g. using magnetoencephalography (MEG), that could shed light on the underlying mechanisms, are contaminated by stimulation artifacts. Recently, a novel tACS stimulation protocol was introduced using amplitude modulation ($tACS_{am}$) reducing contamination of MEG recordings at physiological frequency bands of interest (i.e., 2 – 90 Hz) (Witkowski et al. 2016). However, artifacts induced by non-linearities of the stimulation setup and related to the demodulation of the $tACS_{am}$ signal remain a critical challenge (Karsten et al. 2018). Here we investigated the difference in power and phase locking value (PLV) across both a melon phantom and human head during tACS and $tACS_{am}$. MEG data of 6 healthy volunteers (4 male, 2 female, age 27.7±3.5 years) and a melon phantom were recorded during tACS or $tACS_{am}$. We found that the PLV increase in the phantom model was comparable between both stimulation protocols despite higher power at the target frequency during tACS. When recording MEG in healthy volunteers during $tACS_{am}$ and tACS, PLV was significantly higher during $tACS_{am}$ compared to tACS. This indicates demodulation of the $tACS_{am}$ signal at the target frequency, possibly due to the demodulation properties of neural tissue. More studies are needed to further investigate possible biological and behavioral effects of $tACS_{am}$.

Introduction

Over the last two decades, transcranial electric stimulation (TES) became a widely adopted tool to modulate brain function and behavior. In TES, two or more stimulation electrodes are attached to a person's head delivering a weak and well-tolerable stimulation current (Gandiga et al. 2006, Matsumoto and Ugawa 2017). Depending on the direction and waveform of the stimulation current, various forms of TES can be distinguished, e.g. transcranial direct current stimulation (tDCS), transcranial alternating current stimulation (tACS) or random noise stimulation (RNS). Despite its broad application, strong

electromagnetic artifacts impede online assessment of TES due to contamination of MEG recordings. Recently, a novel strategy combining TES and magnetoencephalography (MEG) was introduced that allowed for *in-vivo* assessment of neuromagnetic brain oscillations during tDCS (Soekadar et al. 2013, Garcia-Cossio et al. 2016). Using advanced spatial filtering based on beamforming, motor-related modulations of neuromagnetic activity could be reliably reconstructed.

It was shown, however, that in case the direction of the stimulation current changes, as in tACS, beamforming does not sufficiently suppress stimulation artifacts (Noury et al. 2016). As the stimulation frequency in tACS is usually set to match the frequency of brain oscillations found to be related to a particular brain function (e.g., frontal theta, parietal beta etc.), insufficient suppression of the stimulation artifact at that frequency can be easily misinterpreted as neuronal response to the stimulation, e.g. *neural entrainment*.

Recently, a novel tACS stimulation protocol was introduced using amplitude modulation ($tACS_{am}$) reducing contamination of MEG recordings at physiological frequency bands of interest (i.e., 2 – 90 Hz) (Witkowski et al. 2016). In this protocol, the amplitude of a high-frequency stimulation signal (e.g., > 200 Hz, carrier signal) is modulated at a lower (envelope) frequency. Biological systems utilize amplitude modulation of brain oscillations for neural transmission and processing in the somatosensory (Lundstrom et al. 2010), visual (Grosof et al. 1993, Mareschal and Baker, 1998) or auditory systems (Giraud and Poeppel, 2012). Therefore, $tACS_{am}$ signal is expected to interact with neurons in the brain. It was shown that $tACS_{am}$ mediated entrainment of frontal midline theta (FMT) oscillations known to be linked to cognitive brain functions and disrupted working memory performance (Chander et al. 2016). While an increasing number of studies suggest that $tACS_{am}$ can be used to effectively target brain oscillations (Negahbani et al. 2018), it remained unknown to what extent $tACS_{am}$ can induce entrainment related power increases in EEG or MEG associated with demodulation of the $tACS_{am}$ signal compared to tACS. This raises the question whether measures broadly used to quantify *neural entrainment*, i.e.

phase lock between the stimulation signal and ongoing brain oscillations, such as phase locking value (PLV) actually reflect functional interaction of $tACS_{am}$ with neurons.

Currently, there is no standardized and accepted artifact rejection method that prevents deterioration of MEG recordings in the physiological frequency bands of interest (i.e., < 90 Hz) during $tACS_{am}$. Improving artifact rejection methods for MEG would allow non-invasive assessment of magnetic oscillations originating in the brain below the stimulation electrodes with good temporal and spatial resolution. Recently, the non-linearity in components of stimulation setups, essentially the stimulator device and the stimulation circuit were found to induce artifacts related to the demodulation of the $tACS_{am}$ signal (Karsten et al. 2018). Besides non-linearity of the stimulation setup, other non-linear components, including biological membranes (Silny, 2007), can influence the level of $tACS_{am}$ signal demodulation. Particularly, development of new stimulators reducing non-linear interactions with MEG data in the frequencies of interest (FOI) might pave the way to successfully unveil the mechanisms underlying TES effects.

Here we investigated the difference in power and phase locking value (PLV) across both a melon phantom and human head during tACS and $tACS_{am}$. As has been shown in previous studies, amplitude-modulated current stimulation, using a voltage controlled electrical stimulator, tend to result in slightly distorted stimulation signals (Karsten et al. 2018). Distortions of the stimulation signal due to non-linearities of the electronics result in spectral components of the $tACS_{am}$ signal in the frequency band of the modulation frequency and its harmonics. Therefore, $tACS_{am}$ does not provide a neuronal stimulation that is completely free of any contamination of the physiological frequency bands by artifacts. In order to quantify demodulation of the $tACS_{am}$-envelope signal, we contrasted $tACS_{am}$ stimulation of human brains with a melon phantom, and compared these results with MEG data recorded during tACS. The melon phantom is like a human head an electrical volume conductor with a layered structure of varying conductivities except that it does not have any neuronal

tissue (Neuling et al. 2017). Given that in $tACS_{am}$ the stimulation energy is directed at a very high frequency usually far beyond the physiological frequency bands of interest (> 200 Hz) and only little activity leaks into the lower frequency band, we expect that in the melon a relatively small portion of the total activity appears in the frequency band of the modulation. In case of human brains, apart from the activity leaking to the lower frequencies, additionally neural entrainment contributes to power increase at the modulation frequency. Moreover, we expected if neural entrainment occurs, that both $tACS_{am}$ and tACS should be associated with a difference in PLV for human volunteers. Since neural entrainment for phantom model is not possible, comparable PLV for $tACS_{am}$ and tACS are expected.

MATERIALS AND PROCEDURES

Study participants

Six healthy volunteers (Age: *M* = 27.7, *SD* = 3.5 years, 2 females) without a history of neurological or psychiatric disorders were invited to participate in the study. The participants were comfortably seated for recording MEG signals. The study was approved by the ethics committee of the Medical Faculty at the University of Tübingen (401/2012BO1). Before entering the study, written informed consent was obtained by all participants.

Melon Phantom

A melon phantom with a mean circumference of 42 ± 1 cm was selected for the study. The melon was placed over a plastic stand and three positions for attaching the head coils were marked at along the circumference consecutively at a distance of one fourth of the circumference.

Whole-head Magnetoencephalography (MEG)

Neuromagnetic activity was recorded using a 275-sensor whole-head MEG system (CTF MEG® by MISL, Coquitlam, BC, Canada) housed in a magnetically shielded room (Vakuumschmelze GmbH, Hanau, Germany). MEG

recordings were digitized at the sampling frequency of 3906.25 Hz and bandwidth of 0 – 976 Hz. Third order synthetic gradiometer configuration was used to attenuate environmental noise. Before MEG recordings, three fiducial localization coils were placed at the nasion, left and right pre-auricular area to determine the participant's head or phantom head position during the MEG recording. Coil positions were continuously recorded and locations stored to allow for offline co-registration with T1-weighted MR images of participants. During MEG recording, participants were asked to rest and minimize head and body movements to avoid movement artifacts. MEG signals were recorded while participants received tACS and $tACS_{am}$ for 240 seconds each as shown below in figure 1.

Study design

Each study block consisted of two consecutive MEG recording of 240 seconds each. During first and second MEG recordings tACS and $tACS_{am}$ was delivered respectively to the participant or melon (Figure 1).

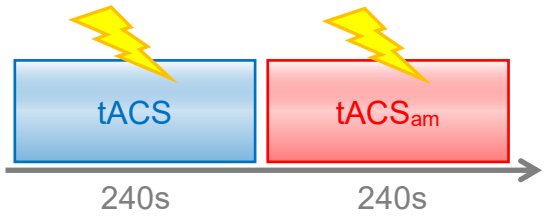

Figure 1: Study design for experiment.

Transcranial electric stimulation (TES)

Alternating current (AC) was applied using a commercial stimulator (DC-STIMULATOR MR®, NeuroConn GmbH, Ilmenau, Germany). The battery-driven stimulator device was located outside the magnetically shielded room housing the MEG system and delivered electric currents via a twisted pair of wires with an peak to peak intensity of 1 mA. A stimulation signal digitized at 24 KHz was generated using a custom made Matlab script and streamed to the DC-STIMULTOR MR®'s remote input channel via National Instrument data acquisition card (NI-9264, National Instruments Corporation, Austin, USA). The

stimulator device linearly converted the input voltage into a corresponding stimulator output current (Stimulator transfer function: Input 1 V = Output 2 mA).

The applied tACS signal was oscillating at 11 Hz and at 220 Hz (as in Witkowski et al. 2016) while the amplitude of stimulation signal was modulated at 11 Hz. Two radio-translucent stimulation electrodes were attached according to the international 10 – 20 system over electrode positions CP4 and O10. A conductive paste (Ten20®, D.O. Weaver, Aurora, CO, USA) was applied to the stimulator electrodes for maintaining impedance between the stimulating electrodes below 18 kΩ.

Magnetic Resonance Imaging (MRI)

Before the first MEG session, participants were invited for a cranial magnetic resonance (MR) imaging exam using a 3-tesla whole body scanner with a 32-channel head coil (Magnetom Prisma syngo MR D13D, Siemens AG, Erlangen, Germany). To minimize head movements within the head coil, foam rubber was used to fixate the participant's head. A T1-weighted structural scan of the whole brain was obtained using the sequence MPRAGE (matrix size = 256 x 256, 176 partitions, 1 mm^3 isotropic voxels, TA = 3:52 m, TR = 2300 ms, TE = 4.18 ms, flip angle = 9◦, FOVRO = 256, FOVPE = 224, PAT = 3, PAT mode = GRAPPA) that served as the anatomical reference for MEG source localization.

Reconstruction of source activity

Recorded MEG data was band-pass filtered between 2 Hz and 90 Hz using a 6^{th}-order Butterworth filter and a notch filter with a width of 4 Hz (± 2 Hz) centered at 50 Hz, using a 20^{th}-order FFT filter. Synthetic Aperture Magnetometry (SAM) beamforming was used for reconstruction of source activity (SA) (Robinson & Vrba, 1999). The covariance matrix for all following processing steps was estimated based on the entire time-series. The weights for each voxel were estimated using the covariance matrix. Source signals were reconstructed by multiplying the estimated weights and preprocessed MEG data. SA activity was estimated at 1 cm resolution on a regular 3D grid using a

single shell head model for human participants (Nolte, 2003). Voxels below the stimulation electrode were selected for subsequent analysis.

Data analysis

The power spectrum at a frequency resolution of 0.05 Hz was estimated as absolute value after Fast Fourier Transform (FFT) of the source activity by applying hanning window on 20 s epochs. The estimated power spectrum was transformed to decibel scale. The ratio of power between the modulation frequency and- the carrier frequency during $tACS_{am}$ was calculated at individual MEG sensors. A normal cumulative distribution test was performed to test whether the single power leakage value for melon belongs to the power ratio distribution of human brains. The PLV spectrum at a frequency resolution of 0.5 Hz was estimated by computing PLV (as in Chander et al. 2016) between the stimulation signal and the source activity after applying a band pass filter with a band width of 1 Hz centered at the frequency of interest. During $tACS_{am}$, PLV was estimated between the source activity and the envelope of the $tACS_{am}$ signal. To test for variation in PLV at target frequency during $tACS_{am}$ and tACS, a two-sided paired Wilcoxon signed-ranks test was performed.

RESULTS

Power Spectrum

The power spectrum for the melon phantom during tACS shows a clear increase in power compared to adjacent frequencies at the stimulation frequency and its harmonics (Figure 2). There is also a power increase during $tACS_{am}$ at the modulation frequency but less compared to tACS as indicated by horizontal line (Figure 2). Further increases could be observed at the harmonics but less evidently (Figure 2).

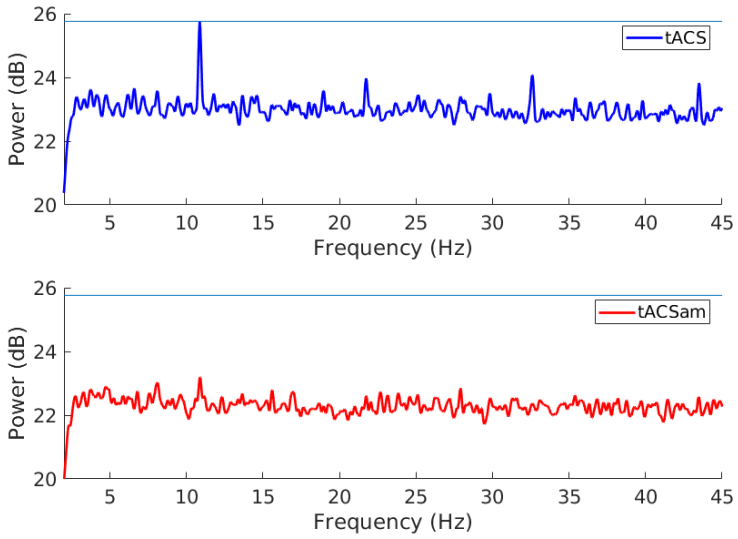

Figure 2: Power spectral analysis for melon phantom showing increase in power at target frequency (11 Hz) during tACS (Blue) and $tACS_{am}$ (Red). The horizontal line hitting the peak of the tACS stimulation serves as reference to compare tACS and $tACS_{am}$.

The power spectrum for human brain during tACS and $tACS_{am}$ shows a clear increase in power compared to adjacent frequencies at the stimulation frequency and its harmonics (Figure 3). The observed increase in power for $tACS_{am}$ is lower compared to the tACS condition as indicated by the horizontal line (Figure 3).

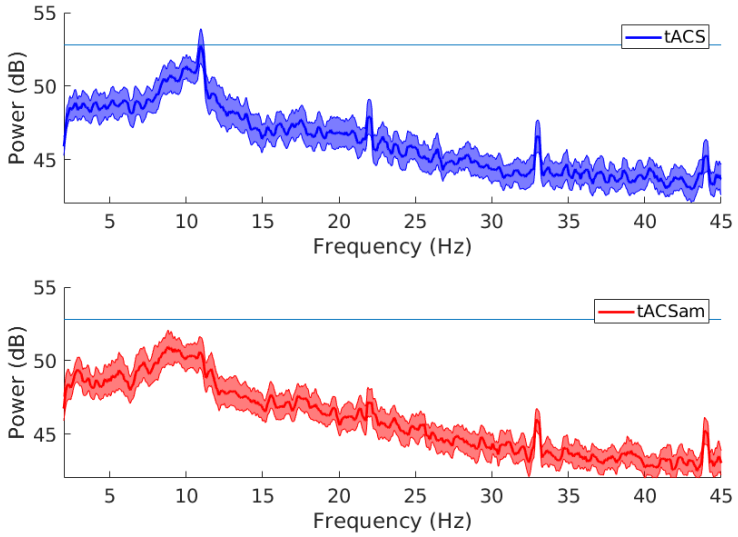

Figure 3: Power spectral analysis for human brain showing increase in power at target frequency (11 Hz) during tACS (Blue) and $tACS_{am}$ (Red) along with SEM. The horizontal line hitting the peak of the tACS stimulation serves as reference to compare tACS and $tACS_{am}$.

While $tACS_{am}$ at 1 mA current was applied to human brains and melon phantom, the ratios of power between the modulation frequency and carrier frequency in percentage reveals ratios of 3.33 % for the melon phantom and on average 13.15 % for the six human participants.

Furthermore, a normal cumulative function distribution test reveals that the ratio of power between the modulation frequency and carrier frequency for human brain (M = -8.81 dB, SD = 1.58 dB) is higher compared to melon (-14.77 dB) ($p < 0.001$). This implies that power leakage for melon phantom is outside the two standard deviations from the mean of the normally distributed power ratio for human brains.

PLV Spectrum

The following PLV spectrums quantify the phase synchrony of the source activity below the stimulation electrode as observed in melon phantom and human brains.

The PLV spectrum for the melon phantom shows similar PLV observed during tACS and $tACS_{am}$ across frequencies (Figure 4).

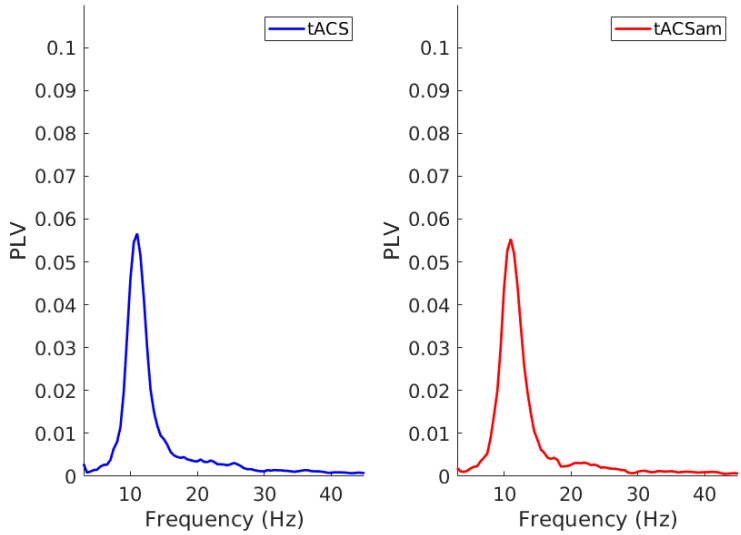

Figure 4: PLV spectrum for melon phantom showing increase in PLV at target frequency (11 Hz) during tACS (Blue) and $tACS_{am}$ (Red)

The PLV spectrums for human brains show an increase in PLV values during tACS and $tACS_{am}$ compared to frequencies around the target frequency of 11 Hz (Figure 5).

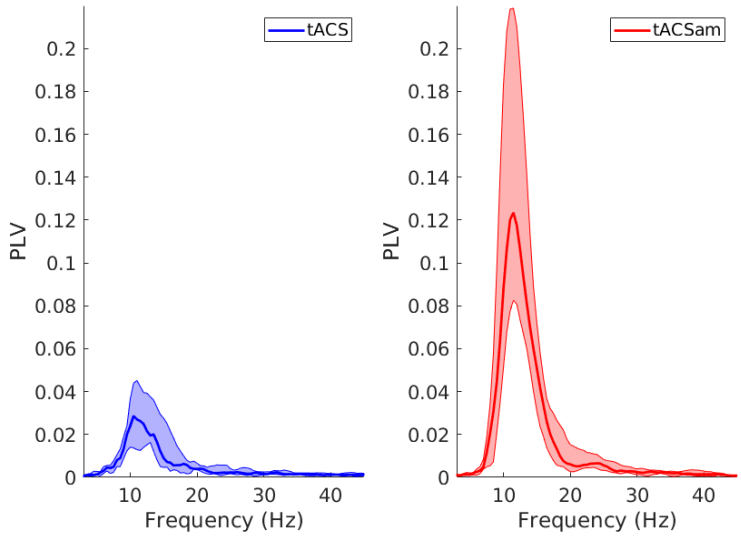

Figure 5: PLV spectrum for human brain showing increase in PLV at target frequency (11 Hz) during tACS (Blue) and $tACS_{am}$ (Red) along with respective maximum and minimum for each frequency

A two-sided paired Wilcoxon signed-ranks test reveals that PLV during $tACS_{am}$ (*Mdn* = 0.120) is higher compared to tACS (*Mdn* = 0.027) (*Z* = 21.00, *p* = 0.031, *r* = 8.57).

Discussion

We found that during $tACS_{am}$ and tACS, signal power and PLV at the target frequency increases. The contrast between human brain and melon phantom revealed differential effect for power and PLV. The power ratio between modulation frequency and carrier frequency was higher for human brain compared to melon implying entrainment in human brains in addition to the power leakage observed in melon phantom. PLV increase during $tACS_{am}$ was approximately four times larger in comparison to during tACS for the human brains. In contrast to human brains, for a melon phantom a stable PLV of 0.057 during $tACS_{am}$ and tACS at the target frequency was found. This observation may suggest possible functional interaction of $tACS_{am}$ with biological tissue, including neuronal populations in the human brain. The increase of PLV during $tACS_{am}$ compared to tACS might be due to additional recruitment of neurons selectively responsive to the envelope of the amplitude-modulated stimulation signal (Middleton et al. 2006, Kawasaki & Guo, 1998)

Since, the non-linearities of biological membranes and stimulation setup are capable of demodulating amplitude-modulated signals (Silny, 2007, Karsten et al. 2018), the PLV increase during $tACS_{am}$ at the modulation frequency compared to other frequencies is probably due to the combination of non-linearities of the biological membranes and stimulation setup. Currently it is not possible to distinguish between the contributions of different non-linear components in the stimulation circuit towards demodulation of $tACS_{am}$ signal and associated increase in power and PLV. The non-linearities of the stimulator setup, attributed to the stimulator device and the stimulation circuit including the

biological tissue being stimulated are not expected to differ between subsequent experiments. Considering only the passive electrical properties of the stimulator setup, similarity in PLV between $tACS_{am}$ and tACS for human brains was expected but only observed for the melon phantom. In contrast, the variation observed in PLV between $tACS_{am}$ and tACS for the human brains cannot be explained only by considering passive electrical properties. If $tACS_{am}$ and tACS have non-linear interactions with only passive electrical properties, the amplitude of PLV for $tACS_{am}$ and tACS should not differ, as observed for the melon phantom. Even though the power at the target frequency is lower for $tACS_{am}$ than for tACS, a stronger increase in PLV for $tACS_{am}$ compared to tACS was found. This suggests that $tACS_{am}$ is associated with demodulation at the target frequency, possibly due to demodulations by biological tissue including neuronal pools.

It remains to be tested to what extend tACS is more suitable for modulating power and $tACS_{am}$ for modulating phase. This is particularly interesting for intermittent stimulation paradigms where stimulation is applied repeatedly for short intervals that do not require assessment of brain activity during stimulation. Under the assumption, that changes in electrical properties of the stimulation circuit including the non-linearities can be minimized or even eliminated, it would be possible to develop brain state dependent stimulation paradigms that can confirm entrainment dependent physiological effects (Thut et al. 2017, Soekadar et al. 2013).

Technical interventions to attenuate artifacts related to demodulation of the $tACS_{am}$ signal due to the hardware should be further explored. For example, introducing band-pass hardware filters centered at the carrier frequency to the stimulation setup could be an option to suppress the artifacts in the modulation frequency range. Another technical intervention could be introducing a low-pass hardware filter before the MEG amplifier to attenuate recording of $tACS_{am}$ signal and potentially avoid any demodulation due to recording hardware (Kasten et al. 2018). Further improvement in stimulation setup possibly by introducing auxiliary stimulation circuit that measure deviations from the programmed

stimulation waveform and inject compensatory currents would improve assessment of non-linear interactions with neurons. More studies are needed to further investigate possible biological and behavioral effects of $tACS_{am}$.

References

Chander, B. S., Witkowski, M., Braun, C., Robinson, S. E., Born, J., Cohen, L. G., ... & Soekadar, S. R. (2016). tACS phase locking of frontal midline theta oscillations disrupts working memory performance. Frontiers in cellular neuroscience, 10, 120.

Gandiga, P. C., Hummel, F. C., & Cohen, L. G. (2006). Transcranial DC stimulation (tDCS): a tool for double-blind sham-controlled clinical studies in brain stimulation. Clinical neurophysiology, 117(4), 845-850.

Garcia-Cossio, E., Witkowski, M., Robinson, S. E., Cohen, L. G., Birbaumer, N., & Soekadar, S. R. (2016). Simultaneous transcranial direct current stimulation (tDCS) and whole-head magnetoencephalography (MEG): assessing the impact of tDCS on slow cortical magnetic fields. Neuroimage, 140, 33-40.

Giraud, A. L., & Poeppel, D. (2012). Cortical oscillations and speech processing: emerging computational principles and operations. Nature neuroscience, 15(4), 511.

Grosof, D. H., Shapley, R. M., & Hawken, M. J. (1993). Macaque VI neurons can signal 'illusory'contours. Nature, 365(6446), 550.

Grossman, N., Bono, D., Dedic, N., Kodandaramaiah, S. B., Rudenko, A., Suk, H. J., ... & Pascual-Leone, A. (2017). Noninvasive deep brain stimulation via temporally interfering electric fields. Cell, 169(6), 1029-1041.

Kasten, F. H., Negahbani, E., Frohlich, F., & Herrmann, C. S. (2018). Non-linear transfer characteristics of stimulation and recording hardware account for spurious low-frequency artifacts during amplitude modulated transcranial alternating current stimulation (AM-tACS). bioRxiv, 246710.

Kawasaki, M., & Guo, Y. X. (1998). Parallel projection of amplitude and phase information from the hindbrain to the midbrain of the African electric fish Gymnarchus niloticus. Journal of Neuroscience, 18(18), 7599-7611.

Lundstrom, B. N., Fairhall, A. L., & Maravall, M. (2010). Multiple timescale encoding of slowly varying whisker stimulus envelope in cortical and thalamic neurons in vivo. Journal of Neuroscience, 30(14), 5071-5077.

Mareschal, I., & Baker Jr, C. L. (1998). A cortical locus for the processing of contrast-defined contours. Nature neuroscience, 1(2), 150.

Matsumoto, H., & Ugawa, Y. (2017). Adverse events of tDCS and tACS: a review. Clinical Neurophysiology Practice, 2, 19-25.

Middleton, J.W., Longtin, A., Benda, J., Maler, L., 2006. The cellular basis for parallel neural transmission of a high-frequency stimulus and its low-frequency envelope. Proc. Natl. Acad. Sci. U S A. 103, 14596-14601.

Negahbani, E., Kasten, F. H., Herrmann, C. S., & Fröhlich, F. (2018). Targeting alpha-band oscillations in a cortical model with amplitude-modulated high-frequency transcranial electric stimulation. NeuroImage, 173, 3-12.

Neuling, T., Ruhnau, P., Weisz, N., Herrmann, C. S., & Demarchi, G. (2017). Faith and oscillations recovered: On analyzing EEG/MEG signals during tACS. Neuroimage, 147, 960-963.

Nolte, G., 2003. 3D imaging, planning, navigation. Minim. Invasive Ther. Allied Technol. 12, 3-4.

Noury, N., & Siegel, M. (2017). Phase properties of transcranial electrical stimulation artifacts in electrophysiological recordings. NeuroImage, 158, 406-416.

Noury, N., Hipp, J. F., & Siegel, M. (2016). Physiological processes non-linearly affect electrophysiological recordings during transcranial electric stimulation. Neuroimage, 140, 99-109.

Robinson, S., Vrba, J., 1999. Functional neuroimaging by synthetic aperature magnetometry (SAM), in: Yoshimoto, T., Kotani M., Kuriki S., Karibe H., Nakasato N. (Eds.), Recent advances in biomagnetism. Tohoku, Japan: Tohoku University Press, pp. 302-305.

Silny, J. (2007). Demodulation in tissue, the relevant parameters and the implications for limiting exposure. Health physics, 92(6), 604-608.

Soekadar, S.R., Witkowski, M., Cossio, E.G., Birbaumer, N., Robinson, S.E., Cohen, L.G., 2013a. In vivo assessment of human brain oscillations during application of transcranial electric currents. Nat. Commun. 4:2032.

Soekadar, S.R., Witkowski, M., Robinson, S.E., Birbaumer, N., 2013b. Combining electric brain stimulation and source-based brain-machine interface (BMI) training in neurorehabilitation of chronic stroke. Journal of the neurological sciences. 333-e542.

Thut, G., Bergmann, T. O., Fröhlich, F., Soekadar, S. R., Brittain, J. S., Valero-Cabré, A., ... & Ziemann, U. (2017). Guiding transcranial brain stimulation by EEG/MEG to interact with ongoing brain activity and associated functions: a position paper. Clinical Neurophysiology, 128(5), 843-857.

Witkowski, M., Garcia-Cossio, E., Chander, B. S., Braun, C., Birbaumer, N., Robinson, S. E., & Soekadar, S. R. (2016). Mapping entrained brain oscillations during transcranial alternating current stimulation (tACS). Neuroimage, 140, 89-98.

2.4. Unpublished work

The phase lock value (PLV) is not affected by linear phase distortions induced by transcranial alternating current stimulation (tACS)

Entrainment of brain oscillations to the applied transcranial alternating current stimulation (tACS) is calculated using phase lock value (PLV) (*Helfrisch et al. 2014, Witkowski et al. 2016, Chander et al. 2016*). PLV estimates synchronization between two signals, for example the tACS signal and the ongoing brain oscillation as a function of instantaneous phase difference between the signals.

Noury and Siegel (*2017*) showed that application of tACS induces steady phase deflections in all MEG sensors relative to the phase of the applied tACS signal. These steady phase distortions project from sensors to the source activity (SA) at location r in the brain while estimating source activity by multiplying beamformer weights with the sensor signal. However, steady phase shifts do not affect PLV estimation as shown below.

Let $b(n)$ be the magnetic field measured by MEG sensors at a discrete time point n represented as a column vector,

$$b(n) = \begin{bmatrix} b_1(n) \\ \vdots \\ b_M(n) \end{bmatrix} \tag{1}$$

where, the magnetic field as measured by m^{th} sensor is given as $b_m(n)$ and M is the total number of MEG sensors.

The Hilbert transform $\big(Y(n)\big)$ of a discrete time series signal is expressed in polar form as,

$$\boldsymbol{Y(n) = A(n) * e^{-i\Phi(n)}} \tag{2}$$

where, $A(n)$ is the amplitude and $\Phi(n)$ is the instantaneous phase at a discrete time point n.

By substituting equation (2) in (1), the Hilbert transform of magnetic fields $(Y_b(n))$ measured by MEG sensors can be expressed as,

$$\boldsymbol{Y_b(n)} = \begin{bmatrix} \boldsymbol{A_1(n)} * \boldsymbol{e^{-i\Phi_1(n)}} \\ \vdots \\ \boldsymbol{A_M(n)} * \boldsymbol{e^{-i\Phi_M(n)}} \end{bmatrix} \quad \textbf{(3)}$$

The Hilbert transform of magnetic field at source $\hat{s}(r,n)$ located at r at discrete time n is given as

$$\boldsymbol{Y_{\hat{s}}(r,n)} = \boldsymbol{\omega^T(r) Y_b(n)} \quad \textbf{(4)}$$

where, $\omega(r)$ is the column vector consisting of a constant weight for each sensor for a tACS signal at a fixed frequency.

Since, sum of multiple sine waves of the same frequency but different amplitudes can be represented as a single sine wave of the same constant frequency with a phase shift, the source activity estimated at a constant frequency (for example the tACS frequency) from weighted sum of sensors activity can be represented with a constant phase shift as shown below.

$$\boldsymbol{Y_{\hat{s}}(r,n)} = \boldsymbol{\omega^T(r) Y_b(n)} = \boldsymbol{A_{\hat{S}}(n)} * \boldsymbol{e^{-i(\Phi_{\hat{s}}(n)+\Phi)}} \quad \textbf{(5)}$$

where, $\boldsymbol{A_{\hat{S}}}$ is the amplitude of the source activity and Φ is the constant phase shift.

As shown by Noury and Siegel (*2017*), tACS induces steady phase deflection for each sensor, thus phase of each sensor ($\Phi_m(n)$) can be represented as a sum of phase due to brain activity ($\Phi_{BA,m}(n)$) and constant

phase shift induced by tACS ($\Phi_{tACS,m}$). Thus during tACS, the resultant phase of the source activity at location $\boldsymbol{r}$ can be represented as the sum of the phase deflection due to the brain activity and the tACS signal as shown below.

$$\boldsymbol{\Phi_{SA}(r,n) = \Phi_{BA}(r,n) + \Phi_{tACS}(r)} \quad \textbf{(6)}$$

where, $\Phi_{BA}(r,n)$ is the resultant phase deflection due to brain activity and $\Phi_{tACS}(r)$ is the resultant phase deflections due to tACS induced constant phase deflections for all sensors.

The $PLV(r)$ between source activity at location $\boldsymbol{r}$ and the applied tACS is calculated as

$$\boldsymbol{PLV(r) = \frac{1}{N}\left|\sum_{n=1}^{N} e^{i\left(\Phi_{SA}(r,n) - \Phi_{stim}(n)\right)}\right|} \quad \textbf{(7)}$$

where, N is the number of discrete samples in the time series signal. $\Phi_{SA}(r,n)$ is the instantaneous phase of the source activity ($\hat{s}(r,n)$) originating from location r and $\Phi_{stim}(n)$ is the instantaneous phase of tACS signal.

Substituting equation (6) in equation (7), $PLV(r)$ between source activity at location r and the applied tACS can be rewritten as

$$\boldsymbol{PLV(r) = \frac{1}{N}\left|\sum_{n=1}^{N} e^{i\left(\Phi_{BA}(r,n) + \Phi_{tACS}(r) - \Phi_{stim}(n)\right)}\right|}$$

$$\boldsymbol{= \frac{1}{N}\left|e^{i(\Phi_{tACS}(r))}\sum_{n=1}^{N} e^{i\left(\Phi_{BA}(r,n) - \Phi_{stim}(n)\right)}\right|}$$

$$\boldsymbol{= \frac{1}{N}\left|e^{i(\Phi_{tACS}(r))}\right|\left|\sum_{n=1}^{N} e^{i\left(\Phi_{BA}(r,n) - \Phi_{stim}(n)\right)}\right|}$$

$$= \frac{1}{N}\left|\sum_{n=1}^{N} e^{i\left(\Phi_{BA}(r,n) - \Phi_{stim}(n)\right)}\right|$$

(8)

where $\left|e^{i(\Phi_{tACS}(r))}\right| = 1$, as the absolute value of a complex exponent is always one. Hence proved, $PLV(r)$ does not depend on the linear phase distortions induced by tACS at sensor level.

3. Chapter 3 – Discussion

Perturbing brain activity to modify behavior has been in practice for decades. Recent advances in neurotechnology have led to the emergence of non-invasive brain stimulation (NIBS) as a promising tool for perturbing brain activity for investigating human behavior. Even though there is substantial evidence supporting NIBS as a tool to modulate behavior, the underlying mechanisms of action of NIBS remained obscure. It was not possible to assess brain activity during NIBS as the noise of the applied stimulation interferes with recording of brain activity.

The proposed amplitude modulated transcranial alternating current stimulation ($tACS_{AM}$) NIBS protocol attenuated tACS stimulation-related artifacts at the physiological frequency bands. Spatial filtering-based algorithms such as Synthetic Aperture Magnetometry (SAM) allow for improved assessment of physiological brain activity during $tACS_{AM}$ compared to classical transcranial alternating current stimulation (tACS). Furthermore, it is possible to entrain and localize the entrained brain activity across the brain, predominantly under the stimulation electrodes by assessing the synchrony between the applied modulation signal of $tACS_{AM}$ at FOI and the ongoing brain activity. The entrainment was limited to the frequency of the amplitude modulation signal of the applied $tACS_{AM}$. While establishing assessment of magnetic activity acquired during electrical stimulation in a phantom head, it was possible to confirm the location of dipolar source synchronized with the applied electric stimulation within millimeter precision.

Entrainment is one of the possible mechanisms of interaction of the applied $tACS_{AM}$ signal with the ongoing brain activity. While entraining, the phase of the ongoing brain activity synchronizes with the phase of the applied amplitude modulation signal. Unlike classical tACS, where power of the applied stimulation signal is concentrated at the FOI, $tACS_{AM}$ entrains brain activity at the frequency of the amplitude modulation signal without delivering most of the power at the FOI. Thus, the mechanism of interaction of $tACS_{AM}$ is different from classical

tACS. For neurons to be susceptible to the amplitude modulation signal, neurons must be able to demodulate the applied $tACS_{AM}$ signal due to the non-linear properties of neuronal cell membrane (*Rise, 1954, Goldman, 1954*). Apart from the amplitude modulation signal, the $tACS_{AM}$ signal also has a carrier signal at 220 Hz and it was not possible to find any influence of the carrier signal on brain activity in the physiological frequencies of interest. However, to ensure there is no influence of the carrier signal on the brain activity, carrier frequencies in the range of kilohertz (kHz) must deliver $tACS_{AM}$ (*Grossman et al. 2017*). Grossman et al. (*2017*) recently showed that neurons do not fire in response to 1 mA tACS when applied at 1 kHz or 2 kHz.

After establishing the mapping of $tACS_{AM}$-entrained brain activity, $tACS_{AM}$ was applied while performing a working memory task to investigate $tACS_{AM}$ mediated behavioral modulation. The results show that delivering $tACS_{AM}$ modulated at each individual's theta peak frequency (4 – 8 Hz) over the medial prefrontal cortex (mPFC) entrains endogenous theta oscillations originating form mPFC and anterior cingulate cortex (ACC). Even though $tACS_{AM}$ was delivered by attaching the stimulation electrodes over the frontal and parietal brain regions, entrainment was not found under the parietal electrode. In addition, entrainment of theta activity interferes with maintenance of temporal order of information essential for performing the n-back task that was used for assessing working memory. Even though power of theta oscillations increases with the difficulty level of n-back task (*Gevins et al. 1997*), the stimuli information seems to be encoded in the phase of theta oscillations as $tACS_{AM}$ induced phase synchrony worsens accuracy in n-back task. Since the inhibition in power-increase occurs only in PFC and not in ACC, hints towards a differential role of PFC and ACC while engaging in an n-back task. PFC has been associated with inhibiting competing stimuli (*Munakata et al. 2011*) whereas ACC is associated with controlling attention (*Gehring and Knight, 2000*). Thus, entrainment of theta oscillations originating from PFC probably interferes with encoding of competing stimuli and therefore does not require n-back task related theta power increase in PFC to inhibit competing stimuli. However, to identify influence of entrainment on encoding and maintenance of

stimuli, requires another working memory task with non-overlapping encoding and maintenance intervals unlike the n-back task, that requires continuous encoding, maintenance and update of stimuli. Unchanged reaction times and power of theta oscillations originating from ACC suggests attention control remains undisturbed.

These findings highlight the importance of phase regulation for performing the n-back task and $tACS_{AM}$ may not influence other working memory tasks that do not require endogenous phase regulation. Contrary to disrupting working memory, it might be possible to disrupt dysfunctional endogenous cortical-subcortical phase synchronization using $tACS_{AM}$ for example in case of depressive disorders and schizophrenia to relieve symptoms, but further investigations are required for a confirmation.

Application of $tACS_{AM}$ disrupts endogenous phase regulation but it might be also possible to boost endogenous phase regulation by applying brain state dependent stimulation. In this study, $tACS_{AM}$ was applied in an open-loop protocol where phase of the stimulation signal is independent of the ongoing brain activity. Therefore, implementation of brain state dependent stimulation (closed-loop) protocol would allow triggering the stimulation at a specific phase of the ongoing brain activity in real-time to boost endogenous phase regulation. In addition, brain state dependent stimulation can perturb brain activity in response to an observed feature of brain activity and utilized for inferring causal links between the perturbed physiological feature and behavior.

However, implementation of brain state dependent stimulation requires minimization of stimulation artifacts in the recordings of brain activity to allow assessment of brain activity during stimulation in an online paradigm. Even though, it is possible to map entrained brain oscillations and assess the induced behavioral modulations, the existence of a residual stimulation artifact in the assessed brain activity cannot be excluded. Even after minimizing the stimulation artifacts in the assessed brain activity, it is not possible to distinguish the contribution of stimulation artifact from the brain activity at the FOI. Recently, demodulation of $tACS_{AM}$ related artifacts were associated with

nonlinear electrical properties of the stimulation setup (*Karsten et al. 2018*). This raised the question whether previously observed entrainment measured as phase-lock value (PLV) were due to the demodulation artifacts of $tACS_{AM}$ signal.

To further characterize power and PLV in $tACS_{AM}$ and tACS, we conducted a series of experiments to contrast between response of $tACS_{AM}$ between human brain and a melon phantom. Under the consideration, the electrical properties of the biological membranes would be similar for human brains and melon phantom except for the functional neurons allows identifying functional interactions of $tACS_{AM}$ signal with neurons. In addition, the layered structure of the melon phantom with different conductivities resembles a human head. Our results show a difference in ratio of power between modulation frequency and carrier frequency reflects demodulation of $tACS_{AM}$ signal plus possible neural entrainment. Since non-linearities of the stimulation circuit including the stimulator and electrical properties of the biological membranes can demodulate the $tACS_{AM}$ signal, leakage of power at carrier frequency to the modulation frequency is expected. One could argue that the observed difference in the power ratio between human brains and melon phantom could be due to differences in conductivities. However, if this were true then one would also expect the PLV values to be comparable between $tACS_{AM}$ and tACS, which is the case for melon phantom but not for human brains. Even though, the power during tACS is higher compared to the $tACS_{AM}$ at the target frequency, one would expect a larger increase in PLV during tACS compared to $tACS_{AM}$, which is contrary to what was found for human brains. This suggests that $tACS_{AM}$ is associated with demodulation at the target frequency, possibly due to biological mechanisms.

Even though, there are indications for a possible functional interaction of $tACS_{AM}$ signal with biological tissue, currently the contribution of demodulation of $tACS_{AM}$ signal due to non-linearities of the stimulator and functional interaction with the neurons in brain cannot be reliably distinguished.

Recently, steady phase deflections were detected in MEG sensors during tACS (*Noury et al. 2017*). These deflections depend on the frequency of applied stimulation and vary across MEG sensors. Under these assumptions, mathematically it was possible to derive that PLV estimate is not affected by steady phase deflections. PLV is a measure of circular variance in phase space and a constant phase deflection does not alter the circular variance, which makes PLV resilient to constant phase deflections. Apart from PLV, other measures such as signal entropy based information estimates might also be resistant or resilient to stimulation artifacts. A random noise signal or a pure sine wave such as the tACS signal does not carry any information. Therefore, estimating the information content or information transfer between brain regions might allow deriving meaningful conclusions. However, further investigations are necessary to establish information theory-based estimates such as rank vector entropy (RVE) and symbolic transfer entropy (STE) as tools to assess brain activity acquired during NIBS (*Robinson et al. 2013*). Apart from testing novel assessment algorithms, technical solutions to eliminate demodulation of $tACS_{AM}$ signal by non-linearities in the stimulation setup must be considered. For example, implementing a hardware band-pass filter centered at the carrier frequency and including the side bands reflecting amplitude modulation, in the stimulation circuit delivering $tACS_{AM}$ can attenuate power leakage to the modulation frequency. Furthermore, implementing auxiliary circuits that measure deviations from the programmed stimulator output and inject current to compensate the measured deviations can potentially eliminate nonlinear stimulation artifacts.

Establishing assessment of brain activity during NIBS would allow brain state dependent stimulation for purposeful manipulation of physiological features. Depending on the physiological feature considered for perturbing, for example tACS for manipulating power and $tACS_{AM}$ for manipulating phase would allow experimenters to select appropriate stimulation paradigms. Perturbing a physiological feature upon estimation in real time would allow facilitating or impeding of underlying physiological processes. Depending on the brain state, applying electrical stimulation can facilitate or impede memory

formation while the observed brain state is classified as poor or optimal for performing a memory task respectively (*Hanslmayr et al. 2017*). Performing NIBS in a brain-state dependent closed-loop stimulation paradigm while engaging in a cognitive task, would allow establishing a tool to determine a causal link between the perturbed feature and performance in the cognitive task. Such causal links might eventually uncover physiological biomarkers as a substrate for NIBS-based therapeutic interventions. Brain-state dependent closed-loop stimulation along with neurofeedback of the perturbed physiological feature as a therapeutic tool would allow for the development of personalized treatment options for various neurological and psychiatric disorders.

4. Chapter 4 – Summary

Application of non-invasive brain stimulation for perturbing brain activity is well established. Various forms of brain stimulation protocols have been effectively demonstrated to modulate behavior associated with the perturbed brain activity. However, the interaction of brain stimulation with ongoing brain activity has been challenging to characterize as the stimulation artifacts in the recordings of brain activity impedes such characterization.

The proposed amplitude modulated transcranial alternating current stimulation ($tACS_{AM}$) attenuates possible stimulation artifacts at the frequency of interest. This is possible by modulating the amplitude of high frequency transcranial alternating current (tACS) signal at a lower physiological frequency of interest to generate the $tACS_{AM}$ signal. Furthermore, application of $tACS_{AM}$ allows localization of the perturbed brain activity with millimeter precision by applying spatial filters on magnetoencephalography (MEG) recordings. For characterization of the $tACS_{AM}$-perturbed brain activity, conventional spectral analysis may not be sufficient. Thus, power and PLV were compared between tACS and $tACS_{AM}$ in a phantom model and MEG data recorded from healthy human volunteers.

The synchronization estimate, phase lock value (PLV), is a measure of circular variance between two signals calculated as a function of instantaneous phase difference between the ongoing brain activity and the applied stimulation signal. Even though, systematic linear phase shifts due to the applied tES signal occur in MEG sensors, mathematically such systematic linear phase shifts nullify while calculating PLV. Systematic evaluation of the MEG data acquired during $tACS_{AM}$ showed increased PLV compared to tACS indicating increased demodulation in such paradigm.

Upon observing $tACS_{AM}$-related increased demodulation, it was still unclear whether such perturbations of brain activity could modulate behavior. To address this question, twenty volunteers while engaging in a working memory paradigm received $tACS_{AM}$ or no stimulation. Working memory is associated

with transient storage and processing of information. Increasing the difficulty of working memory paradigm increases the amplitude of brain activity in the theta band (4 – 8 Hz), while encoding the temporal order of the transient information in the phase of the theta activity. Thus, by targeting individual's theta peak frequency using $tACS_{AM}$, it was possible to modulate the accuracy in the working memory paradigm. The accuracy on a working memory parading of volunteers receiving $tACS_{AM}$ deteriorated compared to the participants who did not receive brain stimulation. Therefore, targeting brain activity in theta band using $tACS_{AM}$ interferes with execution of normal working memory processes, probably by interfering with the maintenance of temporal order of the transient information. Furthermore, $tACS_{AM}$ but not sham stimulation inhibited the increase in amplitude of theta activity during the n-back task, which is essential for working memory processes.

Even though, it is possible to assess the brain activity recorded during $tACS_{AM}$, presence of stimulation artifacts in the assessed brain activity cannot be excluded. However, it was possible to gather evidence that $tACS_{AM}$ is associated with demodulation. $TACS_{AM}$-induced phase synchrony at the modulation frequency was larger compared to tACS even though the power during tACS is larger compared to $tACS_{AM}$. This observation is in favor of possible functional interaction of $tACS_{AM}$ signal with neurons in the brain. However, currently it is not possible to distinguish between the contribution towards demodulation of $tACS_{AM}$ signal by non-linearities of the stimulation setup and functional interactions with neurons in the brain.

In conclusion, $tACS_{AM}$ can alter cognitive function, such as working memory performance, possibly through entrainment. The results obtained from such investigations must be interpreted with great care, as the extent by which possible stimulation artifacts impact the MEG recordings is not entirely clear. Further investigations are necessary to develop quantitative assessment techniques for characterizing artifacts of the stimulation and eventually develop brain state dependent stimulation paradigms in real time as a research tool and therapeutic intervention.

5. German Summary

Derzeit existieren zahlreiche gut etablierte Verfahren der nicht-invasiven Hirnstimulation zur Manipulation von Hirnaktivität. Dabei konnten durch die Anwendung diverser Stimulationsprotokolle Verhaltensweisen, die mit einer Störung der Hirnaktivität in Zusammenhang stehen, effektiv moduliert werden. Jedoch war die Erforschung der Interaktion von Hirnstimulation und der zugrundeliegenden Hirnaktivität bisher mit großen Herausforderungen verbunden, da die Stimulation mit starken Störsignalen einhergeht, die eine Charakterisierung der Hirnaktivität unmöglich machen.

Mit dem hier vorgestellten Stimulationsprotokoll, der amplitudenmodulierten transkraniellen Wechselstromstimulation (engl. amplitude modulated transcranial alternating current stimulation, $tACS_{AM}$), einer Form der transkraniellen elektrischen Stimulation (tES), konnte die Kontamination von physiologischen Frequenzbändern wesentlich reduziert werden. Dies wird erreicht, indem die Amplitude eines hochfrequenten transkraniellen Wechselstromsignals (tACS) auf eine langsamere physiologische Frequenz moduliert wird. Durch die Anwendung von räumlichen Filtern auf simultan zur Stimulation aufgenommene Magnetoenzephalograpie (MEG)-Daten, lassen sich $tACS_{am}$-assoziierte Demodulationen, die möglicherweise durch biologische Mechanismen entstehen, mit Millimeter-Präzision ermitteln.

Da die Existenz von bisher nicht detektierten stimulationsbedingten Störsignalen im untersuchten Frequenzbereich nicht vollständig ausgeschlossen werden kann, wäre für die Charakterisierung der durch $tACS_{AM}$ manipulierten Gehirnaktivität, eine konventionelle Analyse des Frequenzspektrums nicht ausreichend. Aus diesem Grund wurden Maße für die Synchronisation zwischen appliziertem $tACS_{AM}$-Signal und unterliegender Hirnaktivität getestet, um die Auswirkungen der $tACS_{AM}$ auf das Gehirn zu untersuchen.

Als Maß für die Synchronisation wurde der sogenannte Phase Lock Value (PLV) geprüft. Dieser spiegelt die unmittelbare Phasendifferenz zwischen der

momentanen Hirnaktivität und dem applizierten Stimulationssignal wider. Zwar berichten Noury et al. 2017 von systematischen linearen Phasenverschiebungen in Zusammenhang mit dem applizierten tES Signal, diese heben sich jedoch bei der Berechnung des PLV, der auf der unmittelbaren Phasendifferenz basiert, wieder auf.

Während $tACS_{AM}$ konnte bei der systematischen Auswertung der simultan erhobenen MEG Daten eine erhöhte Demodulation in der Zielfrequenz gegenüber tACS beobachtet werden.

Es blieb jedoch unklar, ob eine solche erhöhte Demodulation auch Einfluss auf kognitive Funktionen hat. Um dieser Frage nachzugehen, wurde die Leistung des Arbeitsgedächtnisses bei 20 gesunden Probanden mit und ohne $tACS_{AM}$ untersucht. Das Arbeitsgedächtnis spielt eine wichtige Rolle bei der vorübergehenden Speicherung und Verarbeitung von neuen Informationen. Mit dem Schwierigkeitsgrad der gestellten Aufgabe nimmt auch die Amplitude der Hirnaktivität im Theta-Frequenzband (4 - 8 Hz) zu, wobei die zeitliche Abfolge der eingehenden Information in der Phase der Theta Oszillation kodiert wird. So war es durch die Synchronisation der jeweils am stärksten ausgeprägten individuellen Theta-Frequenz mit der applizierten $tACS_{AM}$ möglich, die Leistung des Arbeitsgedächtnisses während der Durchführung des Experiments zu beeinflussen. Dabei verringerte sich die Genauigkeit mit der die Aufgabe gelöst wurde bei den Teilnehmern, die $tACS_{AM}$ erhielten im Gegensatz zu Teilnehmern, die nicht stimuliert wurden. Demzufolge behindert ein Entrainment der Hirnaktivität im Theta-Frequenzband die normale Ausführung von Prozessen, die wichtig für die Funktion des Arbeitsgedächtnisses sind, vermutlich indem die Beibehaltung der zeitlichen Abfolge der betreffenden Informationen gestört wird. Zudem verhindert $tACS_{AM}$ eine Zunahme der Amplitude von Theta Aktivität, die normalerweise im Zusammenhang mit der Durchführung der Aufgabe beobachtet wird.

Obwohl es grundsätzlich möglich ist, die während $tACS_{AM}$ aufgenommene Hirnaktivität zu analysieren, kann die Existenz von bisher nicht detektierbaren Stimulationsartefakten nicht ausgeschlossen werden. Es konnten jedoch

Anhaltspunkte gefunden werden, die für eine Demodulation des $tACS_{AM}$-Signals sprechen. Durch die Demodulation eines amplitudenmodulierten Trägersignals lässt sich im Leistungsspektrum ein qualitativer Übertrag der Leistungsdichte von der Trägerfrequenz zur Modulationsfrequenz beobachten. Dieser Effekt war bei Messungen mit dem menschlichen Gehirn größer als in einer Melone, die als Phantomkontrolle diente. Zusätzlich bewirkte $tACS_{AM}$ auf der Modulationsfrequenz eine stärkere Phasenkopplung als konventionelle tACS, wenngleich die Leistungsdichte im Vergleich während konventioneller tACS höher war. Diese Beobachtungen stützen die Annahme einer funktionellen Interaktion des $tACS_{AM}$-Signals mit dem Gehirn. Jedoch ist es derzeit nicht möglich zu unterscheiden, in welchem Ausmaß nichtlineare Eigenschaften des Stimulations-Setups zur Demodulation des $tACS_{AM}$-Signals beitragen und zu welchem Grad die Demodulation durch tatsächliche funktionelle Interaktionen mit dem Gehirn hervorgerufen wird.

Es lässt sich zusammenfassen, dass die hier vorgeschlagene $tACS_{AM}$ die zielgerichtete Manipulation von Hirnaktivität erlaubt und während $tACS_{AM}$ erhobenen MEG Daten zu einem gewissen Maß auf das Ausmaß der induzierten Einwirkung auf die Hirnaktivität schließen lassen. Trotz allem sollten die Ergebnisse einer solchen Untersuchung mit Vorsicht interpretiert werden, da die Möglichkeit von bisher nicht erkennbaren Artefakten durch die Stimulation nicht ausgeschlossen werden kann. Aus diesem Grund sind weitere Untersuchungen zur Entwicklung quantitativer Messverfahren für die Beurteilung von stimulationsbedingten Störsignalen notwendig, um vom aktuellen Hirnzustand abhängige Echtzeit-Stimulationsparadigmen entwickeln zu können, die in der Forschung oder im Rahmen therapeutischer Eingriffe eingesetzt werden können.

6. Bibliography

Ali, M. M., Sellers, K. K., & Fröhlich, F. (2013). Transcranial alternating current stimulation modulates large-scale cortical network activity by network resonance. Journal of Neuroscience, 33(27), 11262-11275.

Anderson, K. L., Rajagovindan, R., Ghacibeh, G. A., Meador, K. J., & Ding, M. (2009). Theta oscillations mediate interaction between prefrontal cortex and medial temporal lobe in human memory. Cerebral Cortex, 20(7), 1604-1612.

Antal, A., & Paulus, W. (2013). Transcranial alternating current stimulation (tACS). Frontiers in human neuroscience, 7, 317.

Axmacher, N., Henseler, M. M., Jensen, O., Weinreich, I., Elger, C. E., & Fell, J. (2010). Cross-frequency coupling supports multi-item working memory in the human hippocampus. Proceedings of the National Academy of Sciences, 107(7), 3228-3233.

Bawin, S. M., Kaczmarek, L. K., & Adey, W. R. (1975). Effects of modulated VHF fields on the central nervous system. Annals of the New York Academy of Sciences, 247(1), 74-81.

Beason, R. C., & Semm, P. (2002). Responses of neurons to an amplitude modulated microwave stimulus. Neuroscience Letters, 333(3), 175-178.

Beckmann, M., Johansen-Berg, H., & Rushworth, M. F. (2009). Connectivity-based parcellation of human cingulate cortex and its relation to functional specialization. Journal of Neuroscience, 29(4), 1175-1190.

Blatow, M., Rozov, A., Katona, I., Hormuzdi, S. G., Meyer, A. H., Whittington, M. A., ... & Monyer, H. (2003). A novel network of multipolar bursting interneurons generates theta frequency oscillations in neocortex. Neuron, 38(5), 805-817.

Brignani, D., Ruzzoli, M., Mauri, P., & Miniussi, C. (2013). Is transcranial alternating current stimulation effective in modulating brain oscillations? PloS one, 8(2), e56589.

Brittain, J. S., Probert-Smith, P., Aziz, T. Z., & Brown, P. (2013). Tremor suppression by rhythmic transcranial current stimulation. Current Biology, 23(5), 436-440.

Brookes, M. J., Wood, J. R., Stevenson, C. M., Zumer, J. M., White, T. P., Liddle, P. F., & Morris, P. G. (2011). Changes in brain network activity during working memory tasks: a magnetoencephalography study. Neuroimage, 55(4), 1804-1815.

Buzsaki, G. (2006). Rhythms of the Brain. Oxford University Press.

Buzsáki, G., & Draguhn, A. (2004). Neuronal oscillations in cortical networks. science, 304(5679), 1926-1929.

Cavanagh, J. F., Zambrano-Vazquez, L., & Allen, J. J. (2012). Theta lingua franca: A common mid-frontal substrate for action monitoring processes. Psychophysiology, 49(2), 220-238.

Chander, B. S., Witkowski, M., Braun, C., Robinson, S. E., Born, J., Cohen, L. G., ... & Soekadar, S. R. (2016). tACS phase locking of frontal midline theta oscillations disrupts working memory performance. Frontiers in cellular neuroscience, 10, 120.

Citri, A., & Malenka, R. C. (2008). Synaptic plasticity: multiple forms, functions, and mechanisms. Neuropsychopharmacology, 33(1), 18.

Clayton, M. S., Yeung, N., & Kadosh, R. C. (2015). The roles of cortical oscillations in sustained attention. Trends in cognitive sciences, 19(4), 188-195.

Colgin, L. L. (2011). Oscillations and hippocampal–prefrontal synchrony. Current opinion in neurobiology, 21(3), 467-474.

Cox, R. W. (1996). AFNI: software for analysis and visualization of functional magnetic resonance neuroimages. Computers and Biomedical research, 29(3), 162-173.

Curio, G., Mackert, B. M., Burghoff, M., Neumann, J., Nolte, G., Scherg, M., & Marx, P. (1997). Somatotopic source arrangement of 600 Hz oscillatory magnetic fields at the human primary somatosensory hand cortex. Neuroscience letters, 234(2-3), 131-134.

De Smedt, B., Grabner, R. H., & Studer, B. (2009). Oscillatory EEG correlates of arithmetic strategy use in addition and subtraction. Experimental brain research, 195(4), 635-642.

Donkers, F. C., Schwikert, S. R., Evans, A. M., Cleary, K. M., Perkins, D. O., & Belger, A. (2011). Impaired neural synchrony in the theta frequency range in adolescents at familial risk for schizophrenia. Frontiers in psychiatry, 2, 51.

Düzel, E., Penny, W. D., & Burgess, N. (2010). Brain oscillations and memory. Current opinion in neurobiology, 20(2), 143-149.

Fetz, E. E. (2015). Restoring motor function with bidirectional neural interfaces. In Progress in brain research (Vol. 218, pp. 241-252). Elsevier.

Fröhlich, F., & McCormick, D. A. (2010). Endogenous electric fields may guide neocortical network activity. Neuron, 67(1), 129-143.

Fründ, I., Ohl, F. W., & Herrmann, C. S. (2009). Spike-timing-dependent plasticity leads to gamma band responses in a neural network. Biological cybernetics, 101(3), 227-240.

Gandiga, P. C., Hummel, F. C., & Cohen, L. G. (2006). Transcranial DC stimulation (tDCS): a tool for double-blind sham-controlled clinical studies in brain stimulation. Clinical neurophysiology, 117(4), 845-850.

Garcia-Cossio, E., Witkowski, M., Robinson, S. E., Cohen, L. G., Birbaumer, N., & Soekadar, S. R. (2016). Simultaneous transcranial direct current stimulation (tDCS) and whole-head magnetoencephalography (MEG): assessing the impact of tDCS on slow cortical magnetic fields. Neuroimage, 140, 33-40.

Gehring, W. J., & Knight, R. T. (2000). Prefrontal–cingulate interactions in action monitoring. Nature neuroscience, 3(5), 516.

Gevins, A., Smith, M. E., McEvoy, L., & Yu, D. (1997). High-resolution EEG mapping of cortical activation related to working memory: effects of task difficulty, type of processing, and practice. Cerebral cortex (New York, NY: 1991), 7(4), 374-385.

Giraud, A. L., & Poeppel, D. (2012). Cortical oscillations and speech processing: emerging computational principles and operations. Nature neuroscience, 15(4), 511.

Goldman, D. E. (1943). Potential, impedance, and rectification in membranes. The Journal of general physiology, 27(1), 37-60.

Grosof, D. H., Shapley, R. M., & Hawken, M. J. (1993). Macaque VI neurons can signal 'illusory'contours. Nature, 365(6446), 550.

Grossman, N., Bono, D., Dedic, N., Kodandaramaiah, S. B., Rudenko, A., Suk, H. J., ... & Pascual-Leone, A. (2017). Noninvasive deep brain stimulation via temporally interfering electric fields. Cell, 169(6), 1029-1041.

Hanslmayr, S., & Roux, F. (2017). Human Memory: Brain-State-Dependent Effects of Stimulation. Current Biology, 27(10), R385-R387.

Hanslmayr, S., & Staudigl, T. (2014). How brain oscillations form memories—a processing based perspective on oscillatory subsequent memory effects. Neuroimage, 85, 648-655.

Helfrich, R. F., Knepper, H., Nolte, G., Strüber, D., Rach, S., Herrmann, C. S., ... & Engel, A. K. (2014). Selective modulation of interhemispheric functional connectivity by HD-tACS shapes perception. PLoS biology, 12(12), e1002031.

Hsieh, L. T., & Ranganath, C. (2014). Frontal midline theta oscillations during working memory maintenance and episodic encoding and retrieval. Neuroimage, 85, 721-729.

Ishihara, T., & Yoshii, N. (1972). Multivariate analytic study of EEG and mental activity in juvenile delinquents. Electroencephalography and clinical neurophysiology, 33(1), 71-80.

Jensen, O., & Tesche, C. D. (2002). Frontal theta activity in humans increases with memory load in a working memory task. European journal of Neuroscience, 15(8), 1395-1399.

Joundi, R. A., Jenkinson, N., Brittain, J. S., Aziz, T. Z., & Brown, P. (2012). Driving oscillatory activity in the human cortex enhances motor performance. Current Biology, 22(5), 403-407.

Jurkiewicz, M. T., Gaetz, W. C., Bostan, A. C., & Cheyne, D. (2006). Post-movement beta rebound is generated in motor cortex: evidence from neuromagnetic recordings. Neuroimage, 32(3), 1281-1289.

Kanai, R., Chaieb, L., Antal, A., Walsh, V., & Paulus, W. (2008). Frequency-dependent electrical stimulation of the visual cortex. Current Biology, 18(23), 1839-1843.

Kasten, F. H., Negahbani, E., Frohlich, F., & Herrmann, C. S. (2018). Non-linear transfer characteristics of stimulation and recording hardware account for spurious low-frequency artifacts during amplitude modulated transcranial alternating current stimulation (AM-tACS). bioRxiv, 246710.

Kawasaki, M., & Guo, Y. X. (1998). Parallel projection of amplitude and phase information from the hindbrain to the midbrain of the African electric fish Gymnarchus niloticus. Journal of Neuroscience, 18(18), 7599-7611.

Klimesch, W., Schimke, H., Doppelmayr, M., Ripper, B., Schwaiger, J., & Pfurtscheller, G. (1996). Event-related desynchronization (ERD) and the Dm effect: does alpha desynchronization during encoding predict later recall performance?. International Journal of Psychophysiology, 24(1-2), 47-60.

Kolev, V., Yordanova, J., Schürmann, M., & Başar, E. (2001). Increased frontal phase-locking of event-related alpha oscillations during task processing. International Journal of Psychophysiology, 39(2-3), 159-165.

Kolomytkin, O., Kuznetsov, V., Yurinska, M., Zharikova, A., & Zharikov, S. (1994). Response of brain receptor systems to microwave energy exposure. In: Frey, A.H. (Ed.), On the

Nature of Electromagnetic Field Interactions with Biological Systems. R.G. Landes Co, Austin, TX, pp. 194–206.

Kotecha, R., Xiang, J., Wang, Y., Huo, X., Hemasilpin, N., Fujiwara, H., & Rose, D. (2009). Time, frequency and volumetric differences of high-frequency neuromagnetic oscillation between left and right somatosensory cortices. International Journal of Psychophysiology, 72(2), 102-110.

Laakso, I., & Hirata, A. (2013). Computational analysis shows why transcranial alternating current stimulation induces retinal phosphenes. Journal of neural engineering, 10(4), 046009.

Lachaux, J. P., Rodriguez, E., Martinerie, J., & Varela, F. J. (1999). Measuring phase synchrony in brain signals. Human brain mapping, 8(4), 194-208.

Laske, C., Sohrabi, H. R., Frost, S. M., López-de-Ipiña, K., Garrard, P., Buscema, M., ... & Bridenbaugh, S. A. (2015). Innovative diagnostic tools for early detection of Alzheimer's disease. Alzheimer's & dementia: the journal of the Alzheimer's Association, 11(5), 561-578.

Liew, S. L., Santarnecchi, E., Buch, E. R., & Cohen, L. G. (2014). Non-invasive brain stimulation in neurorehabilitation: local and distant effects for motor recovery. Frontiers in human neuroscience, 8, 378.

Lundstrom, B. N., Fairhall, A. L., & Maravall, M. (2010). Multiple timescale encoding of slowly varying whisker stimulus envelope in cortical and thalamic neurons in vivo. Journal of Neuroscience, 30(14), 5071-5077.

MacDonald, A. W., Cohen, J. D., Stenger, V. A., & Carter, C. S. (2000). Dissociating the role of the dorsolateral prefrontal and anterior cingulate cortex in cognitive control. Science, 288(5472), 1835-1838.

Mareschal, I., & Baker Jr, C. L. (1998). A cortical locus for the processing of contrast-defined contours. Nature neuroscience, 1(2), 150-154.

Marshall, L., Helgadóttir, H., Mölle, M., & Born, J. (2006). Boosting slow oscillations during sleep potentiates memory. Nature, 444(7119), 610.

Matsumoto, H., & Ugawa, Y. (2017). Adverse events of tDCS and tACS: a review. Clinical Neurophysiology Practice, 2, 19-25.

Meiron, O., & Lavidor, M. (2013). Unilateral prefrontal direct current stimulation effects are modulated by working memory load and gender. Brain Stimulation: Basic, Translational, and Clinical Research in Neuromodulation, 6(3), 440-447.

Middleton, J. W., Longtin, A., Benda, J., & Maler, L. (2006). The cellular basis for parallel neural transmission of a high-frequency stimulus and its low-frequency envelope. Proceedings of the National Academy of Sciences, 103(39), 14596-14601.

Missonnier, P., Hasler, R., Perroud, N., Herrmann, F. R., Millet, P., Richiardi, J., ... & Baud, P. (2013). EEG anomalies in adult ADHD subjects performing a working memory task. Neuroscience, 241, 135-146.

Mitchell, D. J., & Cusack, R. (2007). Flexible, capacity-limited activity of posterior parietal cortex in perceptual as well as visual short-term memory tasks. Cerebral Cortex, 18(8), 1788-1798.

Mitra, P. P., & Pesaran, B. (1999). Analysis of dynamic brain imaging data. Biophysical journal, 76(2), 691-708.

Moliadze, V., Antal, A., & Paulus, W. (2010). Boosting brain excitability by transcranial high frequency stimulation in the ripple range. The Journal of physiology, 588(24), 4891-4904.

Moretti, D. V., Pievani, M., Fracassi, C., Binetti, G., Rosini, S., Geroldi, C., ... & Frisoni, G. B. (2009). Increase of theta/gamma and alpha3/alpha2 ratio is associated with amygdalo-hippocampal complex atrophy. Journal of Alzheimer's Disease, 17(2), 349-357.

Munakata, Y., Herd, S. A., Chatham, C. H., Depue, B. E., Banich, M. T., & O'Reilly, R. C. (2011). A unified framework for inhibitory control. Trends in cognitive sciences, 15(10), 453-459.

Negahbani, E., Kasten, F. H., Herrmann, C. S., & Fröhlich, F. (2018). Targeting alpha-band oscillations in a cortical model with amplitude-modulated high-frequency transcranial electric stimulation. NeuroImage, 173, 3-12.

Neske, G. T. (2016). The slow oscillation in cortical and thalamic networks: mechanisms and functions. Frontiers in neural circuits, 9, 88.

Neuling, T., Ruhnau, P., Fuscà, M., Demarchi, G., Herrmann, C. S., & Weisz, N. (2015). Friends, not foes: magnetoencephalography as a tool to uncover brain dynamics during transcranial alternating current stimulation. Neuroimage, 118, 406-413.

Neuling, T., Ruhnau, P., Weisz, N., Herrmann, C. S., & Demarchi, G. (2017). Faith and oscillations recovered: On analyzing EEG/MEG signals during tACS. Neuroimage, 147, 960-963.

Nolte, L. P. (2003). 3D imaging, planning, navigation. Minimally Invasive Therapy & Allied Technologies, 12(1-2), 3-4.

Norman, K. A., Newman, E. L., & Detre, G. (2007). A neural network model of retrieval-induced forgetting. Psychological review, 114(4), 887.

Norman, K. A., Newman, E. L., & Perotte, A. J. (2005). Methods for reducing interference in the complementary learning systems model: oscillating inhibition and autonomous memory rehearsal. Neural Networks, 18(9), 1212-1228.

Noury, N., & Siegel, M. (2017). Phase properties of transcranial electrical stimulation artifacts in electrophysiological recordings. NeuroImage, 158, 406-416.

Noury, N., Hipp, J. F., & Siegel, M. (2016). Physiological processes non-linearly affect electrophysiological recordings during transcranial electric stimulation. Neuroimage, 140, 99-109.

Nunez, P. L. (1981). A study of origins of the time dependencies of scalp EEG: II-experimental support of theory. IEEE Transactions on Biomedical Engineering, (3), 281-288.

Olbrich, S., & Arns, M. (2013). EEG biomarkers in major depressive disorder: discriminative power and prediction of treatment response. International Review of Psychiatry, 25(5), 604-618.

Oostenveld, R., Fries, P., Maris, E., & Schoffelen, J. M. (2011). FieldTrip: open source software for advanced analysis of MEG, EEG, and invasive electrophysiological data. Computational intelligence and neuroscience, 2011, 1.

Papadelis, C., Poghosyan, V., Fenwick, P. B., & Ioannides, A. A. (2009). MEG's ability to localise accurately weak transient neural sources. Clinical Neurophysiology, 120(11), 1958-1970.

Paulus, W. (2011). Transcranial electrical stimulation (tES–tDCS; tRNS, tACS) methods. Neuropsychological rehabilitation, 21(5), 602-617.

Pfurtscheller, G., Neuper, C., Andrew, C., & Edlinger, G. (1997). Foot and hand area mu rhythms. International Journal of Psychophysiology, 26(1-3), 121-135.

Poghosyan, V., & Ioannides, A. A. (2007). Precise mapping of early visual responses in space and time. Neuroimage, 35(2), 759-770.

Polanía, R., Nitsche, M. A., Korman, C., Batsikadze, G., & Paulus, W. (2012). The importance of timing in segregated theta phase-coupling for cognitive performance. Current Biology, 22(14), 1314-1318.

Rice, S. O. (1955). Mathematical analysis of random noise. In: Wax, N. (Ed.), Selected papers on noise and stochastic processes. Dover, New York, pp. 133–294.

Robinson, S. E. (1999). Functional neuroimaging by synthetic aperture magnetometry (SAM). Recent advances in biomagnetism, 302-305.

Robinson, S. E., Mandell, A. J., & Coppola, R. (2013). Spatiotemporal imaging of complexity. Frontiers in computational neuroscience, 6, 101.

Rossini, P. M., Barker, A. T., Berardelli, A., Caramia, M. D., Caruso, G., Cracco, R. Q., ... & De Noordhout, A. M. (1994). Non-invasive electrical and magnetic stimulation of the brain, spinal cord and roots: basic principles and procedures for routine clinical application. Report of an IFCN committee. Electroencephalography and clinical neurophysiology, 91(2), 79-92.

Saad, Z. S., & Reynolds, R. C. (2012). Suma. Neuroimage, 62(2), 768-773.

Santarnecchi, E., Polizzotto, N. R., Godone, M., Giovannelli, F., Feurra, M., Matzen, L., ... & Rossi, S. (2013). Frequency-dependent enhancement of fluid intelligence induced by transcranial oscillatory potentials. Current Biology, 23(15), 1449-1453.

Sauseng, P., & Klimesch, W. (2008). What does phase information of oscillatory brain activity tell us about cognitive processes?. Neuroscience & Biobehavioral Reviews, 32(5), 1001-1013.

Schutter, D. J. (2016). Cutaneous retinal activation and neural entrainment in transcranial alternating current stimulation: a systematic review. Neuroimage, 140, 83-88.

Silny, J. (2007). Demodulation in tissue, the relevant parameters and the implications for limiting exposure. Health physics, 92(6), 604-608.

Soekadar, S. R., Birbaumer, N., Slutzky, M. W., & Cohen, L. G. (2015). Brain–machine interfaces in neurorehabilitation of stroke. Neurobiology of disease, 83, 172-179.

Soekadar, S. R., Witkowski, M., Birbaumer, N., & Cohen, L. G. (2014). Enhancing Hebbian learning to control brain oscillatory activity. Cerebral cortex, 25(9), 2409-2415.

Soekadar, S. R., Witkowski, M., Cossio, E. G., Birbaumer, N., Robinson, S. E., & Cohen, L. G. (2013). In vivo assessment of human brain oscillations during application of transcranial electric currents. Nature communications, 4, 2032.

Soekadar, S. R., Witkowski, M., Garcia Cossio, E., Birbaumer, N., & Cohen, L. (2014). Learned EEG-based brain self-regulation of motor-related oscillations during application of transcranial electric brain stimulation: feasibility and limitations. Frontiers in behavioral neuroscience, 8, 93.

Soekadar, S. R., Witkowski, M., Robinson, S. E., & Birbaumer, N. (2013). Combining electric brain stimulation and source-based brain-machine interface (BMI) training in neurorehabilitation of chronic stroke. Journal of the neurological sciences, 333, e542.

Suk, J., Ribary, U., Cappell, J., Yamamoto, T., & Llinas, R. (1991). Anatomical localization revealed by MEG recordings of the human somatosensory system. Electroencephalography and clinical neurophysiology, 78(3), 185-196.

Thompson, M., & Thompson, L. (2003). The Neurofeedback Book: An Introduction to Basic Concepts in Applied Pychophysiology. Association for Applied Psychophysiology and Biofeedback.

Thut, G., Bergmann, T. O., Fröhlich, F., Soekadar, S. R., Brittain, J. S., Valero-Cabré, A., ... & Ziemann, U. (2017). Guiding transcranial brain stimulation by EEG/MEG to interact with ongoing brain activity and associated functions: a position paper. Clinical Neurophysiology, 128(5), 843-857.

Thut, G., Miniussi, C., & Gross, J. (2012). The functional importance of rhythmic activity in the brain. Current Biology, 22(16), R658-R663.

Thut, G., Schyns, P., & Gross, J. (2011). Entrainment of perceptually relevant brain oscillations by non-invasive rhythmic stimulation of the human brain. Frontiers in psychology, 2, 170.

Veniero, D., Vossen, A., Gross, J., & Thut, G. (2015). Lasting EEG/MEG aftereffects of rhythmic transcranial brain stimulation: level of control over oscillatory network activity. Frontiers in cellular neuroscience, 9, 477.

Vogt, B. (Ed.). (2009). Cingulate neurobiology and disease. Oxford University Press.

Voss, U., Holzmann, R., Hobson, A., Paulus, W., Koppehele-Gossel, J., Klimke, A., & Nitsche, M. A. (2014). Induction of self awareness in dreams through frontal low current stimulation of gamma activity. Nature neuroscience, 17(6), 810.

Vossen, A., Gross, J., & Thut, G. (2015). Alpha power increase after transcranial alternating current stimulation at alpha frequency (α-tACS) reflects plastic changes rather than entrainment. Brain Stimulation: Basic, Translational, and Clinical Research in Neuromodulation, 8(3), 499-508.

Voytek, B., & Knight, R. T. (2015). Dynamic network communication as a unifying neural basis for cognition, development, aging, and disease. Biological psychiatry, 77(12), 1089-1097.

Witkowski, M., Garcia-Cossio, E., Chander, B. S., Braun, C., Birbaumer, N., Robinson, S. E., & Soekadar, S. R. (2016). Mapping entrained brain oscillations during transcranial alternating current stimulation (tACS). Neuroimage, 140, 89-98.

Woods, A. J., Antal, A., Bikson, M., Boggio, P. S., Brunoni, A. R., Celnik, P., ... & Knotkova, H. (2016). A technical guide to tDCS, and related non-invasive brain stimulation tools. Clinical Neurophysiology, 127(2), 1031-1048.

Zaehle, T., Rach, S., & Herrmann, C. S. (2010). Transcranial alternating current stimulation enhances individual alpha activity in human EEG. PloS one, 5(11), e13766.

7. Declaration of Author Contributions

I hereby declare that the doctoral dissertation submitted with the title: “Assessment of whole-head magnetoencephalography during transcranial electric entrainment of brain oscillations” was written independently using only the stated sources and aids and that quotes and excerpts, literal or otherwise, are marked correspondingly. I declare on oath that these statements are true and that I have concealed nothing. I am aware that false declarations or affirmations in lieu of an oath can be punished with a jail sentence of up to three years or with a fine.

Bankim Subhash Chander

7.1. Mapping entrained brain oscillations during transcranial alternating current stimulation (tACS)

Matthias Witkowski*, Eliana García Cossio*, **Bankim S. Chander**, Christoph Braun, Niels Birbaumer, Stephen E. Robinson, Surjo R. Soekadar

* These authors contributed equally

Matthias Witkowski and Eliana García Cossio conceived and designed the study in cooperation with Christoph Braun and Surjo R. Soekadar. Bankim S. Chander established the phase locking value (PLV) as a measure of synchronization between the applied tACS signal and ongoing brain oscillations to demonstrate entrainment. In addition, Bankim S. Chander prepared the methods section describing the PLV. The data of phantom and human experiments was acquired by Bankim S. Chander under the supervision of Matthias Witkowski and Eliana García Cossio. Bankim S. Chander generated the results required for production of figure 5a and figure 6. Stephen E. Robinson prepared the toolbox for analyzing the data.

7.2. TACS phase locking of frontal midline theta oscillations disrupts working memory performance

Bankim S. Chander, Matthias Witkowski, Christoph Braun, Stephen E. Robinson, Jan Born, Leonardo G. Cohen, Niels Birbaumer, Surjo R. Soekadar

Bankim S. Chander conceived and designed the study in cooperation with Matthias Witkowski, Surjo R. Soekadar and Christoph Braun. The working memory paradigm was established by Bankim S. Chander. All the data was acquired and analyzed by Bankim S. Chander. The data analysis was performed using the SAM toolbox developed by Stephen E. Robinson. Bankim S. Chander interpreted the results along with Matthias Witkowski and Surjo R. Soekadar. Bankim S. Chander wrote the first

draft and prepared all the figures of the manuscript under supervision of Surjo R. Soekadar. All other co-authors provided critical reviews and assisted in drafting the final manuscript.

7.3. Amplitude-modulated transcranial alternating current stimulation (tACS) in magnetoencephalography (MEG): An update

Bankim S. Chander, Matthias Witkowski, David Haslacher, Shuka Shibusawa, Stephen E. Robinson, Christoph Braun, Surjo R. Soekadar

Bankim S. Chander conceived and designed the study in cooperation with Matthias Witkowski, Surjo R. Soekadar and Christoph Braun. Bankim S. Chander acquired all the data from human participants and from phantom. David Haslacher and Shuka Shibusawa assisted in collecting data from phantom experiments. Bankim S. Chander analyzed all the data using the toolbox developed by Stephen E. Robinson. David Haslacher and Shuka Shibusawa assisted in analyzing the data from phantom experiments. Bankim S. Chander interpreted the results along with Matthias Witkowski and Surjo R. Soekadar. Bankim S. Chander wrote the first draft and prepared all the figures of the manuscript under supervision of Surjo R. Soekadar. Stephen E. Robinson and Christoph Braun provided critical insights for optimizing the experimental setup for performing concurrent transcranial electric stimulation during magnetoencephalography. All other co-authors provided critical reviews and assisted in drafting the final manuscript.

Acknowledgements

First, I would like to express my gratitude towards PD Dr. med. Surjo Soekadar for always being an inspiration and supportive mentor throughout the course of my thesis. He has always encouraged me to strive for success and motivated me to excel beyond my limits. Thank you very much for supervising my thesis and preparing me for the future.

I would also like to thank my thesis advisors Prof. Dr. Niels Birbaumer, Prof. Dr. Christoph Braun and Prof. Dr. med. Gerhard Eschweiler for taking their valuable time for giving constructive criticism. Again, special thanks to Prof. Dr. Braun for trouble shooting numerous times during inadvertent failures in the MEG lab.

Next, I would like to thank Dr. Matthias Witkowski and Dr. Eliana Garcia for teaching me fundamentals of data analysis and helping in interpretation of results. Heart-felt gratitude for Dr. Stephen Robinson for teaching advance data analysis techniques that allowed me to gain deeper understanding of brain physiology.

I would like to thank Jürgen Dax for eagerly developing new hardware to improve the efficiency and quality of data acquisition.

Special thanks to PD Dr. Susanne Diekelmann, Dr. Anja Wühle and Dr. Katharina Zinke for advice on programming and analyzing the study paradigm.

I would like to thank the members of Applied Neurotechnology Lab: Matthias, Eliana, Marius, Anne, David, Mareike and Shuka for numerous memorable days in office.

Sincere thanks to Mrs. Birgit Teufel for helping in administrative work and taking time out for translating numerous documents from German to English.

Last but not the least I would like to thank my friends Ujwal, Ashish, Raviteja, Marcos, Vinod, Joana, Diljit, Chaitanya, Kousik, Manish, Katja, Konstantina, Ioannis, Solmaz, Peter, Aurelie and Trevor for all the happy memories in Tübingen for a lifetime.

I would also like to thank my friends Manisha, Ishita, Ankur, Swati, Dinesh, Netrapal, Clarisse, Swati, Sneha, Satya and Mrityunjay for begin there through good and bad times.

Finally, I would like express my gratitude towards Dr. Maja Strohal, Dr. Sven Gehring, Dr. Avdhoot Shivanand, Shubhi and my family, though for this words are not enough.